



**Pilkington Library**

Author/Filing Title ..... STURLEY, G.G. .....

Accession/Copy No. ....

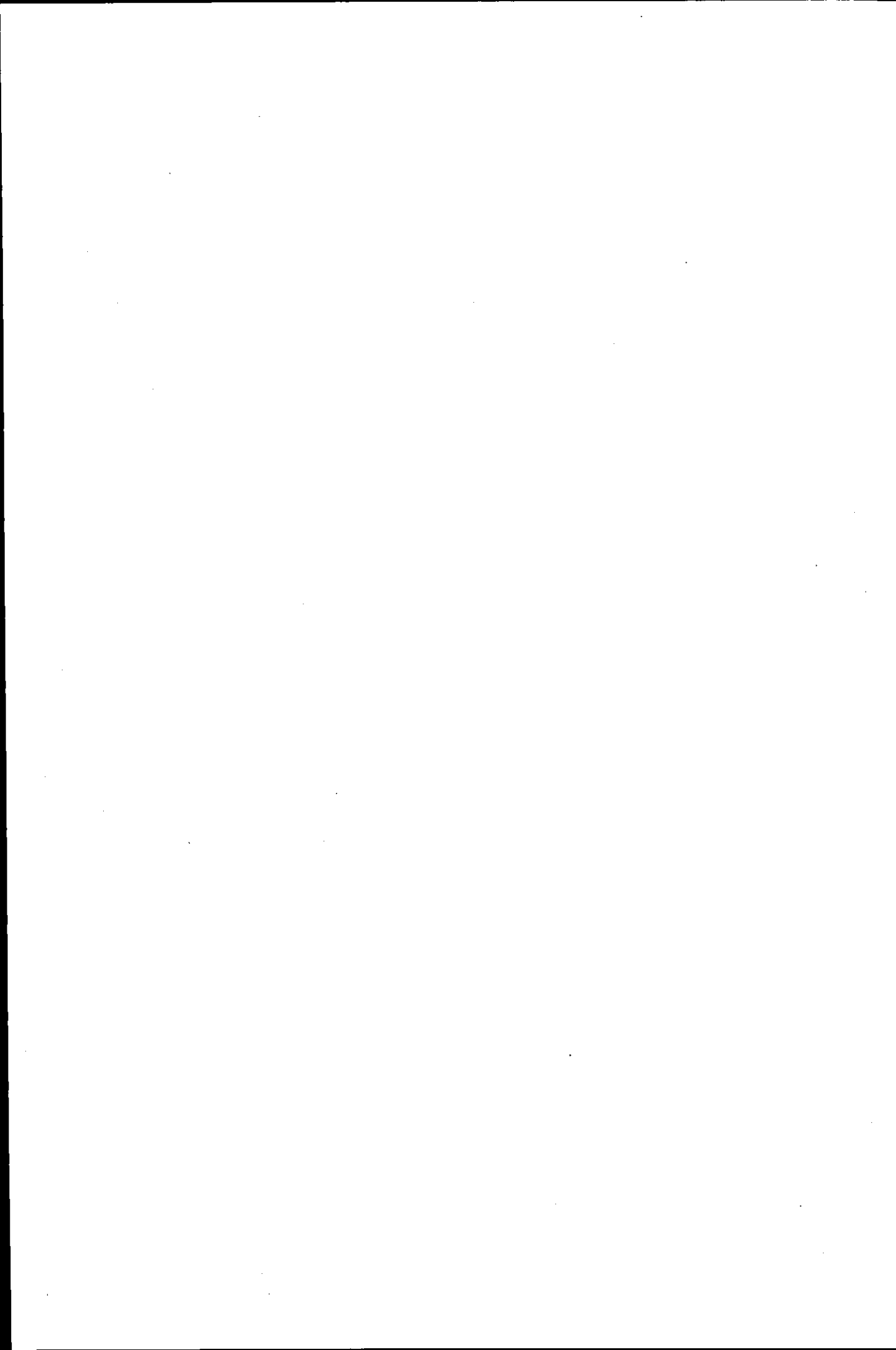
Vol. No. ....

Class Mark ..... T .....

LOAN COPY

040165902X





**PHOTOCHEMISTRY OF 3,3',4',5 - TETRACHLOROSALICYLANILIDE AND  
3,4',5 - TRIBROMOSALICYLANILIDE AND THEIR INTERACTIONS WITH  
HUMAN SERUM ALBUMIN**


**By**

**Garry Graham Sturley**

**A Doctoral Thesis Submitted in Partial Fulfilment of the Requirements for  
The Award of Doctor of Philosophy of Loughborough University.**

**September 30<sup>th</sup> 1997**

**© Garry Graham Sturley 1997**

 Loughborough University Faculty of Engineering
Date Jul 98
Class
Acc No. 040165902

U 0631746

I could quote 'Punctuality is the biggest thief of time' [1] or 'It takes two to lie, one to lie and one to listen' [2] but I won't, because they are not my quotes, however this is 'At last!'

[1] Oscar Wilde

[2] Homer Simpson

To My Mother and Father, Ann and John Sturley

With Love and Thanks

## Acknowledgements

First and foremost I would like to thank my supervisor Professor Frank Wilkinson for his help, encouragement, guidance and incredible patience throughout this project. I would like to thank Unilever for sponsorship of this project. Thanks to Dr. W. Lovell for his advice, use of equipment and Mrs Pendlington for her assistance in making protein samples. I would also like to acknowledge EPSRC for financial support.

A very special thank you to my parents, John and Ann Sturley for all their financial and moral support throughout the years and thanks to my brother Nathan who no matter how melancholic I felt could still split my sides with his humour and to Dr. John Davey for his advice and guidance.

Thanks also to the Photochemistry group past and present: Darren Greenhill, Dr. David Mandley, Prof. Andres Olea, Dr. Jon Hobley, Dr. Ayman Abdel-Shafi, Dr. Richard James, Dr. Marek Sikorski, Anita Jones, Robin Vincent, Jill Crossley, Dr. Sian Williams, Dr. Dave Worrall, Dr. Andy Goodwin, Anabela Oliveiros, Dr. Miquel Mir and my erstwhile girlfriend Dr. Lisinka Jansen.

Thanks must also go to the electrochem' boys for their laconic witticisms: Simon Foster, Phil Naylor, Andy Wallace, Chris Dudfield and fellow Hammers fan Dr. Roger Mortimer.

And finally cheers to my close friends: Steve Phillips, Mukesh Shimnar, Gordon Wright and Dominic "Suggs" Kearney.

# Contents

Abstract .....	i
<b>Chapter 1: Introduction</b>	
1.1 Photochemical Principles .....	2
1.1.1 Photochemical Reactions .....	2
1.1.2 Absorption of Radiation .....	3
1.1.3 Electronic States of Molecules .....	5
1.1.4 Excited States .....	6
1.1.5 Electronic Transitions .....	7
1.1.6 State Diagrams .....	9
1.1.7 The Jablonski Diagram .....	10
1.1.8 Radiative Transitions .....	11
1.1.9 Non Radiative Transitions .....	12
1.1.10 Intermolecular Electronic Energy-Transfer Processes .....	13
1.1.11 Quenching by Molecular Oxygen .....	18
1.1.12 Singlet Oxygen .....	20
1.2 Laser Light .....	23
1.2.1 Historical Development .....	23
1.2.2 Solid State Lasers .....	26
Chapter 1 References .....	28
<b>Chapter 2: Photoallergy, Tetrachlorosalicylanilide Chemistry and Serum Albumin</b>	
2.1 Introduction .....	30
2.2 Photoallergy Vs Phototoxicity .....	31
2.3 Photoallergic Compounds .....	32
2.4 Photoallergic Drug Reaction .....	33
2.4.1 Requirements for a Photoallergic response .....	34

2.5	Photodermatitis due to Tetrachlorosalicylanilide .....	34
2.6	Photobinding to Proteins .....	37
2.7	The Photochemistry of Tetrachlorosalicylanilide .....	40
2.8	Serum Albumin .....	46
2.8.1	Introduction .....	46
2.8.2	Structure .....	47
2.8.3	Survey of Ligands Bound to Albumin .....	49
	Chapter 2 References .....	50

### Chapter 3: Experimental

3.1	Ground State Absorbance Spectra .....	54
3.2	Steady State Emission Spectra .....	54
3.3	Nanosecond Laser Flash Photolysis .....	54
3.3.1	Data Collection .....	56
3.3.2	Data Analysis .....	57
3.4	Phosphorescence Measurements .....	58
3.5	Singlet Oxygen Luminescence Detection .....	59
3.6	Preparation of Solutions .....	60
3.6.1	Preparation of mHSA in 0.1 M Potassium Phosphate buffer solution pH 7.4 .....	60
3.6.2	Preparation of Salicylanilide Solutions .....	61
3.7	Degassing Solutions .....	62
3.8	Materials .....	62

### Chapter 4: Results with $T_4CS^-$ and $TBS^-$

4.1	Absorption Spectroscopy .....	64
4.1.1	Ground State Absorbance Spectra .....	64
4.1.2	$pK_a$ of $T_4CS-H$ in 50% ethanolic aqueous solution .....	69
4.1.3	Calculation of Molar Absorption Coefficients and Verification of Beer's Law .....	73
4.2	Laser Induced Degradation of $T_4CS^-$ .....	75



4.3	Emission Spectroscopy .....	81
4.3.1	Fluorescent Spectra .....	81
4.3.2	Quantum Yield of Fluorescence .....	82
4.3.3	Phosphorescence Measurements.....	85
4.3.4	Singlet-Triplet Energy Splitting .....	87
4.4	Dark Binding Studies of $T_4CS^-$ with mHSA .....	89
4.4.1	Emission Spectroscopy ( $T_4CS^-$ with mHSA) .....	90
4.4.2	Results of Dark Binding Data .....	91
4.4.3	Analysis of Dark Binding Data .....	93
4.5	Flash Photolysis Studies .....	97
4.5.1	Excited State Photochemistry of $T_4CS^-$ in Solution .....	97
4.5.2	Analysis of the Long Wavelength Band ( $\lambda = 650$ nm) .....	98
4.5.3	Triplet-Triplet Energy Transfer .....	103
4.5.4	Quenching Results.....	108
4.5.5	Discussion .....	110
4.5.6	Radical Anion and Product Absorption ( $\lambda = 425$ nm) .....	114
4.5.7	Kinetics of the Radical Species .....	121
4.5.8	Excited State Photochemistry of $TBS^-$ in Solution .....	123
4.5.9	Singlet-Triplet Intersystem Crossing Quantum Yields .....	127
4.5.10	Triplet State Molar Absorption Coefficient of $T_4CS^-$ .....	132
4.5.11	Singlet-Triplet Intersystem Crossing Quantum Yield for $TBS^-$ .....	133
4.6	Flash Photolysis studies with of $T_4CS^-$ and $TBS^-$ with mHSA .....	134
4.6.1	Addition of Human Serum Albumin (mHSA) to $T_4CS^-$ .....	134
4.6.2	Laser Induced Degradation of $T_4CS^-$ / mHSA solutions .....	140
4.6.3	Addition of Bovine Serum Albumin (BSA) to $T_4CS^-$ .....	141
4.6.4	Addition of Human Serum Albumin (mHSA) to $TBS^-$ .....	143
4.7	Singlet Oxygen formation Quantum Yield Determinations for $T_4CS^-$ and $TBS^-$ .....	144
4.8	Excited State Photochemistry of Omadine in solution .....	148
4.9	Excited State Photochemistry of Rose Begal in solution .....	150

Chapter 4 References .....	152
<b>Chapter 5: Summary, and Conclusions and Recommendations for Further Work...</b>	<b>154</b>
Chapter 5 References .....	168

## Abstract

Many substituted salicylanilides, particularly halogenated salicylanilides have strong anti-bacterial properties and in the past have been employed as bactericides in soaps. However, this has led to photoallergy causing serious adverse skin reactions. Although most photoallergens will elicit a response in only a small fraction of the people exposed 3,3',4',5-tetrachlorosalicylanilide ( $T_4CS-H$ ) is unusual in inducing photoallergy in a high fraction of those exposed and displays a high specificity towards serum albumin. The proposed mechanism of the protein-photoallergen binding is thought to proceed via the formation of highly reactive species such as free radicals. The albumin in the skin is believed to be the carrier protein in the skin that binds with  $T_4CS^-$  to form an antigen.

The technique of time resolved nano-second laser flash photolysis has been employed to study the photochemistry of the anion  $T_4CS^-$  and a structurally similar photoallergen 3,4',5-tribromosalicylanilide ( $TBS^-$ ) in solution when excited with U.V radiation. The transient absorption spectrum obtained from exciting solutions of  $T_4CS^-$  in polar solvents has been assigned as comprising of the triplet state, radical anion  $T_3CS^-$ , and the build up of a product. The assignment of the triplet state with ( $\lambda_{max} = 650$  nm) was based on oxygen quenching and triplet-triplet energy transfer experiments. Transient absorption in the range 400-470 nm is attributed to the radical anion:  $T_3CS^-$ . This was not significantly affected by the presence of molecular oxygen. The addition of monomer human serum albumin (mHSA) to solutions of  $T_4CS^-$  had significant affects on both the kinetics and yields of observed transients. It also leads to a marked reduction in the oxygen quenching rate constant of the triplet state. This demonstrates that the triplet state is protected from molecular oxygen upon binding to mHSA. To determine the stoichiometry and affinity of binding, dark-binding studies were carried out to investigate the association of  $T_4CS^-$  with mHSA. The results showed that there are two strong binding sites.

Both  $T_4CS^-$  and  $TBS^-$  were found to be capable of sensitising the production of singlet molecular oxygen ( $^1\Delta_g(O_2)$ ) in 1:19 ethanol:  $D_2O$  solvent. This may explain the weak phototoxicity of  $T_4CS^-$ .

# **CHAPTER 1**

## **Introduction**

# 1 Introduction

## 1.1 Photochemical Principles

### 1.1.1 Photochemical Reactions

The study of photochemistry deals with a unique type of chemical reaction: photochemistry is all about exciting the electrons of molecules with discreet packages of light energy called photons; in what is analogous to a bimolecular interaction between the light and molecule. The remarkable behaviour of molecules once they have captured a photon of light distinguishes photochemical reactions from thermal reactions; a photon of light excites a molecule in a way that heat cannot. One of the major difference lies in the different electron distribution in ground and excited states of an excited molecule; consequently leading to major alterations in chemical behaviour. A second major difference is in the thermodynamics: since an electronically excited state of a molecule has a higher (in most cases a great deal higher) internal energy than the ground state, there exists a much greater choice of reaction pathway for the excited state on thermodynamic grounds. In particular, an excited molecule can give rise to high energy species such as: free radicals, singlet and triplet states, strained ring compounds or rearrange into another isomer that are not readily formed (if they are formed at all) from the ground state.

It is now over a century, since the first laws of the of photochemistry were formulated in the works of Grotthus and Draper which state: *Only the light which is absorbed by a molecule can be effective in producing photochemical change in a molecule.* The second law of chemistry deduced by Stark and Einstein originally stated that: each molecule taking part in a chemical reaction caused by light absorbs one quantum of the radiation that causes the reaction. However, this was later modified by Stark and Bodenstein to take into account secondary chain reactions. The second law restated is: *The absorption of light by a molecule is a one-quantum process, so that the sum of the primary process quantum yields must be unity.* The light that produces photochemical

changes occurs over wavelengths of 200 to 740 nanometres (nm). This is the UV and visible part of the electromagnetic spectrum, and is shown in figure (1.1), it is only a small portion of the spectrum - but happens to be the region that photochemists utilise most.

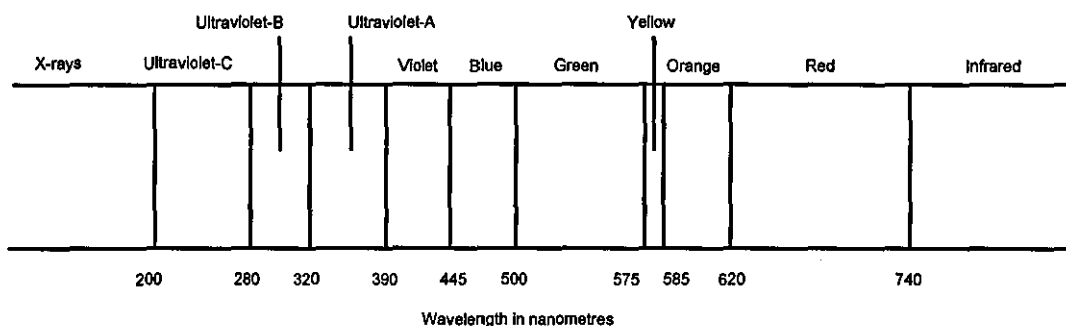


Figure (1.1) *The ultraviolet and visible spectrum of electromagnetic radiation.*

## 1.1.2 Absorption of radiation

When a photon passes close to a molecule, there is an interaction between the electric field associated with the molecule and that associated with the radiation. This perturbation may not result in a permanent change in the molecule, but it is possible for a reaction to occur in which the photon is absorbed by the molecule. This occurs when the molecule absorbs a quantum of radiation whose energy corresponds to a transition within the molecule. Transitions between energy levels take place in instantaneous jumps. The difference in energy between the two levels involved in the transition ( $\Delta E$ ), determines the frequency of the photon that can be absorbed through a relationship first deduced by Niels Bohr: this is  $\Delta E = h \nu$ . Where  $h$  is Planck's constant ( $6.63 \times 10^{-34}$  Js) and  $\nu$  is the frequency of radiation ( $s^{-1}$ ).

Photochemists tend to think in terms of energies in molar quantities; conventionally in  $\text{kJ mol}^{-1}$ , therefore a modification gives:

$$\Delta E = N_A hc/\lambda \quad (1.1)$$

Where  $N_A$  is Avogadro's constant ( $6.022 \times 10^{23} \text{ mol}^{-1}$ ),  $c$  is the velocity of light in a vacuum ( $2.998 \times 10^8 \text{ m s}^{-1}$ ) and  $\lambda$  is the wavelength.

For photochemical experiments, chemists ideally need monochromatic light, *i.e.* light of one wavelength. The absorption of a monochromatic beam of light by a homogenous absorbing system is described well by the Beer-Lambert law, which can be represented by:

$$I = I_0 10^{-\epsilon c l} \quad (1.2)$$

or

$$\log(I_0/I) = \epsilon c l \quad (1.3)$$

which describes how the intensity,  $I$ , of the radiation transmitted through the sample decreases exponentially with increasing path length of the sample,  $l$ , and the sample concentration,  $c$ .  $I_0$  is the incident radiation intensity and  $\epsilon$  is the molar absorption or extinction coefficient.

The quantum yield of a photochemical reaction ( $\phi$ ) can be defined in one of two ways:

$$\phi = \frac{\text{No. of molecules undergoing a process}}{\text{No. of quanta of light absorbed}} \quad (1.4)$$

$$\phi = \frac{\text{Rate of a process}}{\text{Rate of absorption of quanta}} \quad (1.5)$$

Equation (1.4) defines the quantum yield as a ratio of the number of molecules undergoing a process over the number of photons absorbed, and equation (1.5) defines it as a ratio of the rates of the processes involved. In the absence of any competing photochemical processes, the efficiency of the quantum should be unity. If other processes are in competition then the efficiency will be determined by the relative rates of the competing processes.

### 1.1.3 Electronic Structure of Molecules

The electrons in a molecule occupy molecular orbitals, which are often formulated as linear combinations of the valence shell atomic orbitals. One molecular orbital is bonding (*i.e.* more stable than the initial atomic orbitals) the other is antibonding (*i.e.* higher in energy than the initial atomic orbitals). We are concerned with the types of orbitals found in organic molecules that originate from the overlap of atomic s and p orbitals. Orbitals which are completely symmetrical about the internuclear axis are designated  $\sigma$  (sigma) if bonding and  $\sigma^*$  (sigma star) if antibonding. Molecular orbitals derived by mixing two parallel p orbitals are called  $\pi$  (pi) and  $\pi^*$  (pi star). For certain compounds notably those of Groups V, VI or VII, there are non-bonding electrons (designated  $n$ ), which are not involved in bonding and can be regarded as being localised on their atomic nuclei. The most commonly encountered transitions upon excitation are:  $n \rightarrow \pi^*$ ,  $\pi \rightarrow \pi^*$ ,  $n \rightarrow \sigma^*$ , and  $\sigma \rightarrow \sigma^*$ . An energy level diagram showing the different type of transitions is shown in figure (1.2).

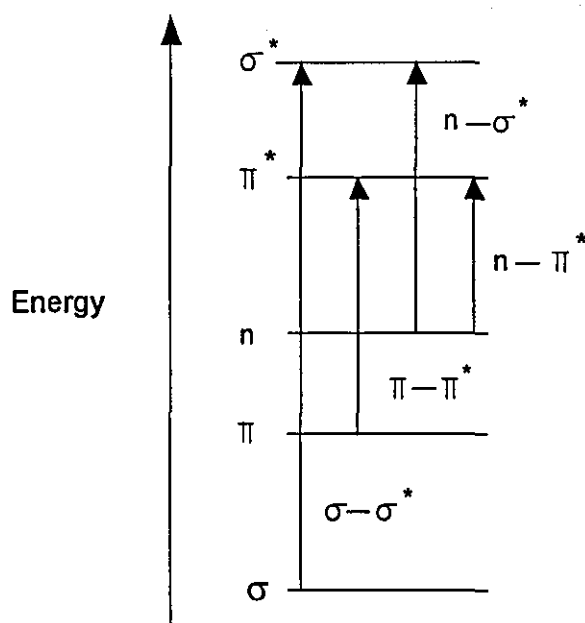


Figure (1.2) *Approximate energy level diagram showing different types of transitions.*



### 1.1.4 Excited States

Excited state molecules contain two unpaired electrons in different orbitals, each electron carrying a spin angular momentum with a spin quantum number  $s$ , and the value of  $m_s$  can be  $\pm 1/2$  depending on the "direction" of the electron spin. The total spin angular momentum possessed by a many electron atom or molecule is represented by the total spin quantum number  $S$ , which may be calculated as the vector sum of all the individual contributions from each electron - from this the spin multiplicity  $M$  gives the number of states expected in the presence of an applied magnetic field, and is given by  $M = 2S + 1$ . Thus, molecules whose electrons have the same (parallel) spin possess  $S = 1$  and a spin multiplicity  $M = 3$  are termed triplet states - triplet states are paramagnetic and can interact strongly with external magnetic fields. If however, the electron spins are different (opposed), then  $S = 0$  and  $M = 1$ , and the resulting states are termed singlet states. These two distinct species, commonly occur in photochemistry and have very different physical and chemical properties. The Pauli exclusion principle states that no two electrons in an atom can have the same values for all four quantum numbers, thus triplet states possess two unpaired electrons in different molecular orbitals. Another rule governing electron configurations is Hund's rule of maximum multiplicity which states that:

1. Electrons will occupy different orbitals whenever energetically possible.
2. Two electrons occupying degenerate orbitals will have parallel spins in their lowest energy state.

As a result of Hund's rule excited triplet states have lower energies than their corresponding excited singlet states.

### 1.1.5 Electronic Transitions

Electronic transitions in polyatomic molecules can be represented pictorially using potential energy / nuclear separation diagrams; these simplify the vibrational motions of a molecule upon excitation by considering the transition along a single “critical coordinate”. The relative intensities of bands are governed in terms of the Franck-Condon principle - this principle states that the time required for absorption of a quantum of light, and the resultant transition of an electron to an excited state is so short ( $\sim 10^{-15}$  s) compared to the period of vibration of the molecule ( $\sim 10^{-13}$  s), that during the act of absorption and excitation the nuclei do not alter appreciably their relative positions (*i.e.*, internuclear distance  $r$ ) or their kinetic energies. As a consequence of this, electronic transitions between two potential energy surfaces can be represented by *vertical lines* connecting them - as shown in figure (1.3).

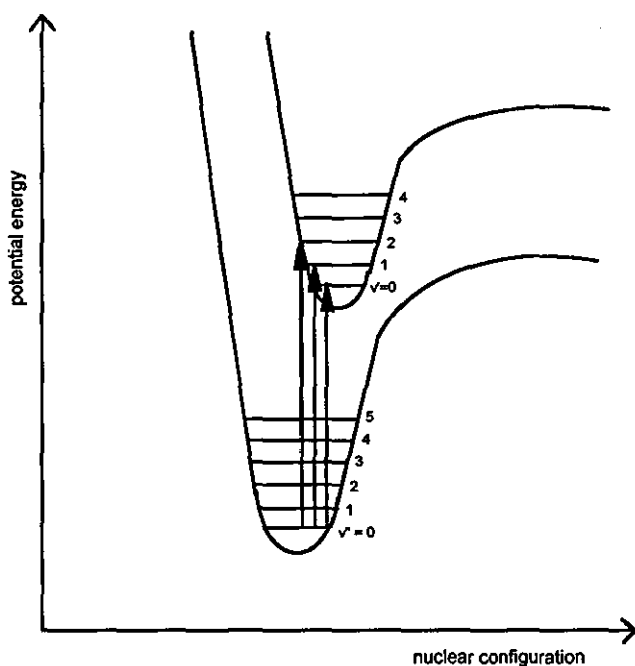


Figure (1.3) Transition between states of similar nuclear geometry.

This example, represents a common situation where excitation leads to stretching of a bond. This is expected whenever the excited electron is promoted into an antibonding orbital, thereby weakening the bond. At room temperature in condensed phase, most molecules will be in their 0th vibrational level as a result of the Boltzmann distribution, so the most favoured transitions occur from  $v'' = 0$ . The vertical line originates at the midpoint of  $v'' = 0$  since the vibrational wave function is maximum here. The probability of transition to a particular vibrational level  $v'$  in the excited state is determined by the product of the vibrational wave functions for the two states *i.e.*, the overlap of the two wave functions. Thus, in the example shown in figure (1.3), transitions from  $v'' = 0$  to  $v' = 1, 2$  and  $3$  occur with the  $v'' = 0 \rightarrow v' = 2$  transition expected to be the strongest; the other transitions will be less probable and therefore less intense - this would lead to an absorption spectrum as illustrated in figure (1.4).

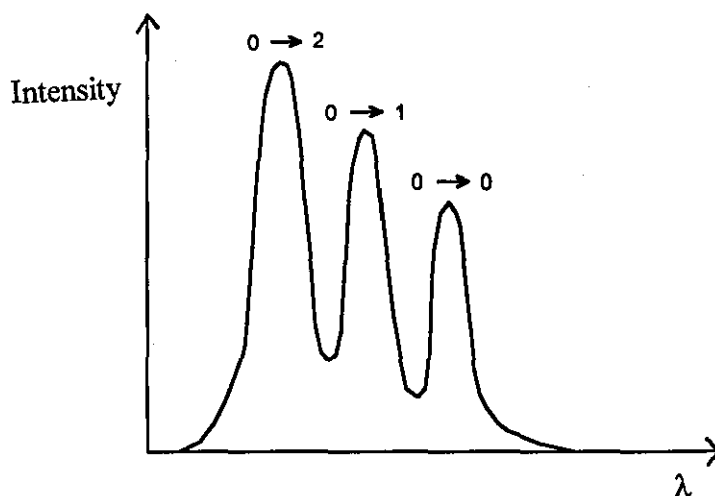


Figure (1.4) Absorption spectrum resulting from the situation in figure (1.3)

The above discussion also applies to the resulting fluorescence bands, with transitions from  $v' = 0 \rightarrow (v'' = n, \dots, 2, 1, 0)$ . The transition probabilities between different electronic states in a molecule are governed by what are known as selection rules. These are summarised as follows:

- 1) *Spin forbidden*: Transitions involving a change of spin, or multiplicity, are strongly

'forbidden' *i.e.*  $\Delta S \neq 0$ . Therefore intercombinations such as singlet  $\rightarrow$  triplet are 'forbidden', whereas singlet  $\rightarrow$  singlet is "allowed".

2) *Symmetry forbidden*: For a transition to be "allowed" there must be good spatial overlap between the orbitals of the states involved. Therefore  $\pi \rightarrow \pi^*$  is allowed whereas  $n \rightarrow \pi^*$  is not.

The fact that spin-forbidden transitions can be seen at all, is due to a phenomenon known "as spin-orbit coupling". Since the electron is charged and spinning, it is expected to have not only spin angular momentum, but also a magnetic moment. The orbital motion of the charged electron produces a magnetic field; which can interact with the nucleus - giving rise to spin-orbit coupling. The magnetic torque thus created, can invert the spin *i.e.* changes the direction of its magnetic moment, resulting in a change in the total spin-angular momentum of the system. Overall, the total angular momentum is conserved by a corresponding change in the orbital angular momentum. As a consequence of spin-orbit coupling, originally pure singlet and triplet states are mixed to a small extent.

### 1.1.6 State Diagrams

Energy level diagrams can be used to represent diagrammatically the various electronic states of a molecule. The singlet and triplet states are arranged in order of increasing energy and numbered in the same order *i.e.*  $S_0, S_1, S_2 \dots$  and  $T_1, T_2$  respectively. With such diagrams, it is possible to represent all the physical processes that can occur upon the absorption of a photon by the ground state, to produce an excited state. This is best represented by what is known as a Jablonski diagram - as shown in figure (1.5).

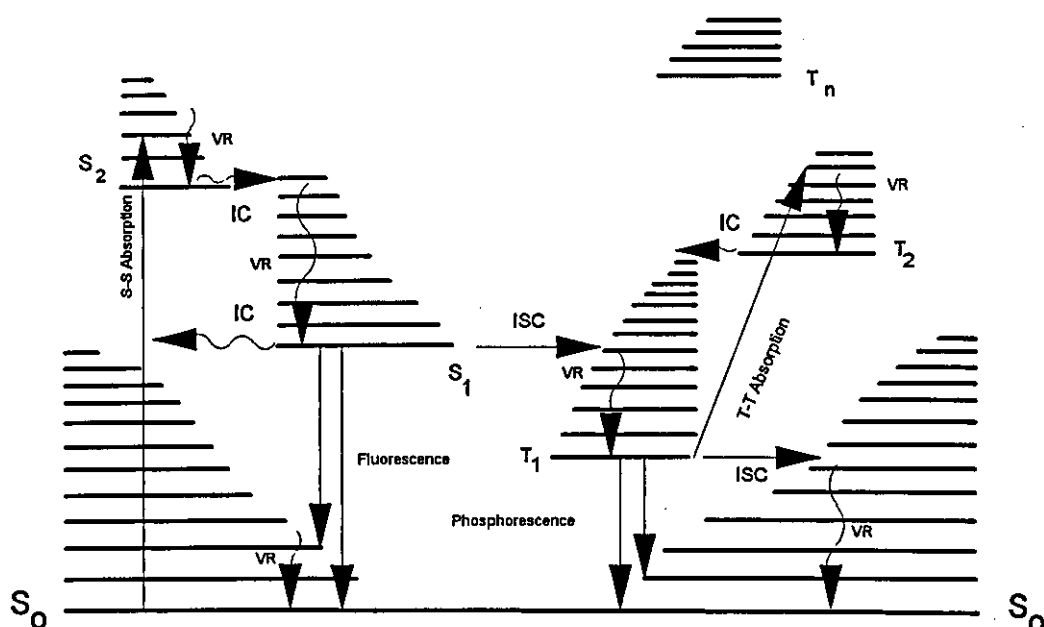


Figure (1.5) *Modified Jablonski diagram for polyatomic molecules.*

### 1.1.7 The Jablonski Diagram

Absorption of radiation by a molecule in its ground state,  $S_0$ , can depending on the frequency,  $\nu$ , lead to population of vibrational levels in  $S_1, S_2 \dots S_n$  states. In figure (1.5), the  $\nu = 2$  of the  $S_2$  level is shown. In solution rapid vibrational relaxation, VR, occurs dissipating this excess vibrational energy with a rate constant in the region of  $10^{11} - 10^{13} \text{ s}^{-1}$ , resulting in the population of the lowest vibrational level of the electronically excited state - here,  $\nu = 0$  of the  $S_2$  level. This may undergo internal conversion, IC, yielding an isoelectronic vibronic level in the  $S_1$ . Again rapid vibrational relaxation occurs to give the lowest vibrational level of  $S_1$ . Deactivation from this energy level can occur by four mechanisms:

1. Fluorescence
2. Internal Conversion, IC
3. Intersystem Crossing, ISC
4. Photochemical processes; yielding products

If ISC occurs to populate the lowest triplet state  $T_1$ , rapid vibrational relaxation occurs resulting in the population of the lowest vibrational level of the  $T_1$  state, where deactivation can occur via three mechanisms:

1. Phosphorescence
2. Intersystem Crossing, ISC
3. Photochemical processes; yielding products

The above deactivation routes can be classified as either being radiative, or non-radiative transitions.

### 1.1.8 Radiative Transitions

*Fluorescence* is a spin allowed process that occurs between states of the same multiplicity. Excitation to  $S_1$  state of an organic molecule in solution may be followed by the emission of fluorescence accompanying the  $S_1 \rightarrow S_0$  transition. Since fluorescence is strongly allowed, it occurs on relatively fast timescales; with a rate constant in the region of  $10^6$ - $10^9$   $s^{-1}$ . The magnitude of this rate constant explains why in most cases, fluorescence does not occur from higher excited states since internal conversion with rate constants in the region of  $10^{12}$   $s^{-1}$  will compete effectively. Experimental observations can be generalised into a set of rules as follows:

1. Kasha's rule [1]: Radiative processes occur from the lowest electronic state of a given spin multiplicity, independent of the energy of the electronic state excited initially.
2. Vavilov's law: The fluorescence quantum yield,  $\phi_f$ , is independent of the energy of the electronic state excited initially, *i.e.* independent of excitation wavelength.

There are exceptions to these rules: notably azulene and related compounds have been shown to fluoresce from  $S_2 \rightarrow S_0$ .

*Phosphorescence* is the radiative transition that occurs between states of different multiplicity; the most common being from the  $T_1 \rightarrow S_0$ . The forbidden nature of the transition ( $\Delta S = 1$ ) does not mean phosphorescence cannot be observed since spin-orbit coupling encourages the mixing of singlet and triplet states - with the result that otherwise forbidden transitions become weakly allowed. The resulting phosphorescence transition is much less intense than the corresponding fluorescence transition, and occurs with an extremely long radiative lifetime  $10^3$ - $10^4$  sec. Allowing collisional electronic vibrational energy-transfer with solvent molecules to compete favourably with the radiative deactivation of the excited triplet states - which is why with the exception of a few compounds such as biacetyl, phosphorescence is rarely seen in fluid solution, but is more commonly associated with rigid media where diffusion of solvent molecules and quenching cannot occur.

### 1.1.9 Non Radiative Transitions

*Internal Conversion* (IC) is a radiationless transition that occurs between states of the same multiplicity. Internal Conversion occurs from the vibrationless level of the higher state to an isoenergetic vibrational level of the lower state, this results in the molecule having some excess vibrational energy above the lowest vibrationless level. In solution phase this excess energy is rapidly dissipated by collisions with solvent molecules; a process referred to as vibrational relaxation (VR). The rate of IC is governed by the energy gap between the initial and final states involved - the smaller the energy gap the higher the rate. The rate of IC from high energy excited states *i.e.*  $S_2 \rightarrow S_1$  or  $T_2 \rightarrow T_1$  is rapid with an associated rate constant of  $\sim 10^{12} \text{ s}^{-1}$ . Internal conversion between  $S_1$  and  $S_0$  however, is slow due to a much larger energy separation; this allows fluorescence and inter-system crossing to compete favourably.

*Intersystem crossing* (ISC) is a radiationless transition that occurs between electronic states of different spin multiplicity. The two most important transitions being  $S_1 \rightarrow T_n$  and  $T_1 \rightarrow S_0$ . The former occurring from the zero point vibrational level of  $S_1$  to an isoenergetic level of  $T_1$  or some higher excited triplet level *i.e.*  $S_1 \rightarrow T_n$ . The

efficiency is determined by the energy gap ( $\Delta E_{S-T}$ ). ISC can occur via a spin-orbit (S-O) coupling mechanism. When the energy gap is small the process is efficient and proceeds at a rate similar to that of fluorescence, *i.e.*  $10^6 - 10^9 \text{ s}^{-1}$ . The presence of heavy atoms can greatly enhance S-O coupling and therefore enhance the rates of ISC transitions.

These processes are the possibilities that occur intramolecularly. Another important phenomenon in photochemistry is the transfer of energy between electronically excited donor molecules and molecules of another species in their ground states. This is known as intermolecular energy-transfer, and the various processes of quenching are described below:

### 1.1.10 Intermolecular Electronic Energy-Transfer Processes

The transfer of energy from an electronically excited donor  $D^*$  to an acceptor molecule A usually in its ground state can be represented by equation (1.6):



This process can result in a "photosensitization" reaction. A becoming "sensitised" to a wavelength of radiation absorbed not by A but by D. Thus, the physical requirement that the molecule of interest absorb the wavelength of radiation being provided in a photochemical experiment, can be relaxed if a suitable sensitizer can be found. Energy-transfer mechanisms are usually classified according to the initial spin multiplicity of  $D^*$  and the final spin multiplicity of  $A^*$ . For example, the process shown in equation (1.7) is termed "triplet-triplet" energy transfer.



There are a number of different mechanisms by which energy transfer can occur:



## Radiative Energy Transfer

*Radiative energy transfer* involves the emission of a photon from the initially excited molecule  $D^*$  and its re-absorption by the molecule A - as represented below:



This process is sometimes referred to as "trivial". The mechanism requires that the emission spectrum of  $D^*$  must overlap with the absorption spectrum of A. The efficiency will be dependent on the degree of overlap of these spectra and on the strength of the transitions.

## Long-Range Coulombic Energy Transfer

As  $D^*$  and A are brought together in solution, they feel each other's presence due to long range coulombic forces experienced by their charge clouds. As  $D^*$  and A approach, the  $D^*$  dipole (excited electron) LUMO (Lowest Unoccupied Molecular Orbital) interacts with the A dipole (an unexcited electron in the HOMO), the resulting dipole-dipole interaction can cause the electron in the HOMO of A to oscillate more violently - therefore becoming more energetic. This may lead to the excitation of the electron in the HOMO of  $D^*$  to be promoted to the LUMO of A (provided this is not greater in energy than the HOMO of  $D^*$ ) - with a corresponding de-excitation of the excited electron on  $D^*$ . This process is shown schematically in figure (1.6).

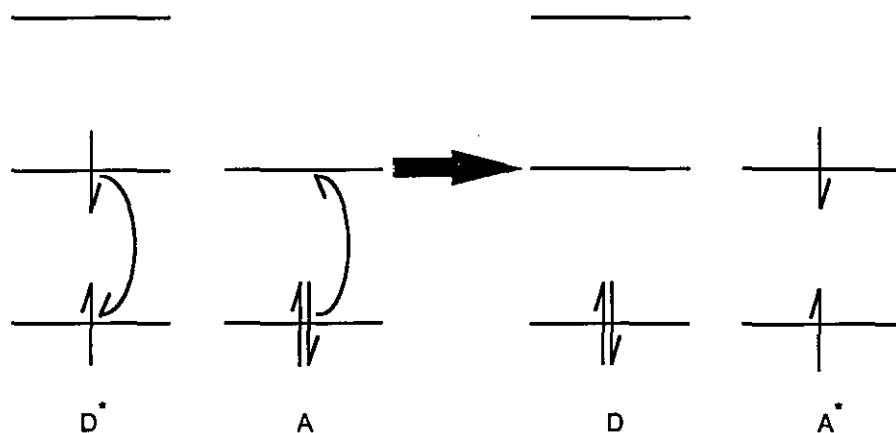


**Figure (1.6)** Energy level diagram showing electron movements in long-range Coulombic energy transfer.

The end result of this is that  $D^*$  has become de-excited and has returned to its ground electronic state,  $D$ , with a simultaneous excitation of  $A$  to  $A^*$ . Energy has been transferred despite the fact that the two species have not come into close contact, *i.e.* no spatial overlap occurs between the clouds of  $D^*$  and  $A$ . Since no actual physical contact is required, energy transfer may take place over distances considerably greater than the molecular radii. Förster [2] obtained the following expression for the rate of energy transfer for a dipole-dipole mechanism:

$$k_{EN}(\text{Coulombic}) = K \frac{\kappa^2 k_D^0}{R_{DA}^6} J(\epsilon_A) \quad (1.10)$$

where  $K$  is a constant accounting for the refractive index of the medium between  $D^*$  and  $A$ ,  $\kappa$  is an orientation factor which accounts for the directional nature of the dipole-dipole interaction, and for a solution containing randomly orientated molecules  $\kappa^2$  has a value of  $2/3$ ,  $k_D^0$  is the radiative rate constant for the decay of the donor,  $R_{DA}$  is the molecular separation and  $J(\epsilon)$  is the spectral overlap integral.

Coulombic energy transfer is subject to strict spin selection rules, and are those that apply to molecules individually: which state that there should be no change in spin

multiplicity of either species. The energy transfer processes favoured by the Coulombic mechanism are, therefore:



### Short-Range Electron-Exchange Energy Transfer

In contrast to energy transfer by a Coulombic mechanism, energy transfer by electron exchange requires that the donor and acceptor are sufficiently close together ( $\sim 1$ - $1.5$  nm), to allow the electron clouds to overlap and an exchange of electrons to take place. The exchange transfer mechanism occurs when the excited electron on  $D^*$  transfers into the LUMO of A with a simultaneous transfer of an electron from the HOMO of A into the corresponding orbital on D, as shown in figure (1.7).

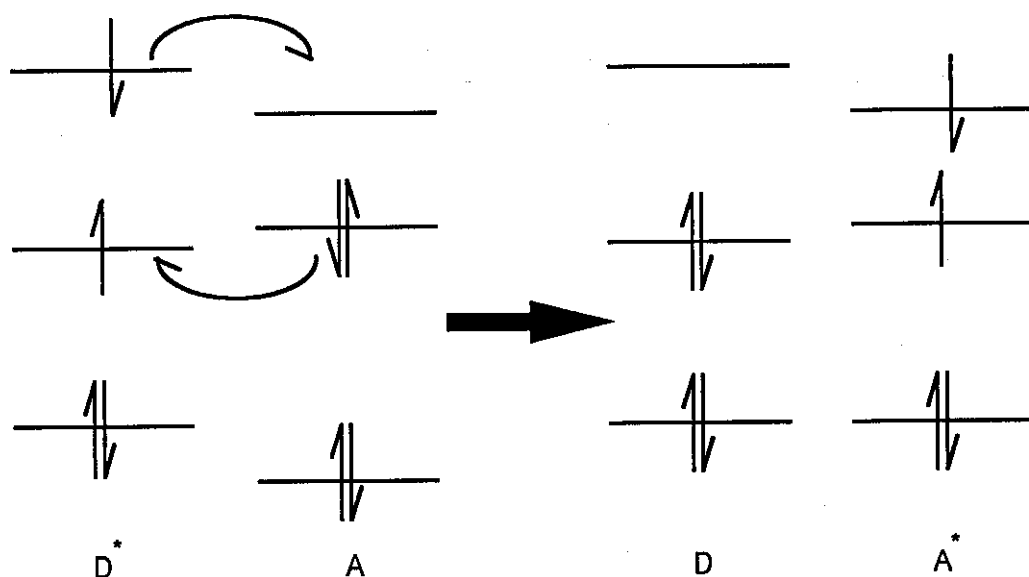
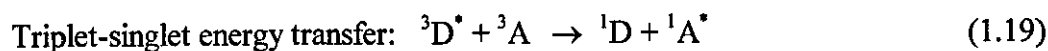
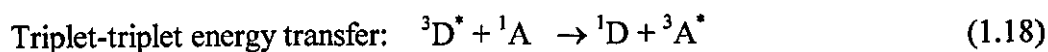
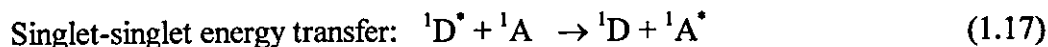


**Figure (1.7)** Energy level diagram showing electron movements in electron-exchange energy transfer.





Molecular oxygen is the most common candidate for  ${}^3\text{A}$ , the ubiquitous nature of oxygen means that it plays a prominent role in photochemistry. Discussed below are the principal reactions of oxygen in photochemical reactions.

### 1.1.11 Quenching by molecular oxygen

Unlike any other homonuclear diatomic molecule having an even number of electrons, oxygen is paramagnetic in its ground state. A simple molecular orbital diagram using the linear combination of atomic orbitals is shown in figure (1.8).

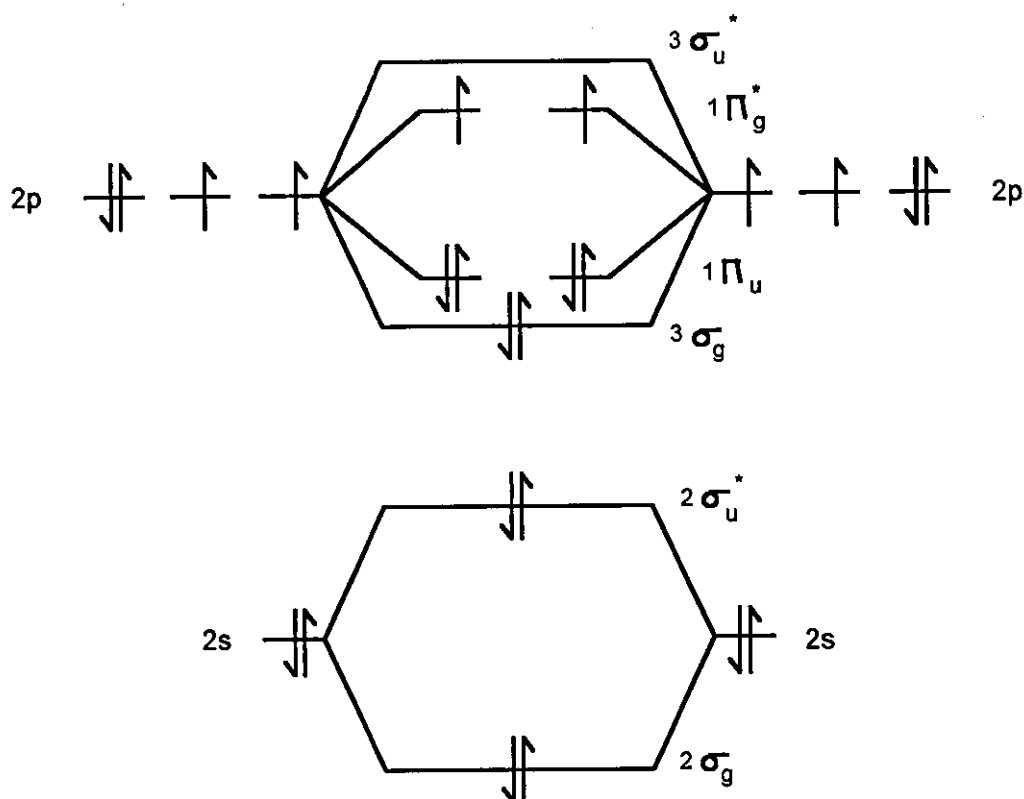
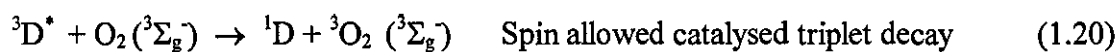


**Figure (1.8)** *Molecular orbital diagram for ground state molecular oxygen.*

The two highest energy unpaired electrons appear in degenerate  $1\pi_g^*$  orbitals, these electrons are of the same spin and hence the ground state of oxygen has triplet multiplicity and has the group theoretical symbol  $^3\Sigma_g^-$ . There are two possible arrangements of the electrons in the  $1\pi_g^*$  orbitals: they can be spin paired in the same orbital or the electrons can be spin paired in separate orbitals. These two electronically excited singlet states of oxygen are known  $^1\Delta_g$  and  $^1\Sigma_g^+$  states respectively and lie 94 and 157 kJ mol<sup>-1</sup> respectively above the ground  $^3\Sigma_g^-$  state. In condensed media, the lifetime of  $O_2^*$  ( $^1\Sigma_g^+$ ) is short due to rapid relaxation to the state  $^1\Delta_g$ . It is the  $^1\Delta_g$  state which is referred to as 'singlet oxygen' because the reactivity of singlet oxygen is almost exclusively observed from this state due to its appreciable lifetime. The most common way of generating singlet oxygen is via organic dye sensitised energy transfer to ground state molecular oxygen. The triplet-singlet energy gap for molecular oxygen results in ground state molecular oxygen quenching the lifetime of almost all the lowest lying triplet states as shown in equations (1.20) and (1.21):



Quenching of excited singlet states can also occur if the excited singlet lifetime is long or a high concentration of oxygen is present according to the equations:



where  $O_2^*(^1\Delta_g)$  represents singlet oxygen.

Reaction (1.23) can only be seen if the singlet-triplet energy gap exceeds 95 kJ mol<sup>-1</sup>, the (0,0) excitation energy of singlet oxygen.

### 1.1.12 Singlet Oxygen

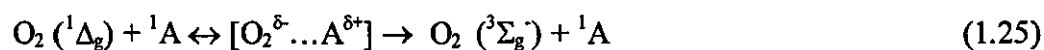
As can be seen not all of the quenching processes lead to the production of singlet oxygen. The overall quantum yield of singlet oxygen production will be given by the sum of the yields of production from oxygen quenching of both the first excited singlet and triplet states:

$$\phi_{\Delta} = \phi_{\Delta}(S_1) + \phi_{\Delta}(T_1) \quad (1.24)$$

The quenching of singlet oxygen may be due to chemical reaction or physical quenching. The principal mechanisms for physical deactivation in fluid solution are outlined overleaf.

**Solvent Quenching:** The lifetime ( $\tau_{\Delta}$ ) of singlet molecular oxygen in solution is extremely variable depending upon the solvent employed. For instance the weak emission at 1270 nm has a maximum lifetime of 28 ms in  $\text{CCl}_4$ , whereas in solvents such as water, hydrocarbons and alcohols this is drastically shortened to a few tens of microseconds. This is thought to be directly related to the absorption of the solvent at 1270 nm, the greater the absorption here the shorter the singlet oxygen lifetime, suggesting that the deactivation route of singlet oxygen is via direct conversion of its electronic excitation energy into vibrational energy in the solvent. This can be demonstrated upon the deuteration of solvents, which reduces the infra-red absorption at 1270 nm so as not to facilitate such an energy transfer, and correspondingly increases considerably the lifetime of singlet oxygen.

**Charge-Transfer quenching:** Quenching of singlet oxygen via a charge transfer or partial charge transfer exciplex by certain compounds such as sulphides, phenols and amines has been suggested, the general mechanism proposed may be represented as:



**Energy Transfer quenching:** The quenching of singlet oxygen in fluid media via the energy transfer mechanism shown in the equation below has been documented for a number of compounds.



The acceptor A is required to have a triplet energy of less than or approximately equal to  $95 \text{ kJ mol}^{-1}$ . The most studied of such compounds is  $\beta$ -carotene having a low lying triplet state ( $88 \text{ kJ mol}^{-1}$ ) [5] and has been widely demonstrated to quench singlet oxygen via electronic energy transfer.

The spontaneous radiative deactivation of singlet oxygen ( ${}^1\Delta_g$ ) to the ground state, producing phosphorescence as shown below:



The above is an inefficient process with a low phosphorescence quantum yield which emits in the near infrared region of the spectrum. It is possible to detect the decay of singlet oxygen luminescence by the development of I-R sensitive germanium photodiodes; allowing detection of this process directly under many experimental conditions.

Details of such apparatus are discussed in the experimental chapter (section 3.4).

Once a molecule has absorbed a photon of UV-VIS radiation and has become excited, the next step is to follow the fate of the excited species. The excited state can last anything from a few seconds down to femtoseconds. Studies on extremely short lived excited states can be carried out thanks to a technique known as flash photolysis - developed in 1949 by a British chemist called George Porter [6] who shared the 1967 Nobel Chemistry Prize for the study of ultra-fast chemical reactions with the German Manfred Eigen and fellow Briton Ronald Norrish.



Principally flash photolysis is an experiment in which a large initial concentration of electronically excited molecules is produced by an intense burst of radiation. The subsequent decay of the excited state may be followed by detection of its emission, or by monitoring its absorption by using a second (often continuous) light source operating at the appropriate wavelength. Experimental details of flash photolysis will be discussed in much greater depth in section 3.3. An important requirement for a photochemical experiment is that the light source must produce a pulse of radiation that lasts for a much shorter time than that of any subsequent processes that we wish to monitor, and ideally be of just one wavelength, these requirements are met by laser light. The special and unique properties of laser light are outlined below.

## 1.2 LASER LIGHT

**Coherence:** Laser light is composed of regular and continuous waves, it is both temporally and spatially coherent. Temporal coherence means that it is nearly a single frequency *i.e.* the spread in frequency or line width is small. If the wave holds its shape with time it is said to be spatially coherent. In contrast ordinary light is incoherent; producing waves over a wide range of frequencies as a result of the random process of spontaneous emission.

**Directionality:** Laser light is highly directional, having a low level of divergence, which allows the beam to be focused on a spot of very small dimensions.

**Monochromaticity:** Most sources of light are white (polychromatic), whereas laser light is monochromatic.

### 1.2.1 Historical Development

The development of laser light had its origins with the work of Einstein who advanced the concept of stimulated emission of radiation in 1917 [7]. This concept of stimulated emission was only used in theoretical discussions, it was not for about 30 years that practical application of this concept was put into practice. Several proposals were

followed for using stimulated emission as a means of amplification, but it was Gordon, Zeiger and Towns [8] who in 1953 obtained continuous micro-wave amplification and oscillation within an ammonia molecule. This device was given the acronym MASER (Microwave Amplification by the Stimulated Emission of Radiation). It was six years later that the same principle was applied to coherent radiation in the visible region, in the form of Maiman's ruby laser [9]. This was soon followed in 1961 by the gas laser of Javan, Bennett and Herriot [10] and the semiconductor laser in 1962. The term LASER is an acronym for Light Amplification by the Stimulated Emission of Radiation. With an atom having only two possible energy states, an upper state  $E_2$  and a lower state  $E_1$ , absorption of radiation can occur if the energy of the photon is such that it exactly matches the energy gap in the molecule *i.e.*  $h\nu = E_2 - E_1$ . Once an atom has absorbed a photon the reverse process can also take place *i.e.* the atom can change from the high energy state to a low energy state with the emission of a photon. An important feature of this emitted light is that there are two processes at work; it was Einstein who showed that emission can be *spontaneous* and *stimulated*. The former is a random process and does not require the presence of radiation, whereas, the latter is found only in the presence of radiation; a photon having an energy equal to the energy difference between the two levels interacts with the atom in the excited state causing it to relax to the lower state with the emission of a second photon. Importantly, the photon emitted travels in the same direction as the stimulating photon. The three radiative processes are shown in figure (1.9).

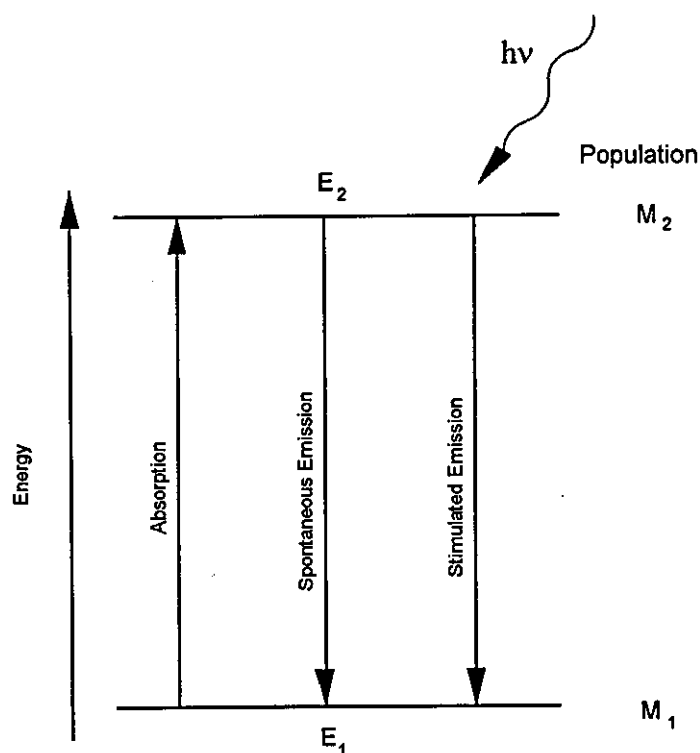
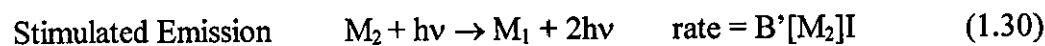
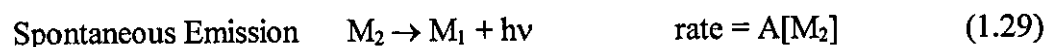
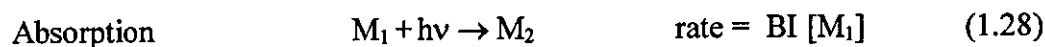


**Figure (1.9)** Schematic representation of the three radiative processes that can occur in a non-degenerate two level energy system.

and can be represented by the following equations and rates:



where  $M_1$  and  $M_2$  are molecules in lower and upper states respectively and  $I$  is the intensity of radiation. The coefficients  $B$ ,  $A$  and  $B'$  were investigated in 1917 by Einstein and are known as the Einstein coefficients, he showed that  $B$  and  $B'$  are in fact identical so the same term can be applied to both. From these expressions the rate of absorption of radiation is given by:

Rate of change of absorption:	$I = -BI[M_1] + A[M_2] + BI[M_2]$	(1.31)
-------------------------------	-----------------------------------	--------

Which can be simplified to:	$I = BI( [M_2] - [M_1] ) + A[M_2]$	(1.32)
-----------------------------	------------------------------------	--------

Under normal circumstances stimulated emission is unlikely to occur, making the  $M_2 + h\nu \rightarrow M_1 + 2h\nu$  encounter of low probability. Therefore the last term in the equation (1.32) being negligible can be ignored giving:

$$I = BI ([M_2] - [M_1]) \quad (1.33)$$

The term  $[M_2] - [M_1]$  is influenced by the Boltzmann distribution which says that the populations will be biased towards the ground state *i.e.*  $[M_2] < [M_1]$ , this being negative shows that the net process is one of absorption. If however it could be arranged for  $[M_2] > [M_1]$  - a situation known as a population inversion, the net process would be emission rather than absorption *i.e.* the sample would emit more light than what was shined on it. Furthermore, if the emitted radiation is '*fed back*' into the system, further emission by the process of stimulated emission of light can occur *i.e.* the light is amplified.

To create a population inversion energy must be supplied to the system. Obviously supplying the system with heat will just increase the population of all levels. Population inversion is achieved by two main methods; one is by passing an electrical discharge through a gas causing ionisation. Examples of these types are: Helium-Neon, Carbon Dioxide and the Argon laser. Alternatively, energy in the form of light can be supplied; this is termed optical pumping and is generally applicable to solid-state lasers. A flash tube is the usual source, discharging photons with energies corresponding to the excited states creating a high density of these excited states.

The above discussion is based on a simple two-level energy system, the difficulty with the two-level arrangement is that any pumping which raises atoms from the lower level to higher, tends almost equally to lower atoms from high to low. The best that can be achieved is to raise 50% of the atoms to the upper level. As of yet no two-level laser has been made, however in three and four level laser systems population inversion is more easily achieved.

## 1.2.2 Solid State Lasers

The first laser, the ruby laser of Maiman is an example of a three level system, a simplified energy level diagram is shown in figure (1.10).

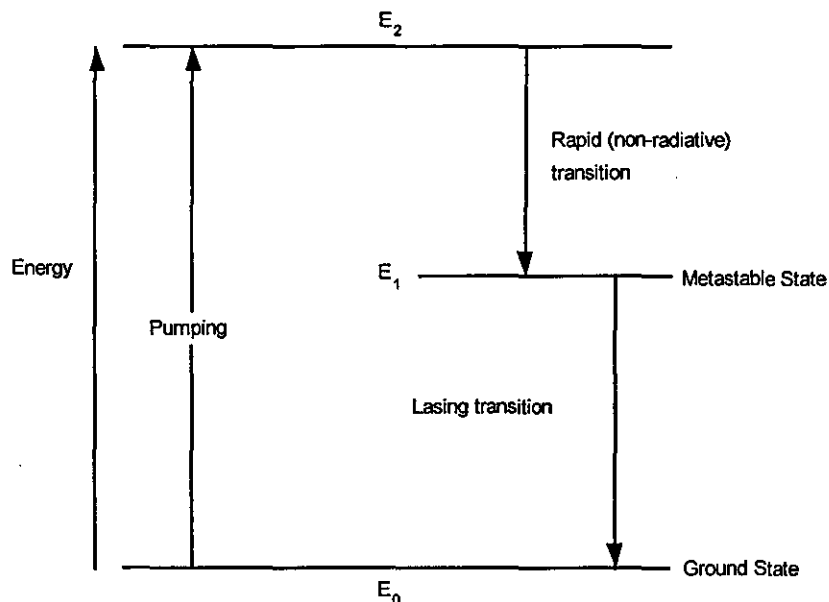
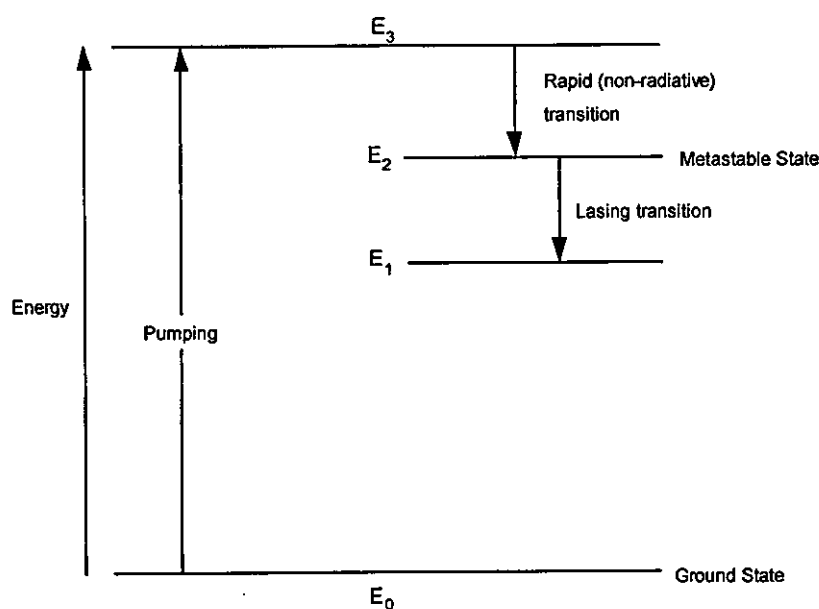


Figure (1.10) Schematic Representation of the three-level Laser.

Ruby is sapphire ( $\text{Al}_2\text{O}_3$ ), containing a small amount of chromium in the form of  $\text{Cr}_2\text{O}_3$ , it is the  $\text{Cr}^{3+}$  ions that are excited to an upper state  $E_2$  by an intense flash of white light. Instead of remaining here fast relaxation occurs to a middle state  $E_1$  by a radiationless transition. Once an atom reaches this middle state it spends an unusually long time there before dropping down by spontaneous emission, to the ground state. States such as this are termed metastable and it is because of this characteristic that the population of the middle state builds up while the ground state is depleted, *i.e.* a population inversion has been achieved. However in a three level laser the method of obtaining population inversion between the middle and ground state is somewhat inefficient. This is because the middle state is effectively empty at the start of the pumping as a result of the Boltzmann distribution, at least half the population of the ground state molecules must be pumped into the middle level before population inversion is achieved. A more recently developed laser is the Neodymium laser, which

employs the triply charged ion of the rare earth metal neodymium ( $\text{Nd}^{3+}$ ), in yttrium aluminium garnet (YAG). The neodymium laser is a four-level system and is the most widely used solid state laser, its major advantage over the ruby laser is its lower lasing level is above its ground state.



**Figure (1.11)** Schematic representation of the four - level laser.

In the four-level laser as shown in figure (1.11) atoms in the ground state  $E_0$  are pumped to the highest level  $E_3$  from which they descend non-radiatively, to the metastable state  $E_2$ . Providing level  $E_1$  is sufficiently high above the ground state then it will be effectively empty and so a comparatively small population in  $E_2$  is needed to ensure a population inversion between  $E_2$  and  $E_1$ , laser action can therefore take place between these levels. It is this type of laser which is employed in Loughborough for flash photolysis experiments, detailed explanation of the laser set up is given in the experimental chapter (section 3.3).

# Chapter 1

## References

- [1] Kasha M., *Discuss. Faraday Soc.*, **9**, 14, (1950)
- [2] Foster T., *Discuss. Faraday Soc.*, **27**, 7, (1959)
- [3] Dexter D.L., *Chem. Phys.*, **21**, 836, (1953)
- [4] Wigner E.P., *Z. Physik Chem.*, **23B 28**, (1933)
- [5] Herkstroeter, W.G., *J. Am. Chem. Soc.* **97**, 4161 - 7 (1975)
- [6] Norrish R.G.H. and Porter G., *Nature*, **164**, 158 (1949)
- [7] Einstein A., *Phys. Z.*, **18**, 121 (1917)
- [8] Gordon J.P., Zeiger H.J. and Townes C.H., *Phys. Rev.*, **99**, 4, 1264, (1955)
- [9] Maiman T.H., *Phys. Rev.*, **123**, 1145, (1961)
- [10] Javan A., Bennett W.R.Jr. and Herriott, D.R., *Phys. Rev. Lett.*, **6**, 106 (1961)

## **CHAPTER 2**

**Photoallergy, 3,3',4',5 - tetrachlorosalicylanilide  
Chemistry and Serum Albumin**



## 2 Photoallergy and 3,3',4',5 - tetrachlorosalicylanilide Chemistry

### 2.1 Introduction

Many substituted salicylanilides, particularly halogenated salicylanilides, have aroused great interest because of their fungicidal and germicidal properties - it was to make use of their potent anti-bacterial properties that salicylanilides like 3,3',4',5-tetrachlorosalicylanilide (T<sub>4</sub>CS-H) have in the past been widely employed as antiseptics and bactericides - commonly used in soaps and deodorants. Unfortunately, after passing the conventional toxicological screening tests and being marketed, they were soon found to lead to photoallergy [1 - 3], causing serious adverse skin reactions. Although most photoallergens will elicit a response in only a small fraction of those exposed [4], tetrachlorosalicylanilide is unusual in being capable of inducing photoallergy in a very high fraction of those exposed. This photoallergy is believed to be brought on by the influence of UV light on the anion of tetrachlorosalicylanilide (T<sub>4</sub>CS<sup>-</sup>) with human skin leading to photodermatitis. Users of these soaps developed an incapacitating photodermatitis after a brief exposure to sunlight, in some cases the skin remained abnormally sensitive to sunlight for months or years after termination of all known contact with the photosensitiser [5]. Cutaneous photosensitivity to tetrachlorosalicylanilide and other salicylanilides is generally accepted as a drug-induced photoallergy. Based on clinical observations and results with experimental animals, this disease has been determined to be an immunologic reaction of the delayed hypersensitivity type. The major difference between contact sensitivity and photoallergy is that light exposure is a necessary prerequisite for the photoallergic response.

Photoallergy can be defined as an acquired altered reactivity of the skin to light in the presence of a photosensitizer [6]. Photosensitivity is a term to describe abnormal or adverse reactions to light energy. Photosensitisers can either be photoallergic or phototoxic in action - the majority of photosensitisers are phototoxic in action. It is

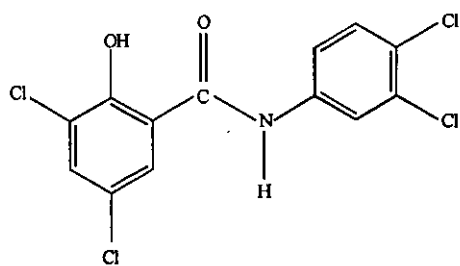
important to distinguish photoallergy from this far more common cutaneous photosensitivity condition, since these two conditions are hard to distinguish clinically.

## **2.2 Photoallergy Vs Phototoxicity**

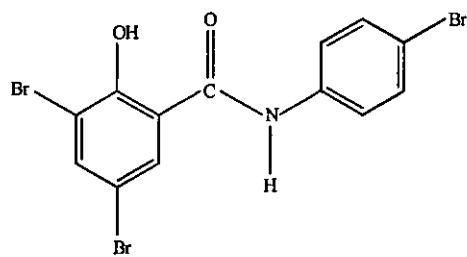
As already stated phototoxicity is much more common than photoallergy - indeed the ordinary sunburn reaction falls into this category. A phototoxic response can be elicited from all individuals if enough light energy of the appropriate wavelengths, and in the case of the photosensitised system, enough of the photosensitiser is present in the skin. Thus, phototoxic responses can be likened to primary irritant reactions, they are characterised by erythema and at times edema occurring within a few minutes to several hours after exposure followed by hyperpigmentation and desquamation confined to the exposed areas. The histology may well show a severely damaged epidermis, particularly if the sensitiser is applied to the skin. In contrast photoallergic reactions are generally uncommon, and where data is available it appears that only a small percentage of an exposed population is susceptible to each photoallergen. The clinical patterns range from immediate urticarial to delayed papular and eczematous lesions. In general less energy is required to induce a photoallergic response than a phototoxic lesion dependent on the same spectrum. The histology is also different - details are given in an excellent review article on photoallergy by J.H. Epstein [6].

## **2.3 Photoallergic compounds**

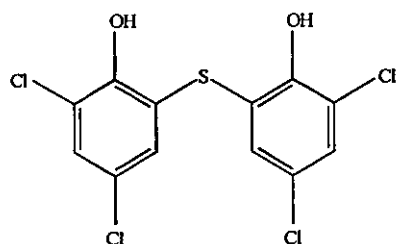
Listed in figure (2.1) are the chemical structures of several known photoallergens with the appropriate reference to their photoallergy indicated in brackets. The best established photoallergic compounds include several halogenated salicylanilide derivatives, most important being tetrachlorosalicylanilide in that it gives the strongest photoallergic response.



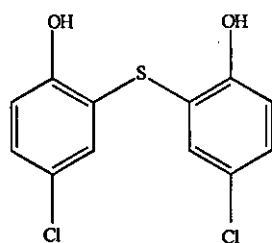
3,3',4',5'-Tetrachlorosalicylanilide [7]



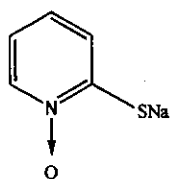
3,4',5-Tribromosalicylanilide [8]



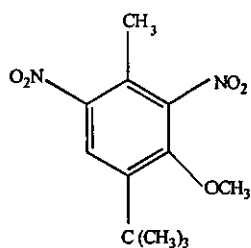
Bithionol [9, 10]



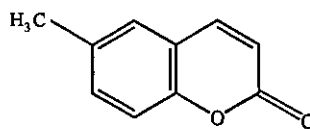
Fentichlor [10 - 12]



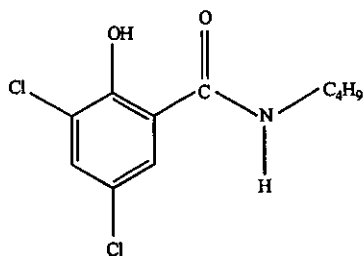
Omadine (Na salt) [13]



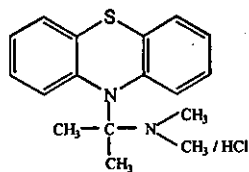
Musk Ambrette [14]



6-methylcoumarin [15]



Buclosamide [16]



Promethazine [17]

**Figure (2.1)** Structures of well-known photoallergens with appropriate reference to their photoallergy in brackets.

The above includes agents used for their antibacterial, antifungal and tranquilliser properties. Structurally, there is some diversity amongst this group of compounds, but obvious features include aromatic rings and in many cases the presence of halogen atoms. However, it must be noted that cellular metabolism may convert these compounds into the actual photoallergic species. The ground state absorption spectrum of all these compounds extends into the UVA (320 - 400 nm) part of the spectrum.

## 2.4 Photoallergic Drug Reaction

The observed skin responses to photoallergic compounds and the appropriate wavelengths of light, are believed to result from a delayed hypersensitivity response to an antigen formed in the skin when certain chemicals penetrate the skin, absorb light and bind to protein. This can lead to a photoallergic response occurring by the pathway shown below [18]:

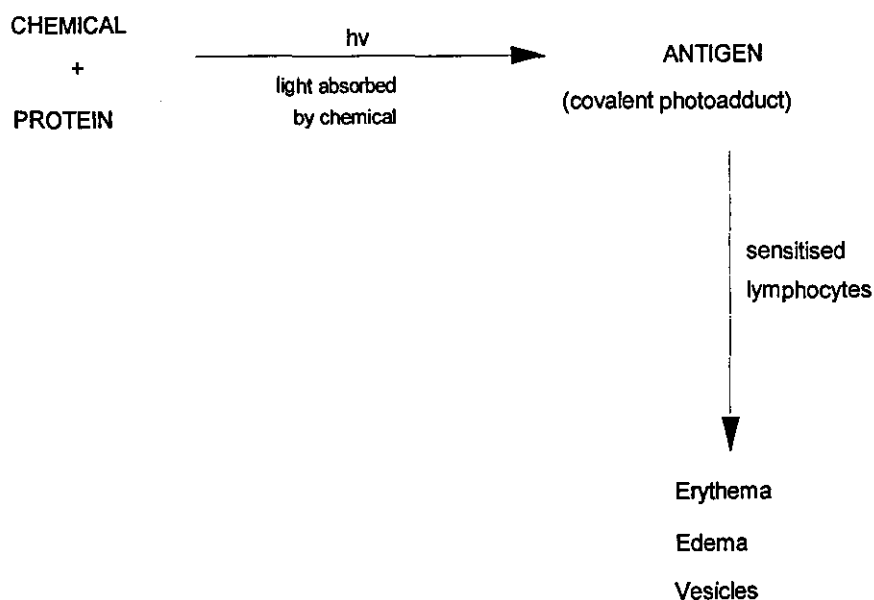


**Figure (2.2)** *Proposed pathway leading to a photoallergic response.*

In photoallergic reactions the photochemical process plays the role of an initiator, *i.e.* light from the sun, whereas the host's own immunologic mechanism may play the role of the effector. The two primary problems in the understanding of photoallergic mechanisms concern the definition of the nature of the antigens (an antigen is a substance that stimulates the production of an antibody) and the antibodies involved.

#### **2.4.1 Requirements for a Photoallergic response**

The first requirement for a photoallergic compound is that it must be able to be adsorbed into the skin, *i.e.* penetrate the skin from the outside or from the interior of the body and remain there long enough for photochemical reaction to take place. Once adsorbed, it or its metabolite must absorb light striking the skin. This absorption of light is followed by a structural change in the substance, to produce a reactive species. The product of this reaction fulfils the structural requirement to be able to bind covalently to protein(s) for the formation of an allergen. Contrast this with many phototoxic compounds that react upon irradiation, producing singlet oxygen, which consequently can produce cellular damage such as oxidation of amino - acid residues.

UV radiation in the UVA and UVB penetrates to various depths in the skin, depending upon the wavelength [19]. So the location at which photochemical reaction takes place will very much depend upon the ground state absorption spectrum of the photoallergic species. Because albumin is a soluble protein present in the skin in a reasonably high concentration it is considered a likely candidate for the carrier protein of the antigen.

#### **2.5 Photodermatitis due to Tetrachlorosalicylanilide**

Late in 1960 there occurred the first of a series of acute photodermatitis due to tetrachlorosalicylanilide, affecting initially a total of 53 people [7], twenty-four of these were hospital cases. Typically, the onset of the dermatitis occurred after the patients had long spells out in the open. The symptoms the patients suffered were: swelling and redness of the skin, erythema, scaling and oedema. In many cases relapses would

occur days later. What was significantly striking, was that the dermatitis was entirely confined to the light-exposed areas, however all light-provoked patch tests proved negative, as were provocative drug tests. Around the same time similar symptoms occurred in a group of factory workers, affecting an eventual total of 27 individuals. It was initially supposed that the manner of the factory work - treating metal at high temperatures with the release of hydrocarbons may be in some way connected with the resulting dermatitis - numerous samples were taken for testing. It was however, noticed that the washing rooms were stacked with bars of a popular germicidal soap. This soap was used rather prodigiously owing to the dirty nature of the men's work, and that the affected men usually reported on Mondays, having become worse at the weekends. Furthermore it was particularly brought to attention that several instances of severe recurrences occurred over the holiday period when the men were away from work. Patch tests against dilutions of suspected oils proved negative. However, it was rather fortuitously discovered in the course of the investigation that a solution of the aforementioned soap was fluorescent. A patch test using 1% solution of the soap was the only sample to give an unequivocal positive result. Further hospital cases revealed that affected patients used the very same soap, therefore, it soon became clear that the debilitating dermatitis was connected with the use of this germicidal soap. Enquiries at the manufacturers revealed that a new germicide: tetrachlorosalicylanilide had been incorporated into the soaps.

Tetrachlorosalicylanilide was developed as a deodorant and bacteriostatic agent, having a wide range of activity against skin organisms. It was patented in the United States in 1955, and had been used in several consumer, industrial and detergent preparations in Great Britain and the United States. The outbreak of photodermatitis caused by tetrachlorosalicylanilide was at the time surprising; the halogenated salicylanilides were not hitherto regarded as photosensitisers, though halogen-substituted fluoresceins had been shown to be photodynamic substances [20]. Indeed tetrachlorosalicylanilide had passed the conventional toxicological screening tests; preliminary patch tests [21, 22] suggested that it was no more an irritant or potential sensitiser than comparable concentrations of bisphenols.

Now it was recognised that the culprit of the incapacitating photodermatitis after relatively brief exposure to light was tetrachlorosalicylanilide, further work on the photochemical behaviour was carried out to try to gain an insight to understanding the problem. In some people the skin remains abnormally sensitive to light for months or even years after all known contact with the offending compound has ceased. Patients suffering these symptoms are known as 'persistent light reactors' or PLR, a term coined by Jillson and Baughman [9] to describe patients suffering from this as a result of photosensitisation to bithionol.

Willis and Kligman [5] carried out *in vivo* experiments to investigate this PLR effect, they carried out phototests at different time intervals after the application of a 1% concentration of the various photosensitisers to human skin. At intervals of two weeks, the patch sites were uncovered and exposed to 3 minutes of radiation, the experiment was carried through for a total of ten weeks. The results showed that for every subject that was exposed to tetrachlorosalicylanilide or tribromosalicylanilide (TBS-H) the skin remained strongly photoreactive for the duration of the experiment *i.e.* up to at least ten weeks after a single application, and significantly there was no great decrease in the intensity of reaction during this time. The blank unirradiated site proved negative, ruling out any contact allergy. Investigation was also performed on how long the reaction would persist at covered and uncovered sites. Again a 1% concentration of each photosensitiser was applied to two sites which were exposed to 3 minutes of xenon arc window glass radiation - one site was covered the other left uncovered. The results showed that when light is totally excluded the reaction does not occur beyond fifteen days. However, on uncovered sites the adverse skin reaction to tetrachlorosalicylanilide and tribromosalicylanilide still persisted from fourteen days to more than six months (six months being the *maximum* period of observation). These observations clearly show that a photoallergic response can occur under the influence of diffuse, low energy light. The persistence of the photosensitiser in the skin was ascertained by extracting dermatatic tissue with ethanol. The extracts were analysed by comparing their ground state absorption spectra and peak fluorescence bands with the authentic chemicals. These methods revealed the presence of the photosensitising compound in the extracts. In conclusion to these findings Willis and Kligman suggest

that the explanation for the PLR, is that the chemical simply remains in the skin for exceptionally long periods.

## 2.6 Photobinding to Proteins

The photochemical binding of tetrachlorosalicylanilide was first reported by Jenkins, Welti and Baines in 1964 [23]. They showed that after exposing a mixture of tetrachlorosalicylanilide and  $\gamma$ -globulin ( $\gamma$ -G) to daylight for 5 hours the eluted protein was found to produce strong fluorescence. When exposure to daylight was omitted, the eluted protein did not fluoresce strongly. Since tetrachlorosalicylanilide itself cannot be eluted, the fluorescence derived from the protein must be due to tetrachlorosalicylanilide combining with the protein via excitation by the sun's light energy to form a conjugate. Hilal [24,25] showed that upon irradiation of a solution containing tetrachlorosalicylanilide and a simple protein type compound: protamine sulphate, a complex was formed between tetrachlorosalicylanilide and protamine, again the findings were based on fluorescence measurements. Later, Kochevar and Harber [26] reported that the anion of tetrachlorosalicylanilide ( $T_4CS^-$ ) binds non-covalently to HSA in the dark, however under the same conditions binding to bovine  $\gamma$ -G did not occur. They also demonstrated the reversible nature of the dark-binding of  $T_4CS^-$  to HSA, by precipitating out the protein with alcohol and re-dissolving in buffer which resulted in a lowering of fluorescence, repetition of this process eventually removed all fluorescence. Irradiation of solutions containing  $T_4CS^-$  with HSA and  $\gamma$ -G resulted in a red shift in the fluorescence maximum in the case with HSA, but with  $\gamma$ -G the fluorescence maximum was the same as observed when irradiation was carried out in the absence of protein, indicating that no photoproduct between  $T_4CS^-$  and the  $\gamma$ -G had formed. In an attempt to determine which amino acid(s)  $T_4CS^-$  covalently binds to on the protein molecule, amino acid analysis was carried out on irradiated samples of  $T_4CS^-$  and HSA and on untreated HSA. In aerated samples it was found a 15% reduction in the histidine content of the irradiated sample, however, analysis in the absence of oxygen revealed no difference in the histidine content. Although these



results do not indicate which amino acid  $T_4CS^-$  covalently binds to, it suggests that  $T_4CS^-$  is sensitising the photooxidation of histidines in albumin.

Stimulated by this work Barrett [27] investigated the behaviour of radio labelled [ $^{14}C$ ]-tetrachlorosalicylanilide ([ $^{14}C$ ]- $T_4CS^-$ ) (labelled at the amide carbon atom) with bovine insulin, a model protein, having a low molecular weight whilst containing most common amino acids. Binding of [ $^{14}C$ ]- $T_4CS^-$  was found to be exclusive to the B-chain of the protein, digestion of this chain with trypsin showed 78% of the original activity to be associated with amino acids 1-22 of the B-chain sequence. Radio tracer techniques indicated the presence of one molecule of [ $^{14}C$ ]- $T_4CS^-$  associated with the peptide; amino acid analysis indicated that one histidine residue from the peptide was missing, presumed to be modified by the covalent binding of [ $^{14}C$ ]- $T_4CS^-$ . When the molar ratio of [ $^{14}C$ ]- $T_4CS^-$  was increased, irradiation resulted in a significant loss of phenylalanine (in addition to histidine). From these results it was concluded that the primary site of  $T_4CS^-$  to bovine insulin is at one of the histidines in the B-chain, with a secondary site at one of the phenylalanine residues. As stated previously, the work of Kochevar and Harber [26] also suggested that the covalent linkage of  $T_4CS^-$  may be close to histidine residues on the HSA molecule.

Rickwood and Barratt [28] investigated the non-covalent binding of  $T_4CS^-$  to monomer HSA. Using a nitroxide spin-label analogue of tetrachlorosalicylanilide, binding studies on enzymatically and chemically modified HSA were carried out using electron spin resonance (ESR) spectroscopy. The spin analogue used was 3,5-dichlorosalicylamido-4-(2,2,6,6-tetramethyl-piperidine-1-oxy) (DCS-TEMPO), which is shown in figure (2.3) along side  $T_4CS-H$  for comparison.

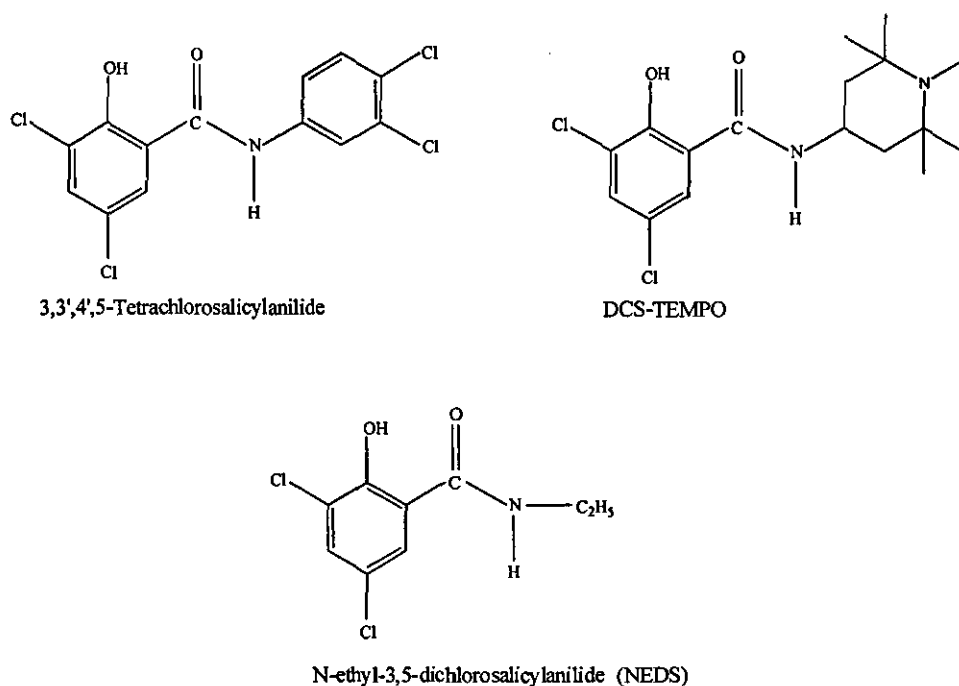


**Figure (2.3)** Chemical Structures of  $T_4CS-H$ , DCS - TEMPO and NEDS.

Kochevar and Harber [26] showed that N-ethyl-3,5-dichlorosalicylanilide (NEDS) which lacks the aniline ring of  $T_4CS-H$  (also shown in figure 2.2) was able to bind and react photochemically with HSA in a similar fashion to  $T_4CS^-$ , thus it appears that the property of photochemical reactivity towards proteins lies in the chlorinated salicyl ring of the  $T_4CS^-$  molecule and the substituted aniline ring appears to be unimportant. Therefore DCS-TEMPO was deemed a suitable substitute compound since the changes in incorporating the nitroxide radical do not alter those properties of interest. Analysing the data obtained by plotting a Scatchard plot of the binding of DCS-TEMPO to HSA monomer in the absence of UV light resulted in a single strong binding site with a binding constant of  $6.1 \times 10^6 M^{-1}$ . There also appeared to be a number of additional sites with much lower binding constants. In the same study it was found that the photochemical binding of  $T_4CS^-$  to HSA significantly reduces the extent of DCS-TEMPO binding to the protein, demonstrating that the major site of photochemical binding of DCS-TEMPO and  $T_4CS^-$  are the same. A later study [29] attempted to identify the major covalent binding site. Solutions of HSA monomer in the presence of [ $^{14}C$ ]- $T_4CS^-$  were irradiated with UV light (360nm) and subjected to

cyanogen bromide cleavage to yield two main fractions C and N. The radioactive counts showed a preference for binding to the N-fragments. On further reduction, carboxymethylation and maleylation seven characteristic cyanogen bromide peptides were produced, by far the greatest degree of radiolabelling with [ $^{14}\text{C}$ ]- $\text{T}_4\text{CS}^-$  was found in residues 124 (cys)-298 (met) of the protein molecule. The position of the covalent binding site was further narrowed down by first performing a tryptic digest which removes residues 1-181 inclusive. The main fragment from the tryptic digestion retained 90-100 % of the activity of the original complex, this then underwent cyanogen bromide cleavage 182-298 of the HSA sequence, and was found to contain 75-80 % of the recovered [ $^{14}\text{C}$ ]- $\text{T}_4\text{CS}^-$  activity; which suggested that the major covalent binding site for  $\text{T}_4\text{CS}^-$  is located between residues 182-298 of the albumin molecule. Further work was carried out on the binding of DCS-TEMPO to enzymically and chemically modified HSA [30]. This was achieved by extensive digestion of HSA with trypsin, to yield a main fragment consisting residues 182-585 of the HSA molecule. A repeat of the Scatchard plot of the binding of DCS-TEMPO to the tryptic main fragment showed a single binding site, with a binding constant of  $3.7 \times 10^5 \text{ M}^{-1}$ , which is 16-times lower than that obtained for the intact HSA. This result shows that although the major binding site is still present in the main fragment, its geometry has been considerably affected by the removal of the N-terminal region of the molecule. Further, it was shown that chemical modification of the single tryptophan (residue 214) of the HSA molecule reduced the binding constant by 60%, evidence of the proximity of this tryptophan residue to the  $\text{T}_4\text{CS}^-$  / DCS-TEMPO binding site; concurring with previous findings since the lone tryptophan residue lies between residues 182-298 of the HSA sequence.

## 2.7 The Photochemistry of Tetrachlorosalicylanilide

It was shown by Jenkins *et al* [23] that upon irradiation of 3,3',4',5-tetrachlorosalicylanilide in aqueous alcoholic phosphate buffer solution (pH = 7.3) by ultra-violet light or sunlight, decomposition to 3',4',5-trichlorosalicylanilide takes place, but no observed decomposition occurred when 3,3',4',5-tetrachlorosalicylanilide

was irradiated in aqueous alcohol alone (pH = 3.3) or in aqueous alcoholic chloride (pH = 2.2). The  $pK_a$  value of tetrachlorosalicylanilide is near 5.6, so these results suggest that it is the ionised form of tetrachlorosalicylanilide ( $T_4CS^-$ ) that is photoreactive; exchanging a hydrogen atom for the 3-chloro atom upon irradiation to give 3',4',5-trichlorosalicylanilide ( $T_3CS^-$ ). An indication of the possible mechanism was shown by the electron spin resonance spectra of tetrachlorosalicylanilide powder; which when irradiated with sunlight or ultra-violet light clearly indicated the presence of free radicals.

Coxon *et al* [31] using infrared spectroscopy to identify products from their 'nujol' mulls, irradiated twenty six different substituted salicylanilides with ultra-violet light and examined the products. It was found that 3,3',4',5-tetrachlorosalicylanilide gave 3',4',5-trichlorosalicylanilide as a product in agreement with Jenkins *et al*. So it appears that the salicylanilide loses its 3-chloro atom through some free radical mechanism. In fact all 3,5 halogen salicylanilide anions lost the 3-halogen atom on irradiation, but halogen atoms on the anilide ring were not affected by near ultra-violet radiation. The first step could be homolytic cleavage of the carbon-chlorine bond in the 3 - position to give a free radical as shown below.

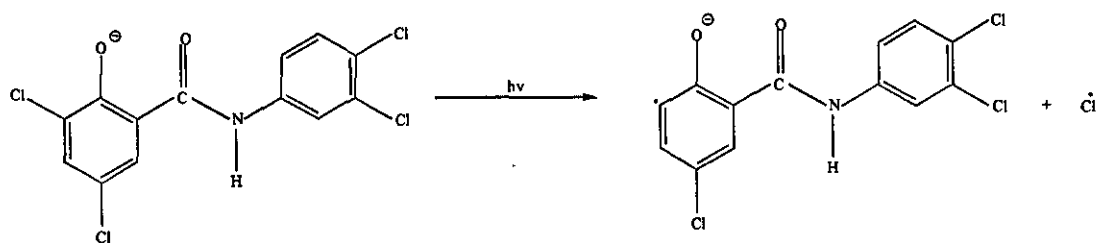
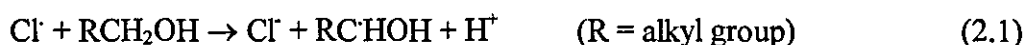


**Figure (2.4)** Irradiation of the ionised form of 3,3',4',5-tetrachlorosalicylanilide leading to homolytic cleavage of the 3 C-Cl bond to produce a free radical.

Evidence for the production of free radicals during the reaction was provided by the release of iodine when potassium iodide was added during irradiation, iodine was

not released from solutions kept in the dark. It was postulated that the initial reaction must be due to the release of halogen atoms as halide ions do not release iodine from potassium iodide. No halogen atoms are removed from unionised salicylanilides - so it appears that a phenolic oxygen atom is essential for the reaction, this could be due to inductive effects as well as hydrogen bonding - the neighbouring oxygen increasing the lability of the 3-halogen atom by induction. Morikawa *et al* [32] confirmed these findings, showing that 3,3',4',5-tetrachlorosalicylanilide undergoes a one-step photodecomposition to 3',4',5-trichlorosalicylanilide.

Davies *et al* [25] utilising 365 nm light irradiated tetrachlorosalicylanilide, and monitored the reaction by potentiometric titration of the chloride ions produced by the reaction:



They found that in 0.02 % aqueous-alcoholic solutions, one molecule of can yield not just one but up to three chloride ions depending on the initial pH of the solution, a solution buffered at physiological pH (7.4) liberated three chloride ions per molecule tetrachlorosalicylanilide photolysed. However no attempt was made to determine the products.

Epling *et al* [33] investigated the primary and secondary photoproducts of tetrachlorosalicylanilide photolysis using gas chromatography to separate the photoproduct mixture. Separation of the mixture showed the complexity of the photoreaction, although the only significant photochemical reaction involved dehalogenation. GC/MS and high field FT-NMR spectroscopy were employed, where the isolated products were compared with authentic materials so a definitive identification of the products could be made. Typically, isolated materials accounted for > 95% of the starting material. It was shown that sequential loss of more than one halogen occurred whenever the pH of the solution was sufficiently high that the anionic form of the salicylanilide was present. Solutions buffered at lower pH's underwent less secondary photodechlorinations. Preferential loss of the chlorine from

the 3-position was observed which is consistent with previous findings and with a general higher reactivity of chlorines "ortho" to a substituent [34, 35], which has been rationalised as a steric effect. The same findings were also found by Chignell and Sik [36] who photolysed 3,3',4',5-tetrachlorosalicylanilide in buffered aqueous ethanol (pH = 7.4) and found a very rapid loss of the 3 - chloro atom, followed by the much slower release of 5- and then 4'- chloro atoms to give 3'-chlorosalicylanilide as a stable photoproduct.

As already stated the first dechlorination results in the formation of 3',4',5-trichlorosalicylanilide as the primary photoproduct. Irradiation of this photoproduct was carried out in order to evaluate the chronology of dechlorination from different positions. Secondary dechlorination was found to involve a loss one of the remaining halogens, the predominant photoreaction found being the formation of 3',4'-dichlorosalicylanilide and 3',5-di-chlorosalicylanilide depending on the solvent composition, see table (2.1):

Solvent	3',4'-di-CS	3',5-di-CS
1% EtOH/H <sub>2</sub> O	27	73
5% EtOH/H <sub>2</sub> O	39	61
45% EtOH/H <sub>2</sub> O	66	34
75% EtOH/H <sub>2</sub> O	92	8
HSA/5%EtOH/H <sub>2</sub> O	90	10

**Table (2.1)** *Products following irradiation of 3',4',5 - trichlorosalicylanilide in various solvent compositions.*

Finally the irradiation of 3',4'-di-chlorosalicylanilide and 3',5-di-chlorosalicylanilide led to the predominant formation of 3'- chlorosalicylanilide, with traces of the other isomers being formed. This variation of product with polarity was explained as being due to the degree of solvation of the phenolic anion; in the more polar media this anion is effectively solvated, and the 'salicylic acid' ring is less photoreactive than the 'aniline' ring. Conversely, in less polar media the anion is less effectively stabilised,

and the ring becomes more reactive. Following the loss of chlorine from  $T_4CS^-$ , an aryl radical is formed. Involvement of the aryl radical has been confirmed upon irradiation of  $T_4CS^-$  in  $CH_3OD / D_2O$  - which led to no incorporation of deuterium into the photoproducts, hence the hydrogen incorporated into the dechlorinated products is a hydrogen atom rather than a proton. Evidence of aryl radical has also been provided by Chignell and Sik - using 2-methyl-2-nitrosopropane (MNP) as a spin trap, irradiation with 365 nm light of a solution of  $T_4CS^-$  in 50% ethanol produced only solvent derived radicals, but  $T_4CS^-$  in a 0.1 N NaOH generated an ESR spectrum consisting of a broad triplet, assigned as an aryl radical, formed from dechlorination of  $T_4CS^-$  in the 3-position; to give an adduct with the structure as shown below:

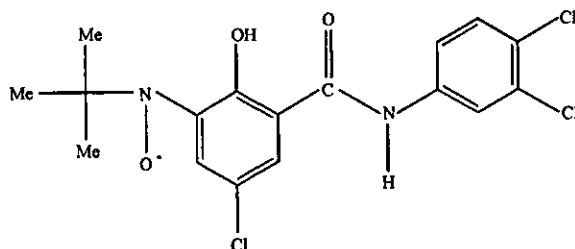


**Figure (2.5)** *Dechlorination of  $T_4CS^-$  to give a photoadduct - showing that an aryl radical is formed.*

Once an aryl radical is formed, it can then either: dimerize, abstract a hydrogen atom as already shown, or attack a reactive site such as an aromatic amino acid in a protein. Elemental analysis and NMR spectra [33] indicated that dimer formation was the greatest in solvents without readily abstractable hydrogens, see table (2.2):

T <sub>4</sub> CS <sup>-</sup> conc. (M)	Solvent composition	Dimer Yield (%)
0.0015	75% i - PrOH/H <sub>2</sub> O	0.1
0.0015	50% i - PrOH/H <sub>2</sub> O	0.5
0.0015	30% EtOH/H <sub>2</sub> O	2.5
0.032	65% MeOH/H <sub>2</sub> O	6.2
0.032	55% MeOH/H <sub>2</sub> O	10.4
0.070	t-BuOH	35

Table (2.2) *Dimer formation in various solvent compositions.*

It was noted that no dimer formation was observed following irradiation of other salicylanilides's nor when T<sub>4</sub>CS<sup>-</sup> was irradiated in the presence of HSA or BSA. This can be explained by the fact that the two T<sub>3</sub>CS<sup>-</sup> moieties required for dimer formation are prevented from reacting with each other due to their fixed positions on the HSA molecule.

Irradiation of T<sub>4</sub>CS<sup>-</sup> in the presence of cysteine led to photoreaction to give tri-chlorosalicylanilide and cystine. When irradiation was carried out in the presence of glycylglycine [36], ESR studies showed the trapping of a carbon-centred radical formed from hydrogen atom abstraction from the backbone methylene carbon atom of the C-terminal glycine residue. On replacing T<sub>4</sub>CS<sup>-</sup> with salicylanilide, no glycylglycine radical was formed; this supports postulates that aryl radicals generated by photodechlorination of T<sub>4</sub>CS<sup>-</sup> are responsible for this hydrogen abstraction reaction. When T<sub>4</sub>CS<sup>-</sup> is irradiated with HSA [21] and then chromatographed on lipophilic Sephadex the associated chlorosalicylanilide fluorescence is found with the eluted protein molecule, but when similar irradiation of HSA containing 3',4',5-tri-chlorosalicylanilide was followed by Sephadex chromatography, the eluted HSA displayed a very weak fluorescence, while other chlorosalicylanilide's showed no tendency to photo-bind to HSA at all. Similar photobinding experiments with BSA showed photobinding of chlorosalicylanilide and to the eluted protein, though not as



efficiently as with HSA, whilst 3',4',5-tri-chlorosalicylanilide failed to show any photobinding to BSA whatsoever. Since the loss of fluorescence in the eluted protein fractions containing chlorosalicylanilide's other than T<sub>4</sub>CS<sup>-</sup> was not due to greatly diminished fluorescence quantum yields by loss of chlorines (see table 2.3), this suggests that T<sub>4</sub>CS<sup>-</sup> is the most capable salicylanilide for binding to protein.

Compound	$\Phi_f$
3'-CS	0.08
3'-5-di-CS	0.19
3',4'-di-CS	0.08
3',4',5-tri-CS	0.19
T <sub>4</sub> CS <sup>-</sup>	0.23

**Table (2.3)** *Fluorescence yield of T<sub>4</sub>CS<sup>-</sup> and other chlorosalicylanilide's in 5% ethanolic water, excited at 251nm.*

## 2.8 Serum Albumin

### 2.8.1 Introduction

Serum albumin occurs in blood plasma and serous fluids, it is the principal and most abundant protein in blood plasma [37] and serves as a depot protein and transport protein for a number of endogenous and exogenous compounds. A prime example for instance is bilirubin which binds with a high affinity to albumin [38], this interaction increases its solubility in plasma and reduces its toxicity. Albumin has also been suggested as a possible source of amino acids for various tissues [39] and is the principal player in the colloid osmotic pressure of blood. The high concentration of albumin in the blood results in it being of great physiological importance and the fact that it can be isolated and purified relatively easy on a large scale has resulted in a

large number of binding studies. These investigations have been further stimulated by the successful determination of the primary sequence of many of the serum albumins.

### 2.8.2 Structure

It was Hunter and McDuffie [40] who in 1959 showed that albumin is a single peptide chain. In fact all serum albumins consist of a single polypeptide chain, and are characterised by a low content of tryptophan and methionine and a high content of cystine and the charged amino acids: lysine, arginine, aspartic and glutamic acids. However, due to the massive size of the protein chain it was a long time before its primary sequence was determined. It was not until 1975 that the peptide sequence of human serum albumin was published by Brown and co-workers [41], this was subsequently slightly modified [42]. Meloun *et al.* [43] independently published the sequence of human serum albumin the same year with extremely good agreement between the two, the peptide sequence of bovine serum albumin was also published by Brown [44]. Comparison of the two sequences show there is about 80% homology between human serum albumin and bovine serum albumin, and what differences there are in the peptide sequence are conservative in nature, *e.g.*, hydrophobic amino acids are replaced by other hydrophobic amino acids and not by polar ones.

The unique three-dimensional structure of human albumin with its characteristic looping structure was described by Saber 1977 *et al* [45] who explained how the nine loops are linked by disulphide bridges, which stabilise the three-dimensional structure of albumin. The amino acid sequence of both human serum albumin and bovine serum albumin with the cysteine linkages are shown in figures (2.6 ) and (2.7).

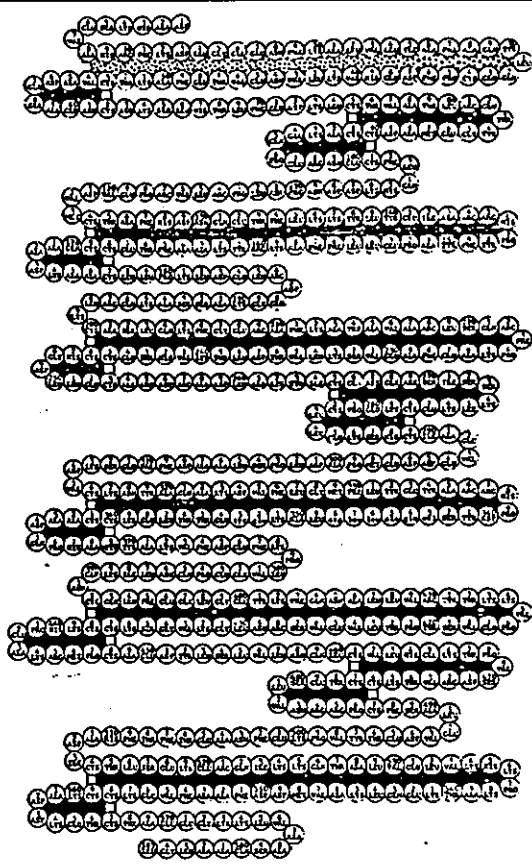


Figure (2.6) *Amino acid sequence of HSA, showing cysteine linkages to form multiple double loops.*

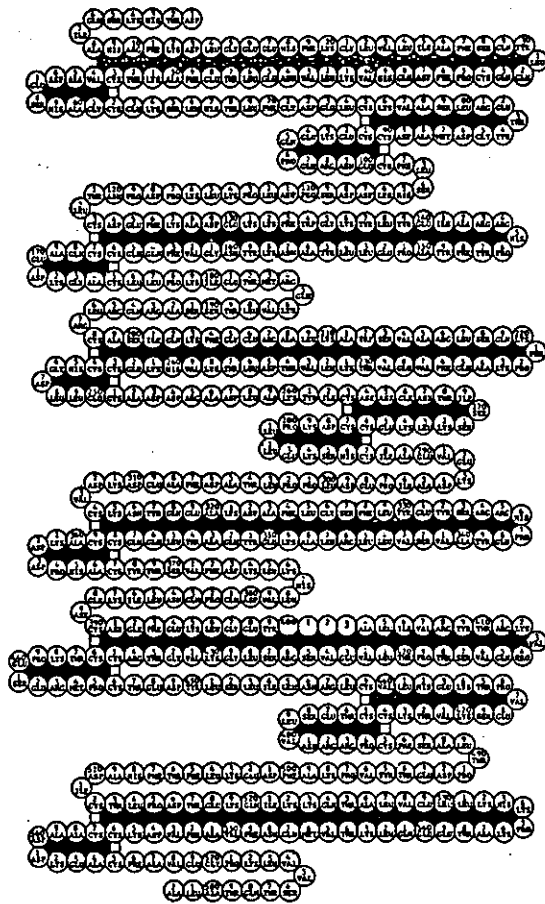


Figure (2.7) *Amino acid sequence of BSA, showing cysteine linkages to form multiple double loops.*

### 2.8.3 Survey of ligands Bound to Albumin [46]

A unique feature of albumin is its ability to bind a wide variety and a large number of biological materials, and its flexibility in adapting its shape to fit the ligand. A survey of ligands bound to albumin shows that nearly all ligands bind to a few high affinity sites plus a greater number of weaker sites. In most cases binding data has been analysed according to the Scatchard model [47] which assumes that the ligand in question is bound to classes of identical, independent binding sites. A large number of negatively charged and electrically neutral drugs bind to albumin with comparable association constants ( $10^4$  to  $10^5$   $M^{-1}$ ). Although albumin itself at physiological pH carries a negative charge, it has been proposed that albumin can bind negatively charged ligands in preference to positively charged ligands. However, albumin is also able to bind several positively charged drugs with an association constant comparable to that of the most negatively charged drugs. It must be noted that when carrying out ligand binding studies to serum albumins, the data does have to be treated with some caution. This is because binding data can be influenced by numerous factors such as temperature, pH, albumin concentration, and type and concentration of salts in the solution studied. It is possible for different batches of albumin which have been purified according to the same principles, resulting in different binding parameters. Therefore, to some extent wide limits have to be accepted when binding results obtained in different laboratories are compared before conclusion of significant differences are drawn.

For a fully comprehensive look at the various structural and ligand binding properties of serum albumin(s) the reader is recommended to refer to two excellent reviews by Theodore Peters and Kragh - Hansen [46, 48].

# Chapter 2

## References

- [1] Smith S.Z. and Epstein J.H., *Arch Dermatol.* **113**, 1372 - 1374 (1977)
- [2] Chung C.W and Giles A.L Jr, *Food Cosmet. Toxicol.* **15**, 325 -330 (1977)
- [3] Harber L.C, Targovnik S.E. and Baer R.L., *Arch. Dermatol.* **96**, 646 - 656 (1967)
- [4] Harber L.C, Armstrong R.B and Ichikawa H., *J. Nat. Cancer Inst.* **69**, 237 -244 (1982)
- [5] Willis I. and Kligman A.M., *J. Invest. Dermatol.* **51**, 378-384 (1968)
- [6] Epstein J.H. *Photoallergy - a review.* *Arch. Dermatol.* **106**, 741-8 (1972)
- [7] Wilkinson DS., *Br.J. Dermatol.* **73**, 213-219 (1961)
- [8] Epstein S. and Enta T., *J. Am. Med. Assoc.* **195**, 1016 (1965)
- [9] Jillson O.F. and Baughman R.D., *Arch. Derm.*, **88**, 409 (1963)
- [10] Barratt M.D and Brown K.R., *Toxicol. Letts.* **24** 1-6 (1985)
- [11] Burry J.N., *Arch. Dermatol.* **95**, 287-291 (1967)
- [12] Rickwood D.M. and Barratt M.D., *Chem.-Biol. Interactions* **52**, 213-22 (1984)
- [13] Maguire H.C.Jr. and Kaidbey K J., *Invest. Dermatol.* **79**, 147-52 (1982)
- [14] Giovanazzo V.J., *Archs Derm.* **117**, 344-348 (1981)
- [15] Kaidbey K.H. and Kligman A.M., *Contact Dermatitis* **4**, 277-82 (1978)
- [16] Ippen H. and Jadit Z., *Haut - Geschl. - Kr.* **31**, 185 -187 (1965)
- [17] Sidi E., Hichy M. and Gervis A., *J. Invest. Dermatol.* **24**, 345-52 (1955)
- [18] Kochevar I.E., *Photochem-Photobiol.* **30**, 437-442 (1979)
- [19] Johnson B.E., Daniels Jr F. and Magnus I.A., *In Photophysiology*, vol IV 139-143 Press, New York
- [20] Blum H.F., *Photodynamic Action and Diseases caused by light.* New York: Reinhold (1941)

- [21] Lennon W.J., Furia T.E. and Zussman H.W., *Soap, Perfum. Cosm. Tr. Rev.*, **33**, 51. (1960)
- [22] Lennon W.J., Furia T.E. and Zussman H.W., *Soap Chem. Spec.*, **36**, 609. (1960)
- [23] Jenkins F.P., Welti D. and Baines D., *Nature* **201**, 213-219. (1964)
- [24] Hilal N.S., *Ph.D. Thesis*, University of Salford. 77-78 (1973)
- [25] Davies A.K., Hilal N.S., Mckellar J.F. and Phillips G.O., *Br. J. Dermatol.* **92**, 143 (1975)
- [26] Kochever I.E. and Harber L.C., *J. Invest. Dermatol.* **68**, 151-156 (1977)
- [27] Barratt M.D., *Photobiochem. Photobiophys.* **3**, 59-65. (1981)
- [28] Rickwood D.M. and Barratt M.D., *Photobiochem. Photobiophys.* **5**, 365-369 (1983)
- [29] Rickwood D.M. and Barratt M.D., *Biophysical Chemistry* **19** 69-73 (1984)
- [30] Rickwood D.M. and Barratt M.D., *Photochem. Photobiol.* **35**, 643-647 (1982)
- [31] Coxon J.A., Jenkins F.P. and Welti D., *Photochem. Photobiol.* **4**, 713-718 (1965)
- [32] Morikawa F., Nakayama Y., Fukuda M., Hamano M., Yokoyama Y., Naguru T., Ishi M. and Toda M. *In Sunlight and Man*. 529-558 Uni. Tokyo Press, Tokyo (1974)
- [33] Epling G.A., Wells J. L. and Young U.C., *Photochem. Photobiol.* **47**, 167-172 (1988)
- [34] Phiney J.T. and Rigby R.D.G., *Tetrahedron Lett.* 1267-1270 (1969)
- [35] Davidson R. S., Goodwin J.W. and Kemp G., *Adv. Phys. Org. Chem.* **20**, 191-233 (1984)
- [36] Chignell C.F. and Sik R.H., *Photochem. Photobiol.* **50**, 287-29 (1989)
- [37] *The British Medical Association Complete Family Health Encyclopedia Second Edition* 1995 Dorling Kindersley Ltd. 80 (1985)
- [38] Jacobsen J., *Int. J. Pept. Protein Res.* **9**, 235 - 239 (1977)
- [39] Peters T.Jr., *In the Plasma Proteins*, ed. by F.W. Putnam, vol. I, 133 - 181 *Academic Press*, New York (1975)
- [40] Hunter M.J. and McDuffie F.C., *J. Am. Chem. Soc.* **81**, 1400 - 1406 (1959)

- [41] Behrens P.Q., Spiekerman A.M. and Brown. J.R., *Fed. Proc.* **34**: 591 (1975)
- [42] Brown J.R., *In Albumin Structure, Function and uses* 27 - 51 Pergamon Press (1977)
- [43] Meloun B., Moravek, L. and Kostka V., *F.E.B.S. (Fed. Eur. Biochem. Soc.) Lett.* **58**: 134 - 137 (1975)
- [44] Brown J.R., *Fed. Proc., Fed. Am. Soc. Exp. Biol.* **34**: 591 (1975)
- [45] Saber M.A., Stockbauer P., Moravek L. and Meloun B., *Collect. Czech. ChemCommun.* **42**: 564 - 579 (1977)
- [46] Kragh-Hansen U., *Pharmacological Reviews* **33**, 17-53 (1981)
- [47] Scatchard G. Ann N.Y., *Acad. Sci.* **51**: 660 - 672 (1949)
- [48] Theodore P.Jr ., *Advances in Protein Chemistry.* Vol **37**, 161 - 242 (1985)

# **CHAPTER 3**

## **Experimental**



## **3 Experimental**

### **3.1 Ground State Absorbance Spectra**

All ground state spectra were recorded using a PU-8800 dual beam UV-VIS spectrophotometer (Philips), spectra being obtained using 1cm x 1 cm quartz or glass cuvettes.

### **3.2 Steady State Emission Spectra**

Emission spectra were recorded using either a Fluoromax spectrophotometer (ISA Instruments S.A (UK) Ltd), or a LS50 Perkin Elmer luminescence spectrometer. All spectra recorded used conventional right angle geometry.

### **3.3 Nanosecond Laser Flash Photolysis**

Two laser flash photolysis lasers are employed in Loughborough. Both are Neodymium doped Yttrium Aluminium Garnet (Nd:YAG) lasers that are operated in Q-switched mode. One is built around a JK Lasers (now Lumonics) JK2000, the other a Lumonics hyper YAG HY200 Laser. A schematic diagram of the flash photolysis system is as shown in figure (3.1).

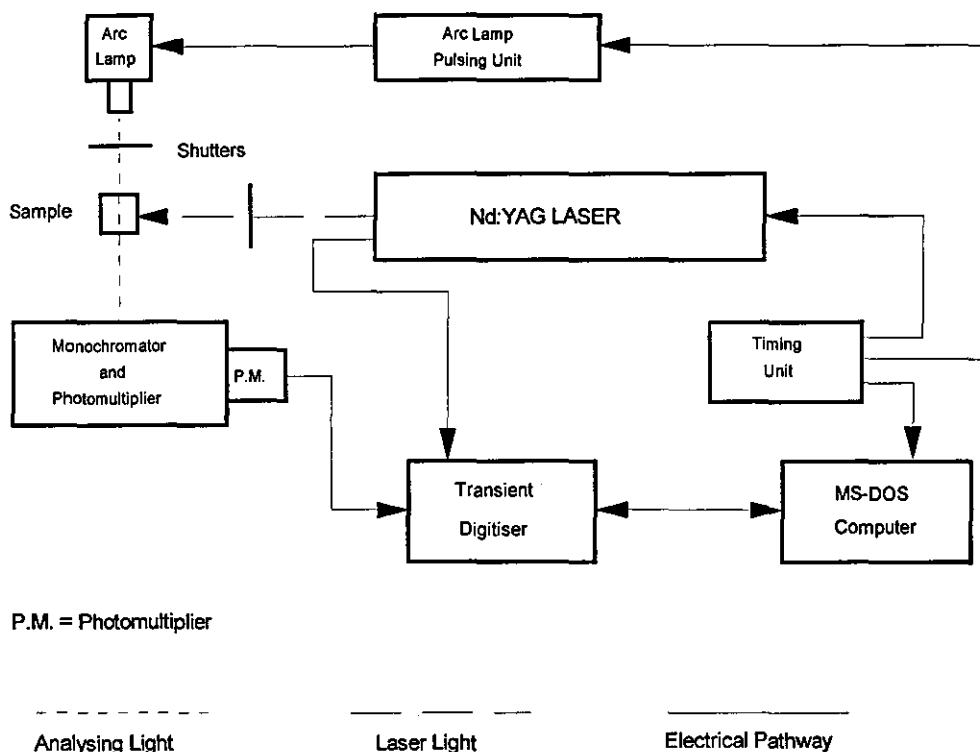


**Figure (3.1)** Schematic diagram of the apparatus used for laser flash photolysis experiments.

The fundamental wavelength of these lasers is located in the near infra-red region of the spectrum at 1064 nm. However, this wavelength is not of use for photochemical investigations - what is required is UV-VIS radiation. This can be obtained by passing the fundamental wavelength through appropriate frequency doubling or mixing crystals, producing second, third and fourth harmonics. Second harmonic generation to give 532 nm is achieved by passing the fundamental wavelength through a deuterated caesium dihydrogen arsenate crystal (DCDA). Frequency mixing of the 532 nm light with the remaining undoubled 1064 nm light in a potassium dihydrogen phosphate (KDP) crystal results in the generation of the third harmonic at 354.7 nm. The fourth harmonic, located at 266 nm, is obtained by frequency doubling the second harmonic in an ammonium dihydrogen phosphate (ADP) crystal. The excitation wavelength used for photochemical studies in this thesis was almost exclusively 354.7 nm with occasional use of 532 nm. The JK and HY laser pulses generated are gaussian with respect to time and have full

width at half maximum (FWHM) of approximately 20 and 8 ns respectively. The analysing source on both systems is a 300W xenon arc lamp (Optical Radiation Corporation). Appropriate filters can be placed between the analysing source and sample to cut off unwanted wavelengths. The detection system comprises a  $f/3.4$  grating monochromator (Applied Photophysics Ltd.) which has fully variable (0 to 8mm) 21 mm height bilateral slits front and back and an R928 side window photomultiplier tube (Hamamatsu Ltd.) The accelerating voltage applied to the photomultiplier tube was by a 412B (FLUKE) high voltage supply. The signal from the photomultiplier tube was directed in the case of the JK laser system either into a 7612D transient digitiser (Tektronix Ltd.) or a TDS420 digitising oscilloscope (Tektronix Ltd.) - both having a maximum single shot digitising rate of 5 ns per point. The HY laser uses a 2432A digital oscilloscope having a maximum single shot rate of 4 ns per point.

Both these devices have the facility of a programmable number of pre-trigger points which were set as 24 and 28 points respectively out of a total data record length of 512 points. Communication of these devices with an IBM compatible personal computer is achieved via a PC2A general purpose interface bus (GPIB - National Instruments), which allows setting of the instrument parameters and the passing of digital data from the instrument direct to the computer. The driver software was provided by National Instruments and Tektronix. The shutters that are placed between the analysing lamp and sample and laser and sample are controlled by the computer via a DT2808 digital / analogue analogue / digital (D/A/AA/D) card (Data Translation Ltd).

### **3.3.1 Data Collection**

The software used to control the operation of both sets of apparatus as well as data collection and storage was written in Loughborough by Dr. D.R Worrall, Dr. G.P. Kelly and Mr. P.A. Leicester. Overall timing of the events leading to data collection for both set of apparatus is controlled by one central timing unit consisting of a quartz oscillator and a series of analogue delay modules. This unit was designed and built in Loughborough. The first step in data collection is the triggering of the computer, once triggered the computer instructs the digitiser to arm its timebase and to digitise a signal

upon receipt of its next signal. The next step is the opening of the appropriate shutters that are situated between the laser beam and the sample and the analysing source and the sample. For a transient absorption experiment the baseline is first collected with only the analysing light shutter open, next the transient absorption itself is collected with both analysing source and laser shutters open. An emission trace is obtained with only the laser shutter open and finally the top line with both shutters closed. The correct opening of the shutters is achieved by the computer that either allows opening or closing of the shutters depending on which data set is being collected. The firing of the laser can trigger the digitiser in one of two ways: the JK2000 laser reflects some of the laser pulse onto a glass slide aimed at a fibre optic cable which is in turn incident upon a photodiode, the HY200 laser triggers the digitiser by residual 1064 nm light incident upon a photodiode. On completion of digitisation of the signal obtained from the photomultiplier, the data is transferred to the computer, displayed on the screen, and stored on disk for later analysis - thus completing a cycle of data collection. Following this the computer awaits another signal from the timing unit for the sequence to begin again.

### 3.3.2 Data Analysis

To obtain an absorbance change of the intermediate under study with respect to time it is necessary to manipulate the traces collected, *i.e.* the baseline, topline, absorption, and emission (see figure 3.2). This is done as follows: a data array corresponding to signal intensity following the laser pulse is generated, it is corrected for emission by subtracting the emission trace (E) from the transient absorption (TA) trace. For reliable results it should be noted that the emission trace should remain on the screen - overloading of the photomultiplier or too strong an emission is not desirable. The range of the screen is calculated by subtracting the topline (TL) from the baseline (BL), thus ensuring that the calculated transmission change is independent of the position of the two traces on the screen. The change in transmission is then calculated according to equation (3.1).

$$\Delta T(t) = 1 - \frac{\text{transmission}_c}{\text{baseline}_c} \quad (3.1)$$

Where the subscripts c denote that baseline and transmission are corrected for topline and emission, respectively.

The value of interest in solution flash photolysis is the change in absorbance as a function of time,  $\Delta A(t)$ . Using the Beer-Lambert law,  $\Delta A(t)$ , is given by:

$$\Delta A(t) = \log_{10} \left( \frac{1}{1 - \Delta T(t)} \right) \quad (3.2)$$

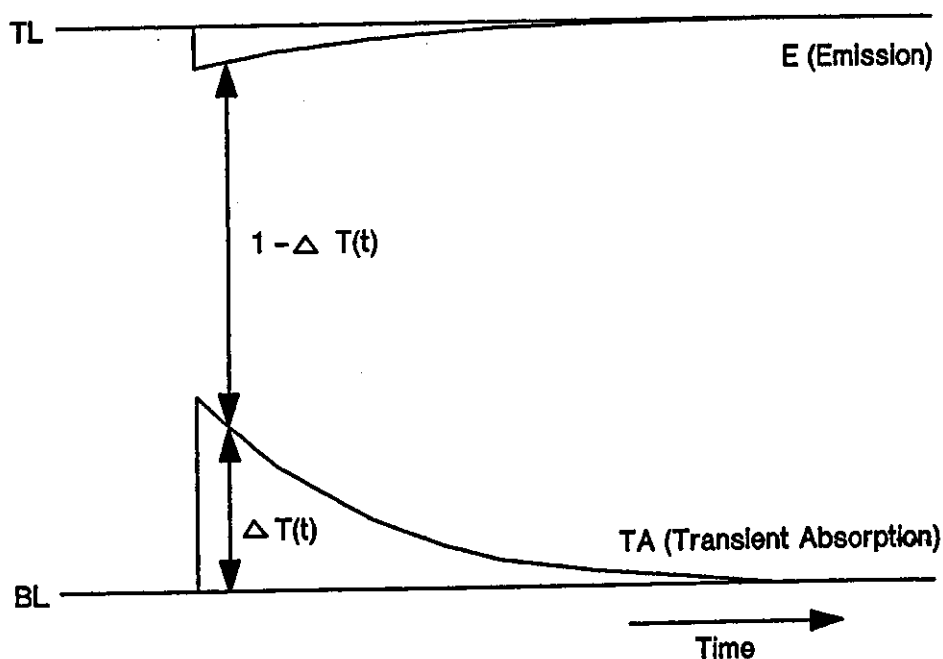


Figure (3.2) Schematic diagram of the experimental data traces recorded for transmission laser flash photolysis experiments.

### 3.4 Phosphorescence Measurements

Phosphorescence emission spectra were carried out using a gated Photodiode Array System (EG & G Princeton Applied Research). The Lumonics hyper YAG HY200 Laser was used as the excitation source at 354.7 nm. In this system the detector controller determines the timing of events, sending out a pulse to trigger the laser. The laser pulse

is detected by a photodiode via a fibre optic cable positioned next to the laser output, and the signal from this photodiode triggers the gate pulse interface. The resulting gate pulse is amplified and applied to a microchannel plate, thus effectively "opening" the optical gate for the gate pulse duration allowing detection by the photodiode array. The emitted light from the sample is collected using a fibre-optic which transfers it to a spectrograph. Gate widths used were up to 100  $\mu\text{s}$ , with delays from the laser pulse of up to 100  $\mu\text{s}$ .

### 3.5 Singlet Oxygen Luminescence Detection

As already discussed in section (1.1.11), the radiative relaxation of the lowest lying excited singlet state of molecular oxygen ( $^1\Delta_g$ ), results in the production of phosphorescence at 1270 nm. Detection of the phosphorescence was achieved using a singlet oxygen luminescence detector. The detector consists of a reverse biased germanium photodiode (Judson J16-8SP-1205M) coupled to a 55dB gain pre-amplifier (Judson PA100). Samples are placed in quartz cuvettes and excited with the 354.7 nm harmonic of the Nd:YAG laser. To prevent light of unwanted wavelengths reaching the detector, filters were used. One was placed in front of the laser beam to filter out any residual 1064 nm light (BG38 Oriel Scientific Ltd.), the other a long pass infra-red silicon filter (Oriel Scientific Ltd. Filter 57900) was placed in front of the photodiode preventing all wavelengths below 1100 nm from reaching the detector. The detector and filter are placed a few millimetres from the face of the sample cuvette so as to detect emission perpendicular to the exciting source. The signal from the detector is then digitised and stored by the computer for later analysis.

## 3.6 Preparation of Solutions

### 3.6.1 Preparation of Monomeric Human Serum Albumin (mHSA) in 0.1 M Potassium Phosphate buffer solution pH 7.4

Potassium dihydrogen orthophosphate ( $\text{KH}_2\text{PO}_4$ ) and di-potassium hydrogen orthophosphate ( $\text{K}_2\text{HPO}_4$ ) solutions were prepared to a concentration of 0.1M. The  $\text{KH}_2\text{PO}_4$  solution is then added to the  $\text{K}_2\text{HPO}_4$  solution whilst stirring until a pH of 7.4 is reached. The prepared buffer solution is then degassed and filtered through a 0.22  $\mu\text{m}$  Millipore filter and stored at 4°C. A Sephadex G-150 column (90 x 2.6 cm) is equilibrated with approximately 1 litre of the 0.1M potassium phosphate buffer (pH = 7.4). About 1mg / 1ml of HSA is dissolved in the buffer solution, and this is loaded onto the G-150 Sephadex column. Elution is then carried out, a typical flow rate being 0.4 ml / min. The eluted solution is collected as 4ml fractions by automation. The absorption at 280 nm is recorded for each fraction, whereby it is possible to identify the fractions that contain the monomer form of HSA. A typical absorption versus fraction plot is shown in figure (3.3).

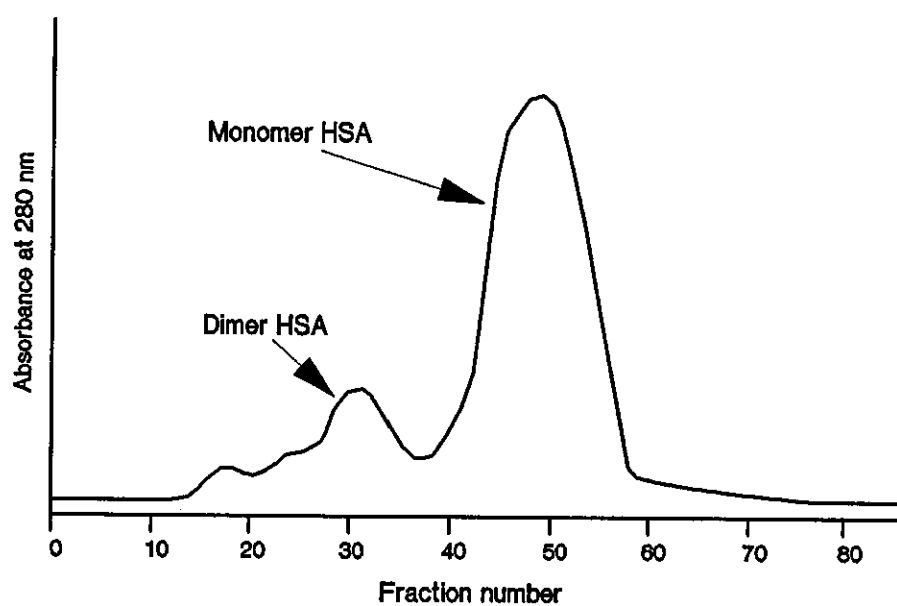


**Figure (3.3)** Typical collection spectrograph showing which fractions contain the monomeric form of HSA.

The fractions that contain the monomeric form of HSA are pooled together. These are then concentrated in an Amicon ultrafiltration cell at 15 psi using a  $\gamma$ m-10 membrane. If there are any signs of bacterial contamination, the solution can be filter sterilised through a 0.45 $\mu$ m Aerodisc filter.

The concentration of the fractionated mHSA is determined by equation (3.3). Dilution of the solution is required, so that the absorption at the peak of 280 nm will not be off-scale.

The concentration is given by:

$$[mHSA] / mg ml^{-1} = \frac{A^{280nm}}{\epsilon \cdot l} \times 10 \times (\text{dilution factor}) \quad (3.3)$$

where:

$\epsilon$  HSA at 280 nm = 5.8

$l$  = the pathlength of the cell (cm)

The concentrated mHSA solution is stored at 4°C.

### 3.6.2 Preparation of Salicylanilide Solutions

Aqueous solutions of T<sub>4</sub>CS<sup>-</sup> and TBS<sup>-</sup> were prepared by first dissolving the salicylanilide in the appropriate alcohol and then adding 0.1 M potassium phosphate buffer (pH = 7.4) solution to make up the requisite ratio. The ratio is indicated throughout the thesis as a volume percentage, where the percentage of alcohol is stated. So that a solution containing by volume 10% alcohol and 90% buffer would be represented as a 10% alcoholic aqueous solution. All pH measurements were carried out using a Corning 220 pH meter.



### 3.7 Degassing Solutions

Using a vacuum line the 'freeze-pump-thaw' (FPT) technique was applied. Solutions were placed in a limb of the reaction vessel and frozen using liquid nitrogen (77K), the air above the frozen solid is evacuated by decreasing the pressure (measurable down to a pressure of  $1 \times 10^{-3}$  mbar). The vacuum tap on the vessel cell was closed and the solution is thawed, allowing trapped air in the solution to equilibrate with the rest of the cell. The cycle is repeated until no further change in pressure is monitored.

To avoid denaturing protein samples, solutions containing mHSA or BSA were purged with nitrogen gas to remove the oxygen content.

### 3.8 Materials

All solvents (methanol, ethanol, propanol, propan-2-ol, cyclohexane, benzene and acetonitrile) were of spectrophotometric grade (Aldrich Ltd.) and were used as received. Chemicals were obtained from the following sources: 3,3',4',5-tetrachlorosalicylanilide (T<sub>4</sub>CS) and 3,5,4'-tribromosalicylanilide (TBS) (Kodak). These were purified by repeated recrystallization from chlorobenzene, until a sharp melting point of 162-164°C was reached for T<sub>4</sub>CS (literature 162 °C) and for TBS 189 -190 °C (literature 190-191 °C). Benzophenone (Aldrich Ltd. Gold Label), 9,10 - diphenylanthracene (Aldrich Ltd. Gold Label), naphthalene (Aldrich Ltd. Scintillation Grade), quinine sulphate (Aldrich Ltd.), biphenyl (Aldrich Ltd. 99%), rose bengal, bis (triethyl-ammonium) salt (Aldrich Ltd. ~ 90%), 1-hydroxypyridine-2-thione (Omadine, Sodium salt) (Sigma 98%).

HSA (fraction V, fatty acid free) and BSA (fraction V) were purchased from Sigma. Monomeric HSA (mHSA) was prepared from the commercial sample with the kind assistance of Mrs. R.U. Pendlington as detailed in section (3.5).

Oxygen and nitrogen were supplied by B.O.C. Ltd and were water free.

## **CHAPTER 4**

**Results with  $T_4CS^-$  and  $TBS^-$**

## 4.1 Absorption Spectroscopy

### 4.1.1 Ground State Absorbance Spectra of ( $T_4CS-H / T_4CS^-$ ) and ( $TBS-H / TBS^-$ ) in Solution

Halogenated salicylanilides like  $T_4CS-H$  and  $TBS-H$  are insoluble in water, therefore other solvents need to be utilised in order to study their photochemistry. It is possible to make aqueous solutions with cosolvents. Thus, alcohol/water mixtures can be used provided that the salicylanilide is first dissolved in the alcohol and the water is added after the anilide has dissolved. The ground state absorption spectra of ( $T_4CS-H / T_4CS^-$ ) and ( $TBS-H / TBS^-$ ) in a selection of solvents are shown in figures (4.1) to (4.5).

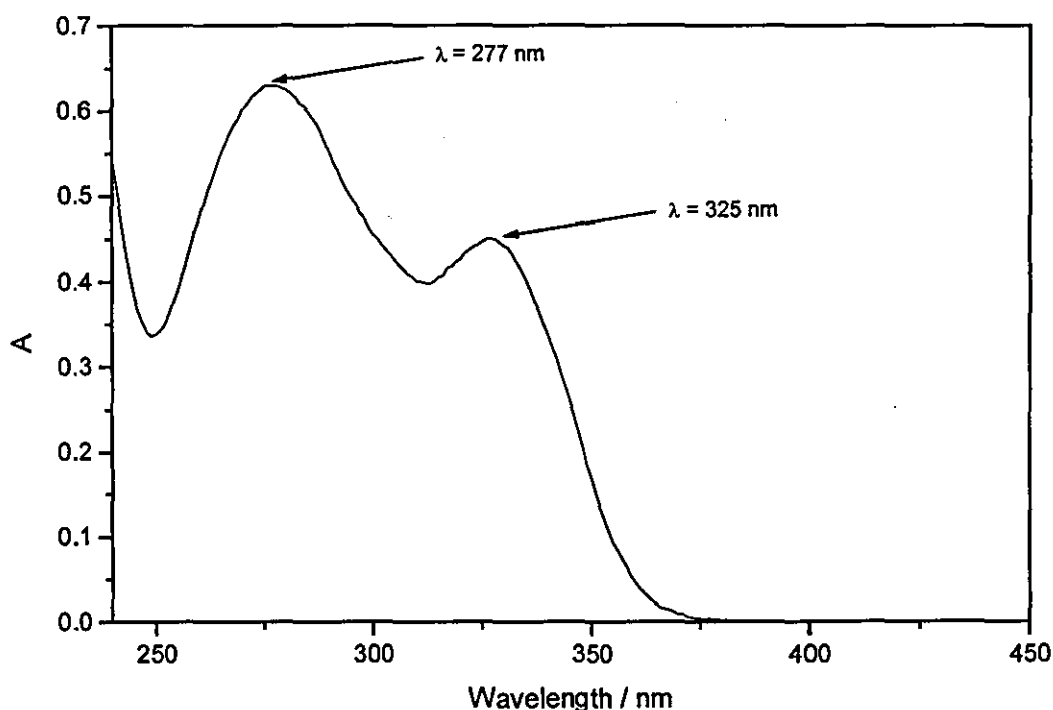


Figure (4.1) Ground state absorption spectrum of  $T_4CS-H$  in acetonitrile ( $50 \mu M$ ).

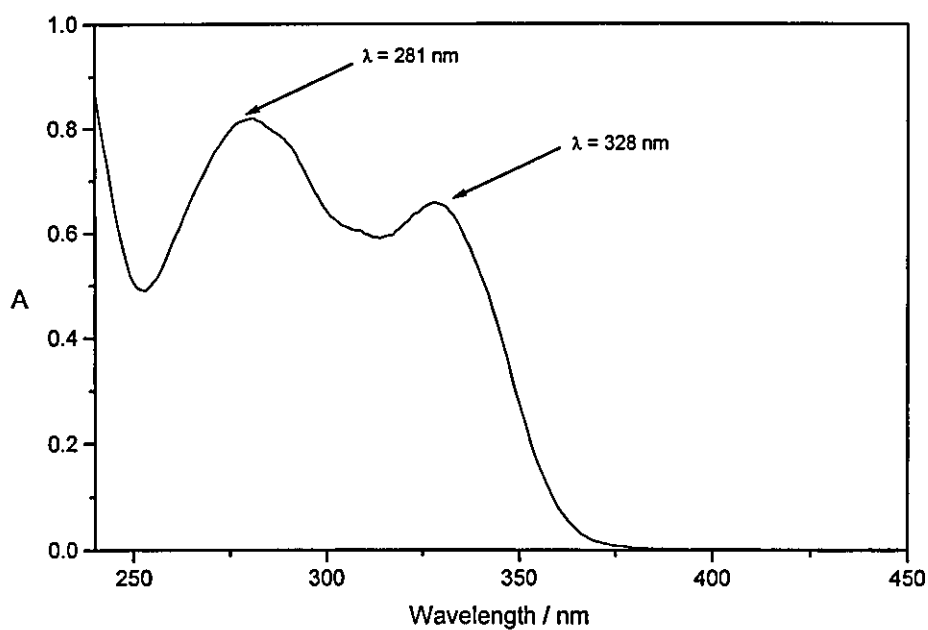


Figure (4.2) *Ground state absorption spectrum of TBS-H in acetonitrile (65 μM).*

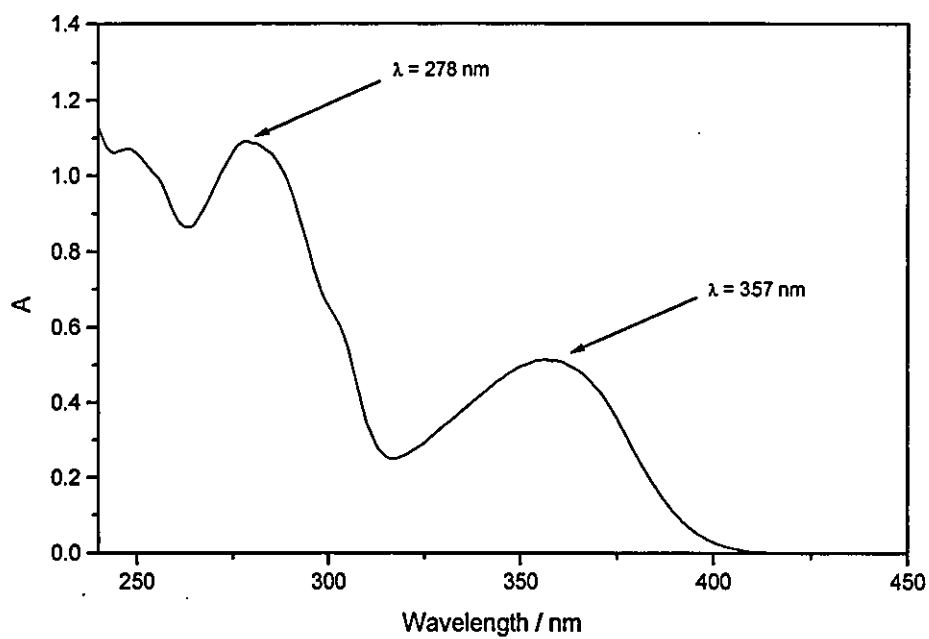


Figure (4.3) *Ground state absorption spectrum of T<sub>4</sub>CS<sup>-</sup> in methanol (60 μM).*

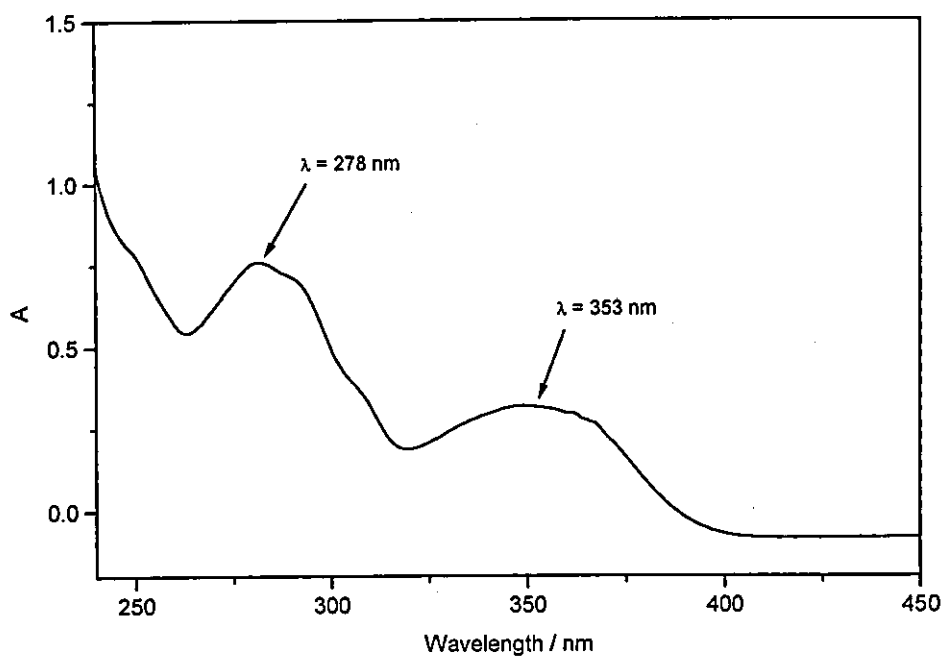


Figure (4.4) Ground state absorption spectrum of TBS-H in methanol (60 μM)

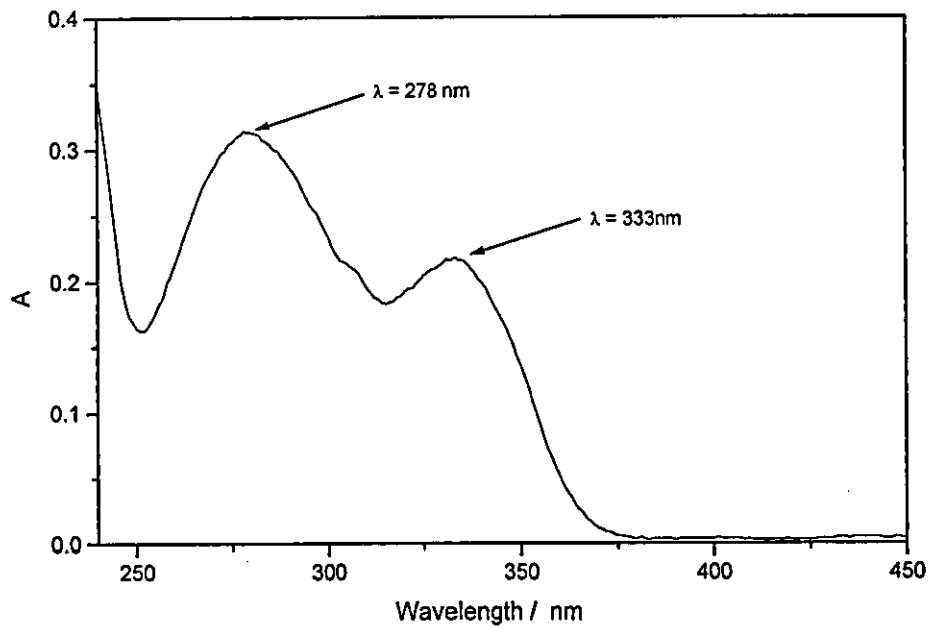
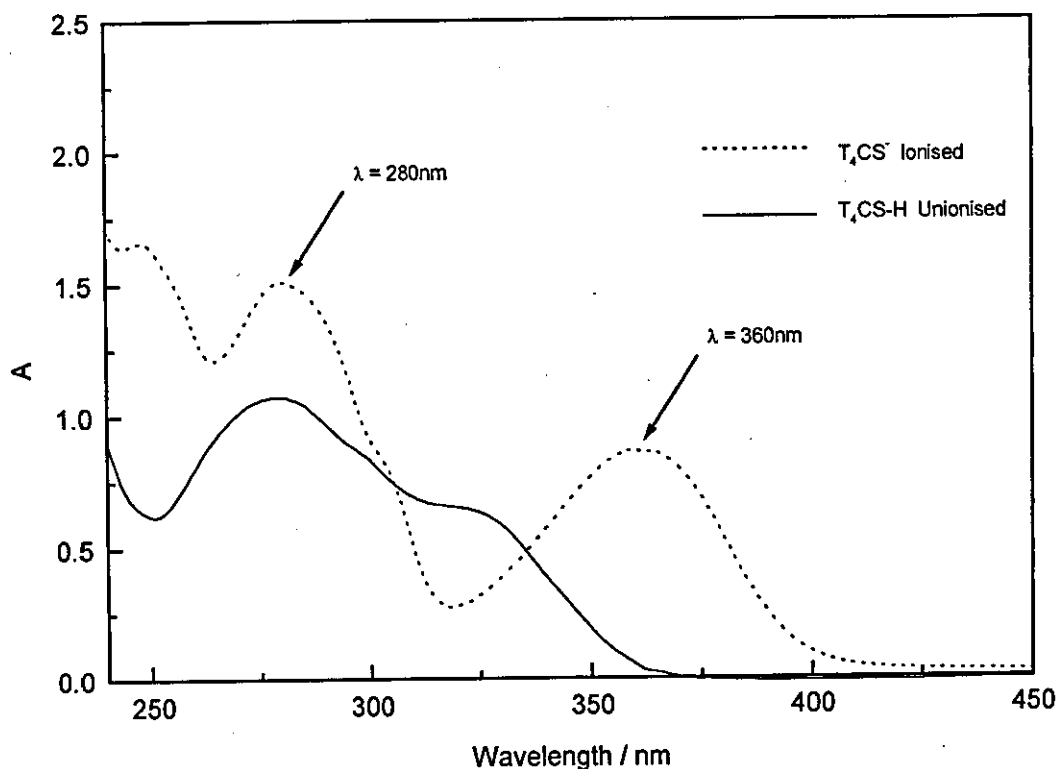


Figure (4.5) Ground state absorption spectrum of T,CS-H in cyclohexane (80 μM).

In aqueous cosolvent solutions ( $T_4CS-H / T_4CS^-$ ) and ( $TBS-H / TBS^-$ ) exhibit similar spectra; they absorb light in the ultra-violet region of the spectrum (below 400 nm). In protic (hydroxylic) solvents under alkaline conditions the molecule is predominantly in its ionic form where there are two main absorption bands, one with  $\lambda_{max}$  approximately 360 nm and the other  $\lambda_{max}$  approximately 280 nm. Changing to acidic, non-polar or aprotic solvents results in a decrease in the absorption coefficient of the 360 nm band and an increase in the absorption coefficient at 319 nm. The 319 nm band is due to the unionised form of  $T_4CS-H$  or  $TBS-H$ , these are illustrated in figures (4.6) and (4.7).



**Figure (4.6)** *Ground state absorption spectra of  $T_4CS^-$  and  $T_4CS-H$  ( $90 \mu M$ ) in 50% aqueous ethanolic solution, showing ionised and unionised forms.*

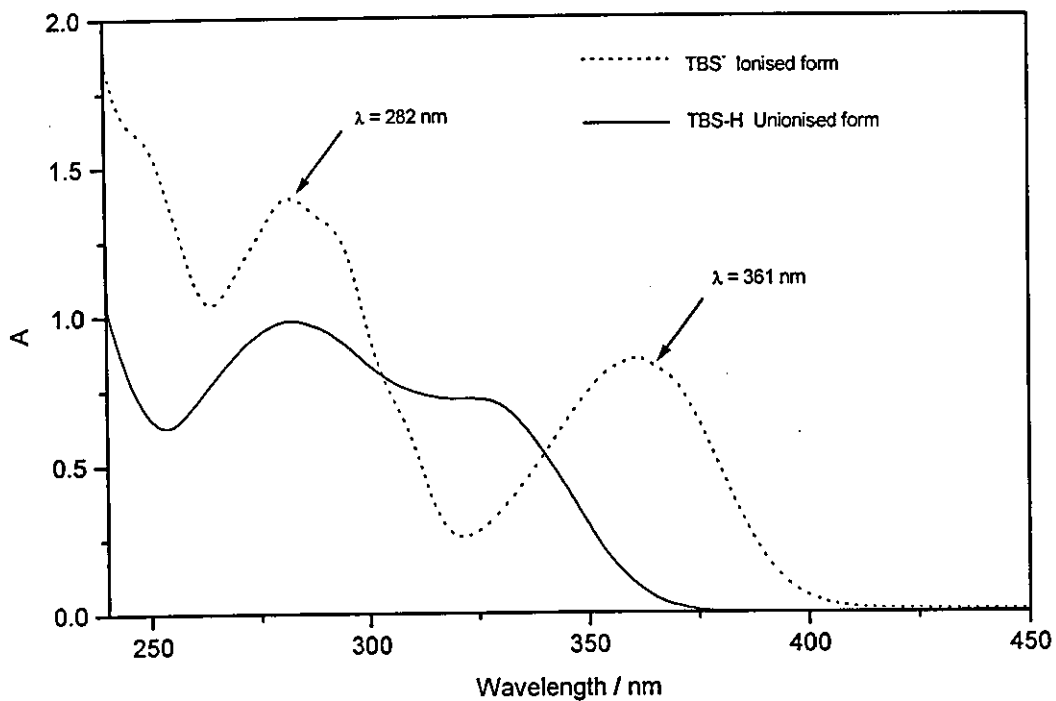


Figure (4.7) Ground state absorption spectra of TBS<sup>-</sup> and TBS-H (100 μM) in 50% aqueous ethanolic solution, showing ionised and unionised forms.

The equilibrium between the two forms in the case of T<sub>4</sub>CS-H may be represented as follows:

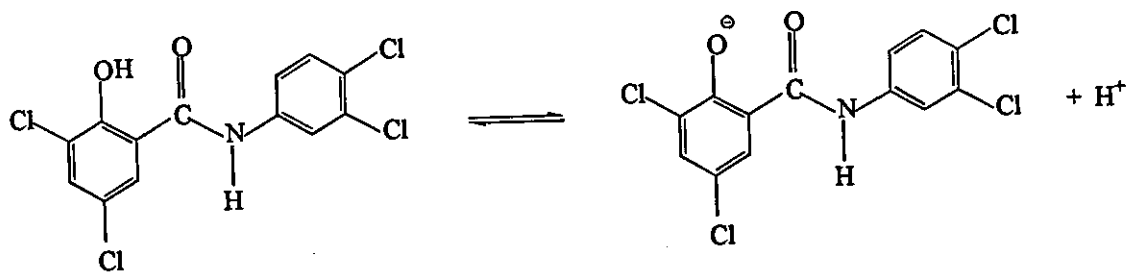


Figure (4.8) Equilibrium between the ionised and unionised forms of T<sub>4</sub>CS-H.

It is the anionic form that is photochemically active to near ultra-violet radiation, and therefore it is this ionised form that is of interest in photochemical studies. The Nd:YAG lasers that will be used in the flash photolysis experiments can produce excitation wavelengths located at 354.7 nm and 532 nm. Since the salicylanilides absorb well at 354.7 nm, this was the excitation wavelength employed in the flash photolysis studies.

#### 4.1.2 Calculation of the $pK_a$ for $T_4CS-H$ in 50% ethanolic aqueous solution

The equilibrium between the unionised and ionised forms can be represented as:



where  $T_4CS-H$  = unionised form and  $T_4CS^-$  = ionised form

The equilibrium association constant is given by:

$$K_a = \frac{[T_4CS^-]_{eqm} [H^+]_{eqm}}{[T_4CS - H]_{eqm}} \quad (4.2)$$

or

$$[H^+]_{eqm} = K_a \frac{[T_4CS - H]_{eqm}}{[T_4CS^-]_{eqm}} \quad (4.3)$$

Taking logs gives:

$$-\log [H^+]_{eqm} = -\log K_a - \log \left( \frac{[T_4CS - H]_{eqm}}{[T_4CS^-]_{eqm}} \right) \quad (4.4)$$



where:  $-\log[H^+]_{eqm} = pH$  (4.5)

$$\therefore pH = -\log K_a - \log \left( \frac{[T_4CS - H]_{eqm}}{[T_4CS^-]_{eqm}} \right) \quad (4.6)$$

The pH of the solution depends on the ratio of the concentrations of acid and base, and not the actual values. When  $[T_4CS-H] = [T_4CS^-]$  then  $pH = -\log K_a$ . Equation (4.6) is of the form of a straight line, such that a plot of pH versus  $\log ([T_4CS-H] / [T_4CS^-])$  should give a straight line with the intercept representing the  $pK_a$ . The absorption spectra of  $(T_4CS-H / T_4CS^-)$  in 50% aqueous ethanol solutions at various pH's are shown in figure (4.9) showing two isosbestic points suggesting two species are present.

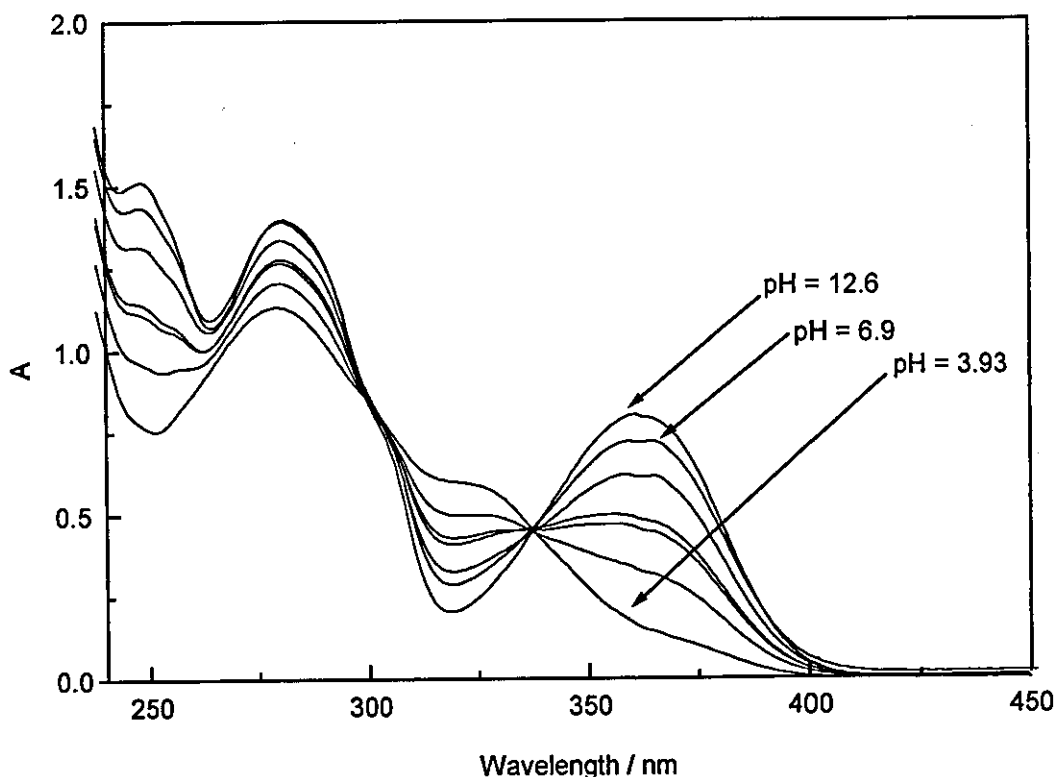


Figure (4.9) Ground state absorption spectra of  $T_4CS^-$  and  $T_4CS-H$  in 50% aqueous ethanol under various pH's, showing two isosbestic points.

The pH of the solutions was made more alkaline by adding  $\text{NaOH}_{(s)}$  or acidified by adding dilute  $\text{H}_2\text{SO}_4_{(aq)}$ . Absorption  $A$  at a given pH and  $\lambda$  (360 nm) can be expressed as the sum of the absorbances of these two species as shown below:

$$A = [\text{T}_4\text{CS-H}][A_{0,\text{T}_4\text{CS-H}}] + [\text{T}_4\text{CS}^-][A_{0,\text{T}_4\text{CS}^-}] \quad (4.7)$$

where  $A_0$  represents the absorption of the pure associated and dissociated forms  $\text{T}_4\text{CS-H}$  and  $\text{T}_4\text{CS}^-$ . These were measured at pH 3.9 and 12.6 respectively.

If only two species are present in solution then:

$$[\text{T}_4\text{CS}^-] = 1 - [\text{T}_4\text{CS-H}] \quad (4.8)$$

Combining equations (4.7) and (4.8) yields equation (4.9):

$$[\text{T}_4\text{CS-H}] = (A - [A_{0,\text{T}_4\text{CS}^-}]) / ([A_{0,\text{T}_4\text{CS-H}}] - [A_{0,\text{T}_4\text{CS}^-}]) \quad (4.9)$$

The concentrations of  $\text{T}_4\text{CS}^-$  and  $\text{T}_4\text{CS-H}$  are calculated according to equations (4.8 and 4.9).

A plot of  $\log ([\text{T}_4\text{CS-H}] / [\text{T}_4\text{CS}^-])$  versus pH is shown in figure (4.10).

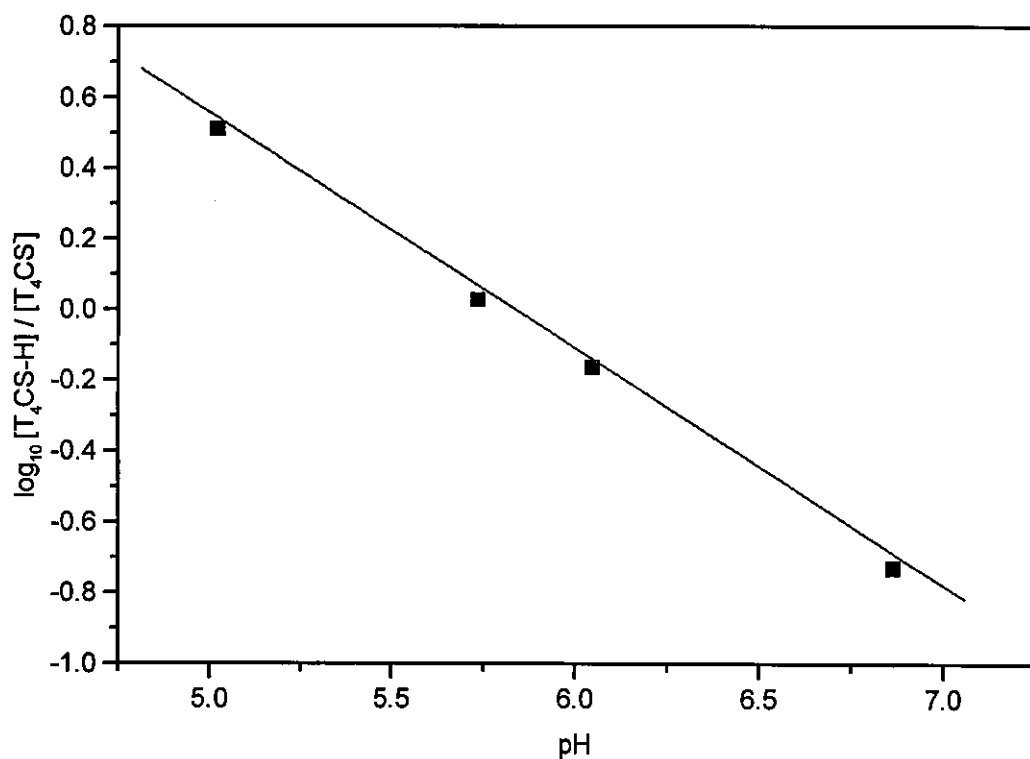


**Figure (4.10)** Plot of  $\log ([T_4CS-H] / [T_4CS])$  vs. pH

The above plot using equation (4.16) should yield a gradient of unity. The actual gradient is 0.7 which means that assuming only two species are present at all pH's is not right. To calculate the  $pK_a$  would mean using different limits of pH. What is clear from figure (4.9) is that solutions at pH = 7.4, contain mainly the ionised form:  $T_4CS^-$  and this was the pH used for making up solutions throughout the thesis.

### 4.1.3 Calculation of Molar Absorption Coefficients and Verification of Beer's Law

Measuring the absorbance spectra at the desired wavelength of a range of solutions of varying concentrations and plotting the absorbance of the solution against the concentration of the solution, should give a straight line through the origin if Beer's law is obeyed. Deviations from Beer's law can occur for several reasons including chemical effects such as dimerisation or cluster formation particularly at high concentrations, or by instrumental artefacts such as non-linearity of the photomultiplier response. Concentrations ranging from  $30\mu\text{M}$  to  $280\mu\text{M}$  of  $\text{T}_4\text{CS}^-$  in 50% and 10% ethanolic aqueous solutions and of  $\text{TBS}^-$  in 10% ethanolic aqueous solutions were prepared. Absorbance measurements were carried out using a 1 cm pathlength cell, with a 0.5 nm resolution slit width and a one second integration time. Figures (4.11) to (4.13) show plots of absorbance against compound concentration measured at the peak of the long wavelength band.

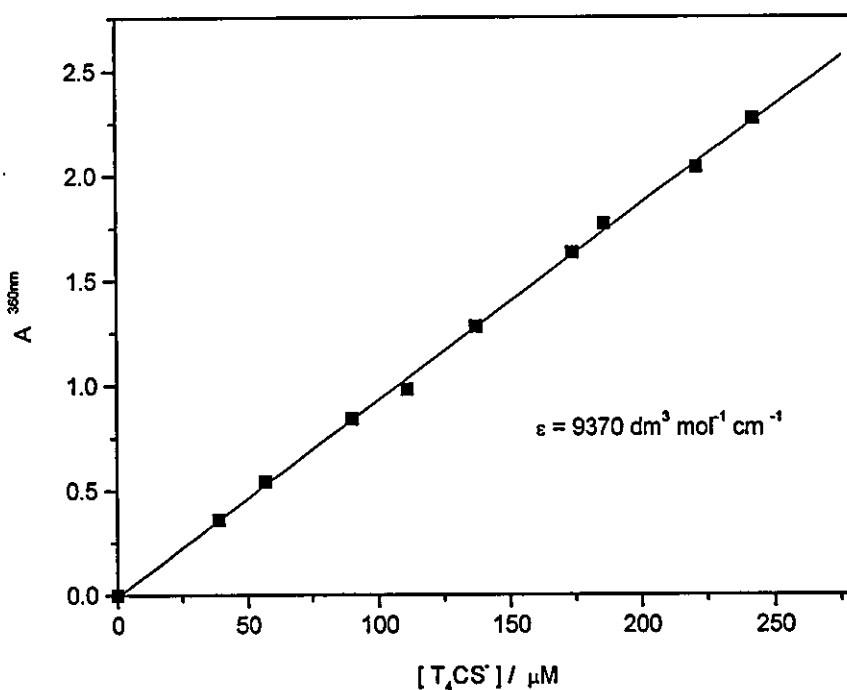


Figure (4.11) *Change in absorbance at 360 nm of  $\text{T}_4\text{CS}^-$  in 50% ethanolic aqueous solution (pH=7.4) with increasing concentration, with the Best Straight Line Fit to the data.*

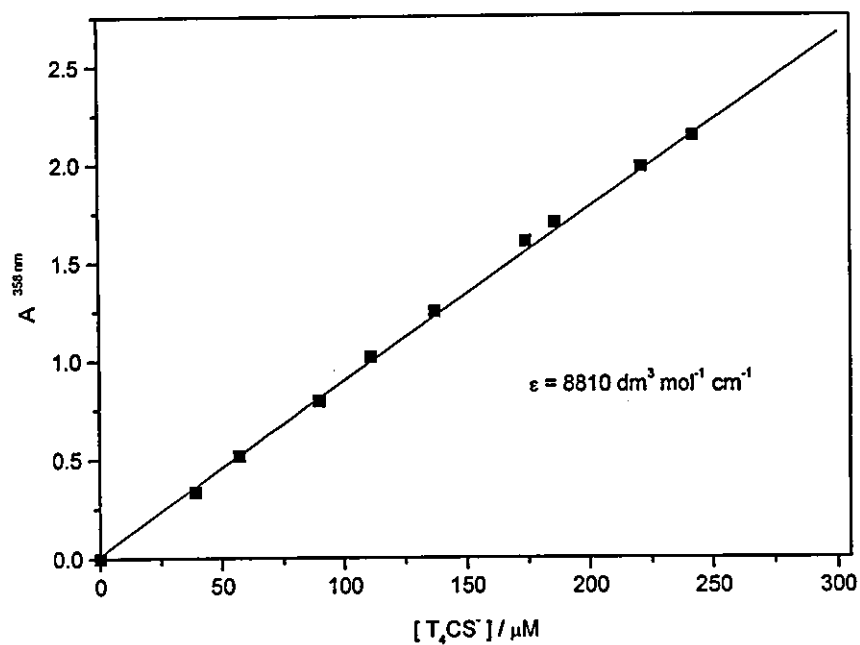


Figure (4.12) Change in absorbance at 358 nm of  $T_4CS^-$  in 10% ethanolic aqueous solution ( $\text{pH}=7.4$ ) with increasing concentration, with the Best Straight Line Fit to the data.

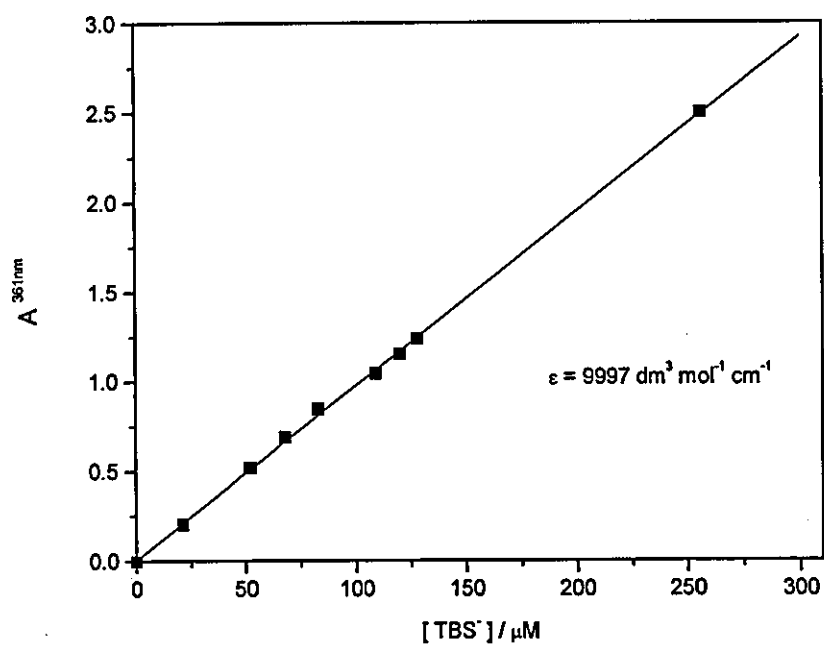


Figure (4.13) Change in absorbance at 361 nm of  $TBS^-$  in 10% ethanolic aqueous solution ( $\text{pH}=7.4$ ) with increasing concentration, with the Best Straight Line Fit to the data.

Figures (4.11- 4.13) show that Beer's law is adhered to up to concentrations of approximately 300  $\mu\text{M}$ . The excitation wavelength to be used in flash photolysis studies is 354.7 nm, where we can be sure that Beer's law is obeyed at least up to this concentration, which is more than adequate for laser flash photolysis experiments.

## 4.2 Laser Induced Degradation of $\text{T}_4\text{CS}^-$

It is well documented that following irradiation, the anion  $\text{T}_4\text{CS}^-$  undergoes cleavage of a C-Cl bond (see section 2.7), resulting in production of a chlorine radical according to:

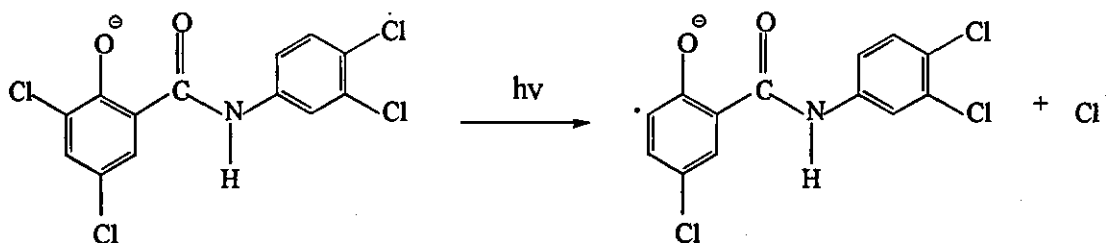
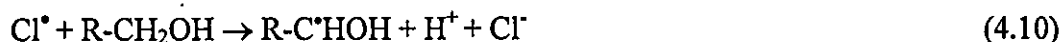


Figure (4.14) Irradiation of  $\text{T}_4\text{CS}^-$  anion, resulting in loss of the 3 - chloro atom.

Following this, reaction of  $\text{Cl}^\cdot$  and alcohol can occur according to the following:



Reaction between the alcohol radical and the  $\text{T}_3\text{CS}^{\cdot-}$  can then lead to the formation of  $\text{T}_3\text{CS-H}$ :



The resulting production of  $\text{HCl}_{(\text{aq})}$  will have the effect of lowering the pH of the system under study, thereby attenuating the ground state absorption in the 360 nm band, as was shown in figure (4.9). This pH change is not desirable for laser flash

photolysis transient absorption experiments, therefore it is necessary to use a buffer solution. It was decided to use 0.1M potassium phosphate buffer with a pH of 7.4, this pH is desirable since the salicylanilide will exist almost entirely in its ionized form (see section 4.12). A pH of 7.4 is also physiological pH and was the pH used to make up human serum albumin (HSA) solutions (for preparation see section 3.6.1). It also means that solutions can be prepared consistently and easily, knowing accurately the pH and molar absorption coefficients for particular solvent compositions.

Preliminary experiments to observe the effect of laser excitation on  $T_4CS^-$  in solution was carried out. Aerated and degassed solutions of  $T_4CS^-$  in 10% and 50% ethanol were flashed up to a 100 times, using 354.7 nm light of the JK laser, the energy being approximately 20 mJ/pulse. The ground state absorption spectrum was then recorded, and the process repeated. The resultant spectra are shown in figures (4.15) and (4.16).

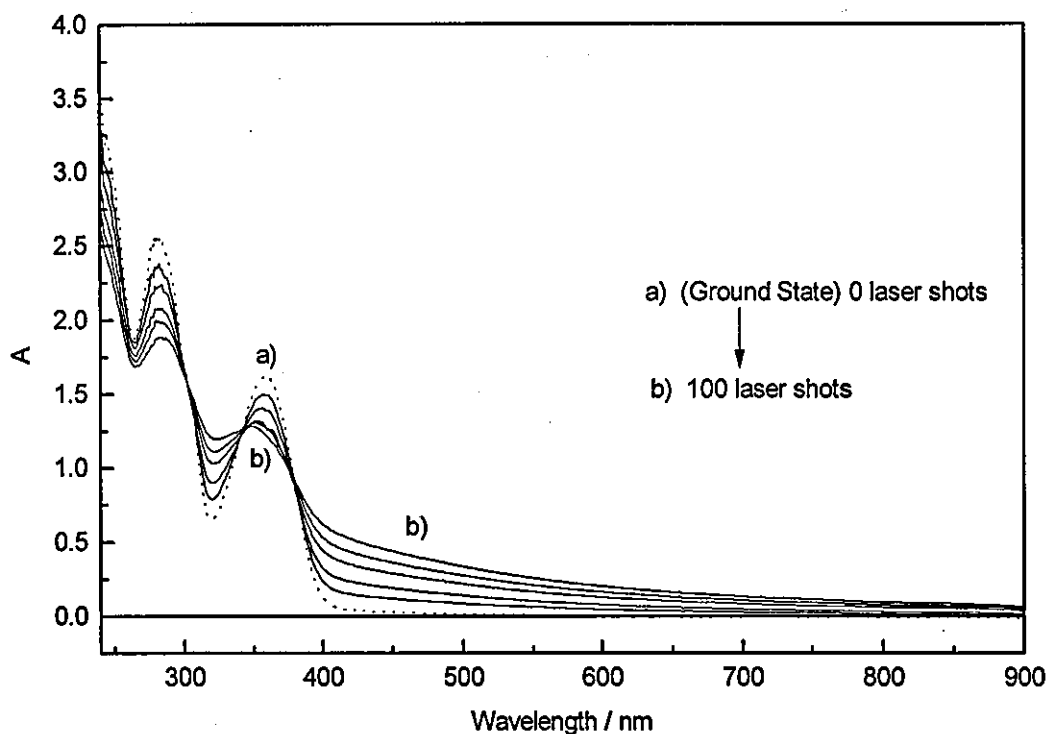


Figure (4.15) *Degradation of  $T_4CS^-$  ( $180 \mu M$ ) in a aerated 10% ethanolic aqueous solution following laser excitation at 354.7 nm.*

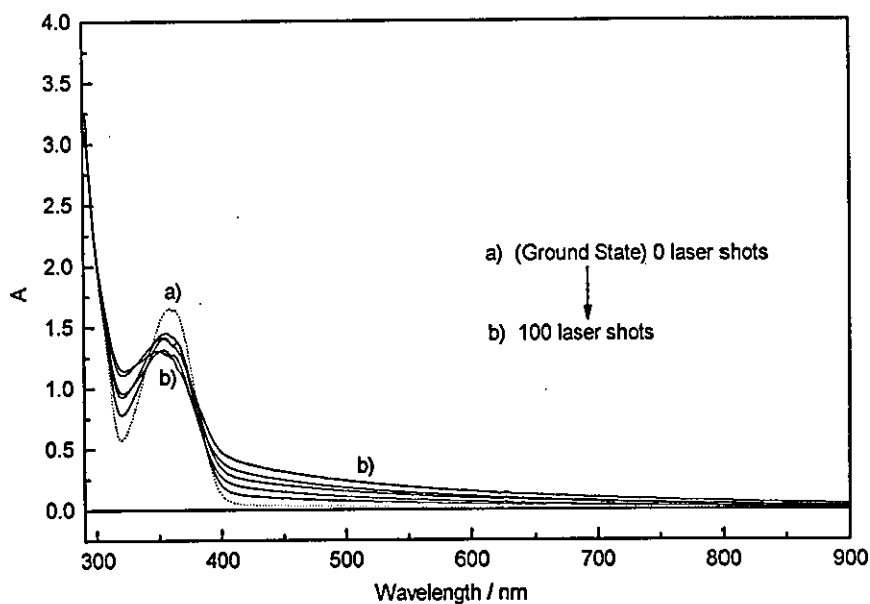


Figure (4.16) Degradation of  $T_4CS^-$  ( $180 \mu M$ ) in a degassed 10% ethanolic aqueous solution following laser excitation at 354.7 nm.

Under the same experimental conditions, aerated and degasses solutions of  $T_4CS^-$  in 50% ethanolic aqueous solutions were flashed. The resultant spectra are shown in figures (4.17) and (4.18).

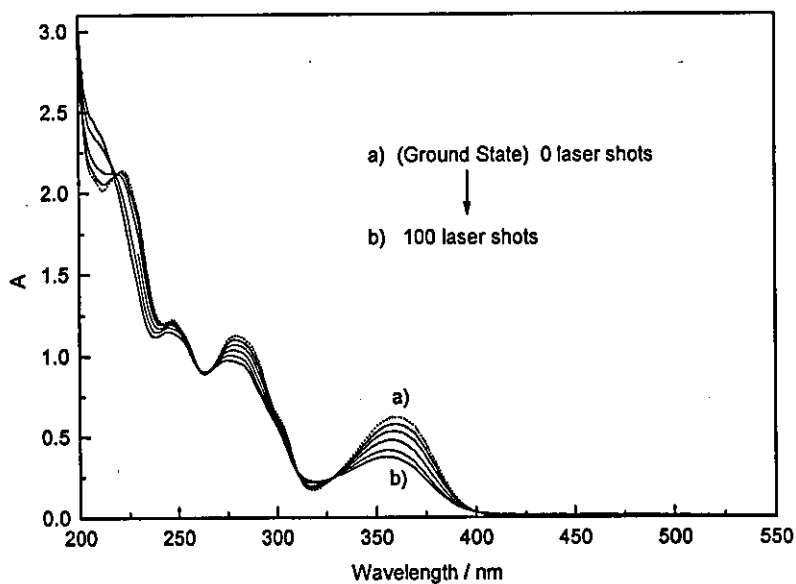


Figure (4.17) Degradation of  $T_4CS^-$  ( $70 \mu M$ ) in an aerated 50% ethanolic aqueous solution following laser excitation at 354.7 nm.



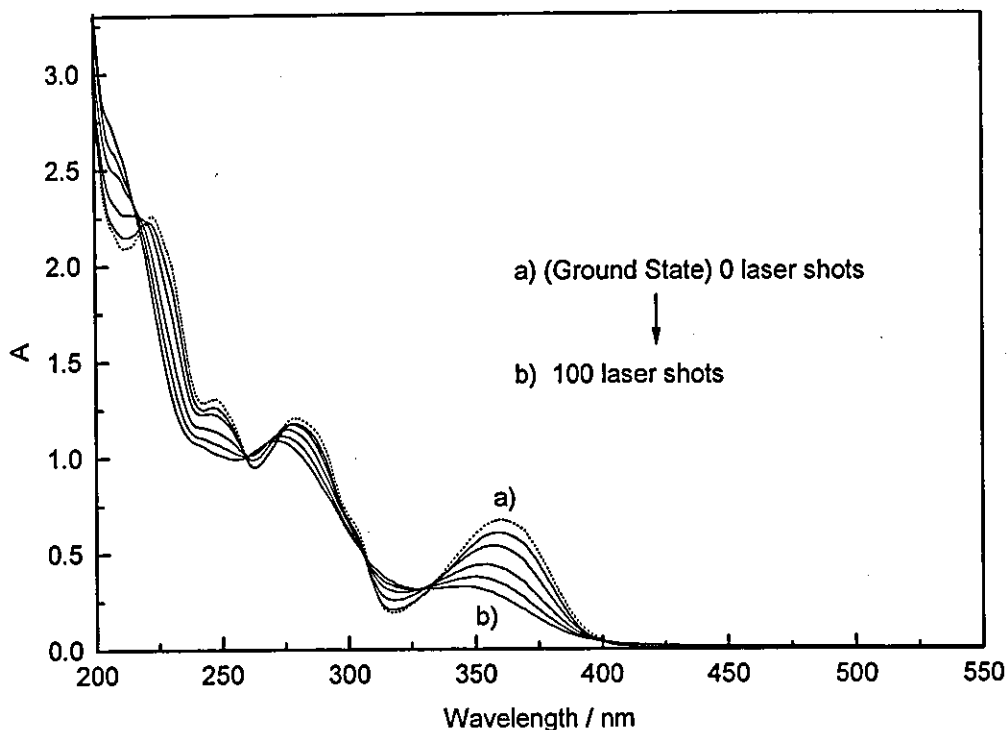


Figure (4.18) *Degradation of  $T_4CS^+$  ( $70 \mu M$ ) in an degassed 50% ethanolic aqueous solution following laser excitation at 354.7 nm.*

In the 10% ethanolic aqueous solutions there can be clearly seen a build up of degradation product, which exhibits absorption throughout the UV region extending up to 900+ nm. The degradation product is not so pronounced in the 50% ethanolic aqueous solutions. In order to observe the build up of product absorption from 400 nm onwards, it is necessary to blow up that part of the spectrum, which is shown in figure (4.19). This reveals a growth in product reaching a maximum at about 450 nm before tapering into a long tail.

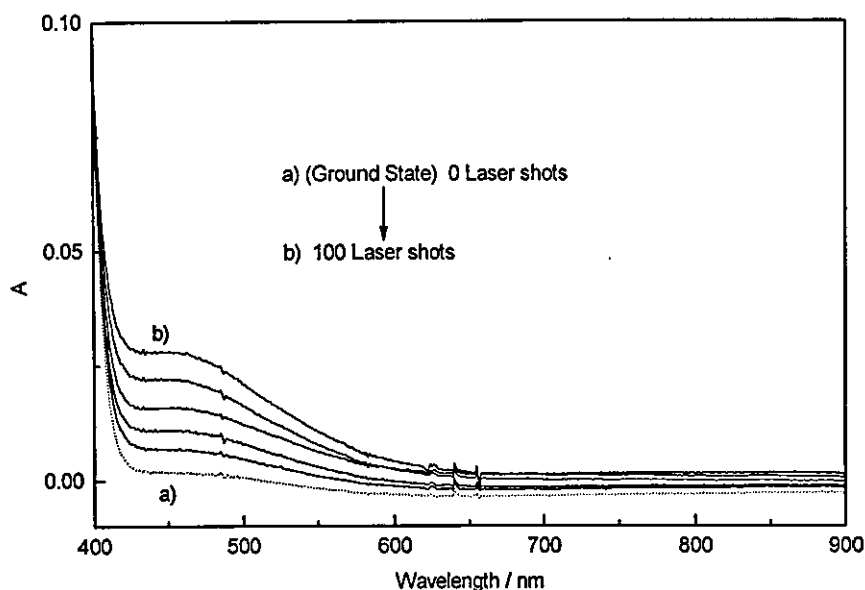


Figure (4.19) A close look at the product absorption, blown up from figure (4.18).

It is advantageous to minimise the degradation that occurs during flash photolysis experiments as much as possible. For aerated solutions degradation is not a significant problem because as long as a large enough volume of stock solution is prepared for the particular experiment in hand, because once a solution is irradiated it can be discarded and exchanged for fresh solution. But solutions held in freeze-pump-thaw cells (F-P-T) that have been degassed on the vacuum line, are enclosed systems and exchange of solution without admitting air is difficult. Conventional F-P-T cells have only one small capacity bulb for holding solutions - so once irradiated any degradation products rapidly build up. Adaptation of these cells is easily achieved, whereby a large volume bulb is used for fresh unirradiated solution and another bulb with vacuum taps fitted is used as a refuge tip for discarded solution that has been irradiated. A schematic diagram is shown in figure (4.20). This type of F-P-T cell is used throughout the thesis for any experimental work that required many laser shots of a degradable compound. An example of a transient absorption spectrum obtained using this cell is given in figure (4.28).

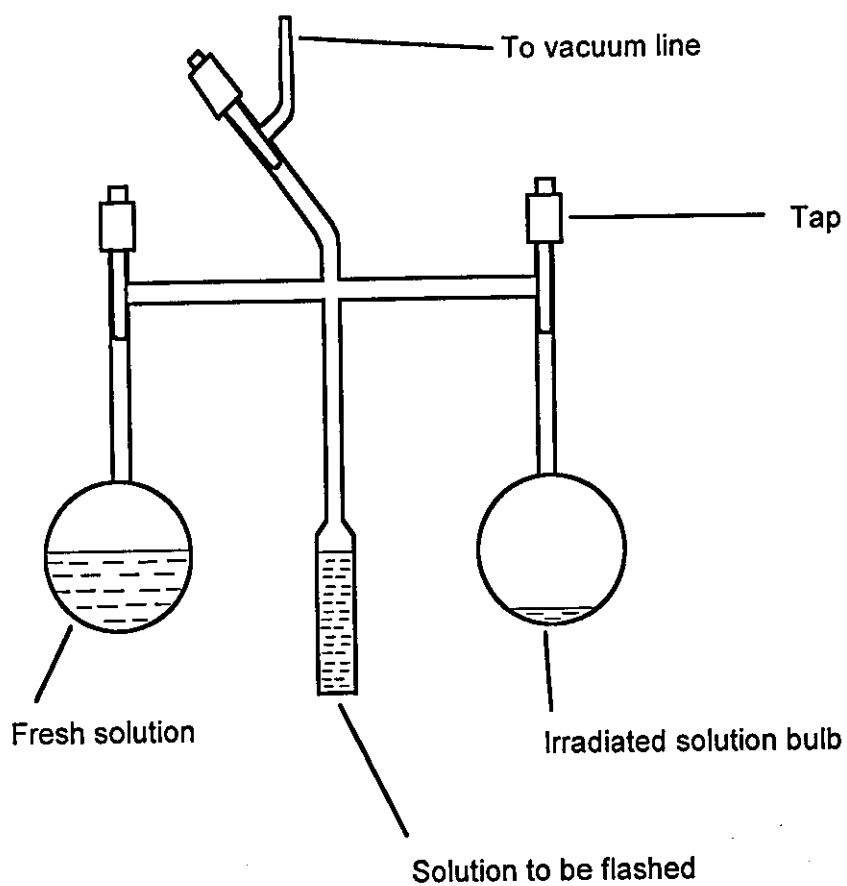


Figure (4.20) *Adapted freeze-pump-thaw cell; used for irradiating degradable solutions.*

## 4.3 Emission Spectroscopy

### 4.3.1 Fluorescence Spectra

The fluorescence spectra of tetrachlorosalicylanilide in various solvents were obtained using absorbances of approximately 0.1 at the excitation wavelength of 360 nm. The spectra along with the peak wavelength of emission are shown in figure (4.21). The spectra are independent of the excitation wavelength, *i.e.* Kasha's rule is obeyed (see section 1.18).

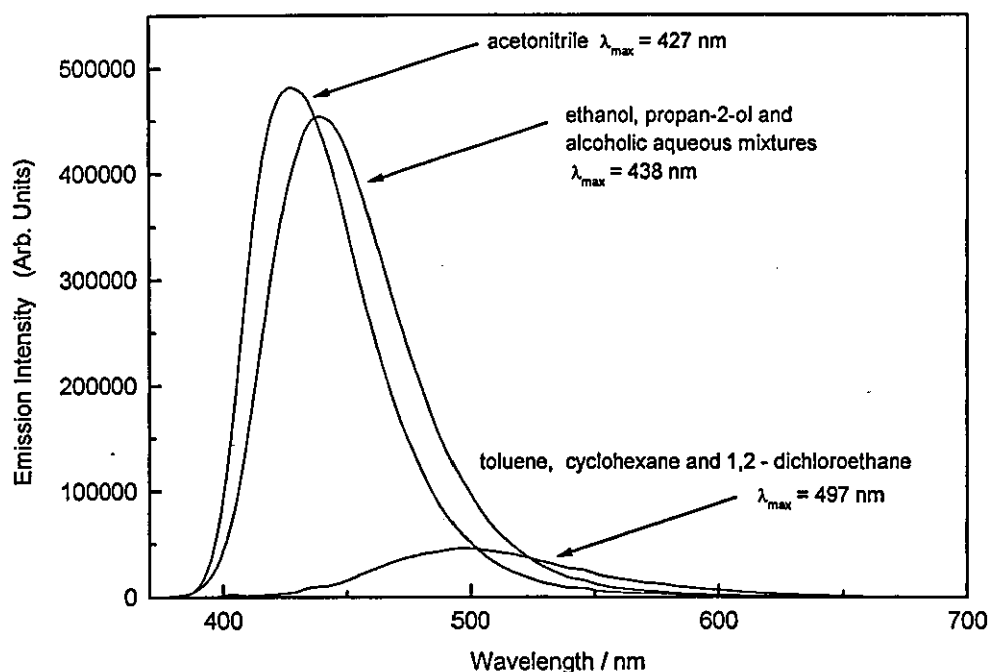


Figure (4.21) Fluorescence spectra obtained by exciting tetrachlorosalicylanilide in a selection of solvents at 360 nm.

Using the relationship:  $\Delta E = N_A hc/\lambda$ , it is possible to estimate the energy of the first excited singlet state,  $S_1$ , for tetrachlorosalicylanilide and tribromosalicylanilide (which have the same fluorescence maximum in the various solvents). This was done by using a value of  $\lambda$  obtained by the midpoint wavelength found between the absorption maximum and fluorescence maximum.

The resultant energies are tabulated below:

Solvent	$\Delta E (S_0 - S_1)$ kJ mol <sup>-1</sup>
acetonitrile	393
ethanol and propan-2-ol aqueous mixtures	300
Toluene, cyclohexane and 1,2-dichloroethane	287

**Table (4.1)** *Singlet state energies calculated in various solvents.*

### 4.3.2 Quantum yield of fluorescence

Measurements of fluorescence yields are accomplished by comparison with a fluorescence standard that absorbs and emits in the same region of the spectrum as those of the unknown. Absorbances of the sample and the standard must be similar and sufficiently dilute to prevent the occurrence of the inner filter effect (self-absorption effects). It is preferable that both unknown and standard be dissolved in the same solvent. If this is not possible, then corrections for the difference between the refractive indices of the solvents must be made according to equation (4.12). The need for refractive index corrections are due to 1) changes in the intensity of radiation as it passes from the solution into the air due to refraction and 2) internal reflection within a cell may occur.

All solutions should be tested for oxygen quenching, if oxygen quenching does occur then the solutions should be purged with oxygen free nitrogen gas or degassed on a vacuum line. Monochromatic excitation of both sample and standard should be carried out using identical excitation and emission slit widths, the former ensuring the excitation intensity impinging on both solutions will be equal.

For a typical molecule following excitation to  $S_1$  energy level:

$$\Phi_F + \Phi_T + \Phi_{IC} + \Phi_R(S_1) = 1 \quad (4.12)$$

$$\Phi_F + \Phi_T + \Phi_{IC} + \Phi_R(S_1) = 1 \quad (4.12)$$

and the fluorescence yield  $\Phi_F$  depends on  $\Phi_T$ ,  $\Phi_{IC}$  and  $\Phi_R(S_1)$  (see section 1.1.2) and is the ratio of fluorescence probability compared to triplet state formation, internal conversion and photochemical reaction probabilities. Using appropriate standards,  $\Phi_F$  for  $T_4CS^-$  and  $TBS^-$  can be calculated by measuring the area under the respective fluorescence spectra and comparing with a standard of known fluorescence quantum yield. The quantum yield of an unknown can be found using the following equation:

$$\phi_u = \left( \frac{(1 - 10^{-A_s}) F_u n^2}{(1 - 10^{-A_u}) F_s n_o^2} \right) \phi_s \quad (4.13)$$

where:

$\phi_u$  = fluorescent yield of the unknown

$\phi_s$  = fluorescent yield of the standard

$A_U, A_S$  = the absorbances of the unknown and standard at the excitation wavelength

$F_U, F_S$  = the integrated emission area across the band for the unknown and standard

$n$  = index of refraction of the solvent containing the unknown

$n_o$  = index of refraction of the solvent containing the standard

Two standards were chosen for the calculation of the fluorescence yields of  $T_4CS^-$  and  $TBS^-$ . These were: 9,10-diphenylanthracene (DPA) in cyclohexane ( $\Phi_F = 0.90$ ) [2] and quinine sulphate in N-sulphuric acid ( $\Phi_F = 0.546$ ) [3]. Their ground state absorption spectra occur in the same region of the spectrum as that of  $T_4CS^-$  and  $TBS^-$ , as do their emission spectra (see figure 4.22), so they are deemed suitable standards to use for fluorescence quantum yield determinations.

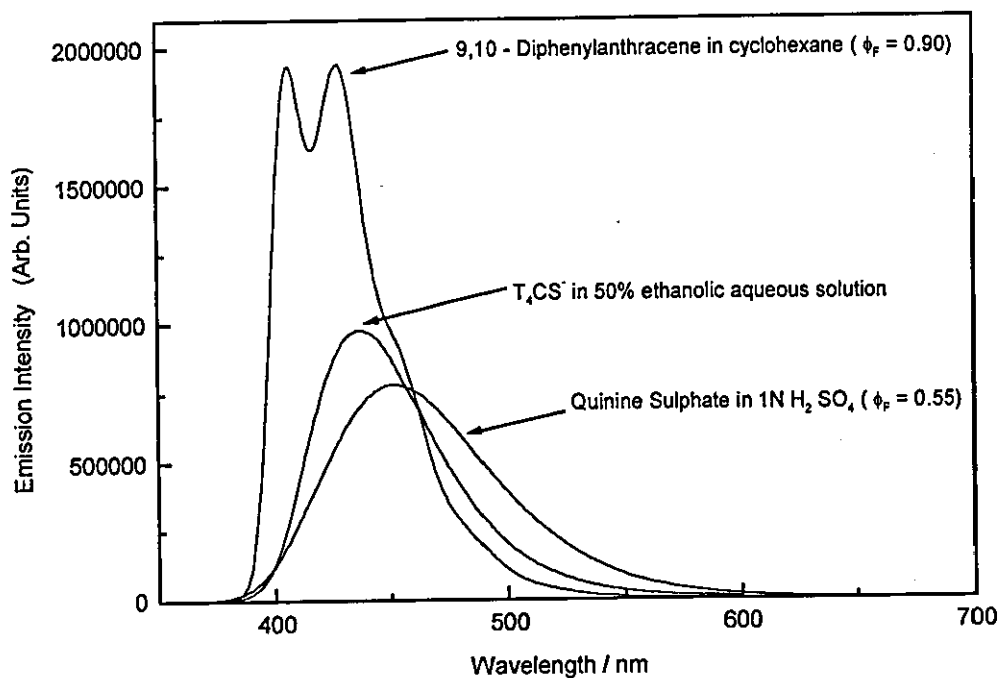


**Figure (4.22)** Emission spectra of the two standards shown with the emission spectrum of  $T_4CS^+$  for comparison.

## Experimental

Fluorescence measurements were carried out on both 10% and 50% ethanolic aqueous solutions of  $T_4CS^+$  and  $TBS^+$ , using small absorbances of approximately 0.1 at the excitation wavelength so as to avoid any self absorption effects. The parameters used were as follows:

Excitation wavelength	= 360 nm
Emission range	= 365 - 700 nm
Excitation slit	= 0.8 nm
Emission slit	= 2 nm
Integration time	= 1 nm / sec

All solutions were degassed on a vacuum line and all spectra recorded with the subtraction of a blank, *i.e.* solvent alone.

## Results

The results are displayed in table (4.2):

Compound	$\phi_F^*$	Solvent	$n_D^{20}$ *
DPA	0.90	Cyclohexane	1.422
Quinine Sulphate	0.55	1N H <sub>2</sub> SO <sub>4</sub>	1.339
T <sub>4</sub> CS <sup>-</sup>	0.50	50% ethanol	1.356
T <sub>4</sub> CS <sup>-</sup>	0.36	20% ethanol	1.343
T <sub>4</sub> CS <sup>-</sup>	0.27	10% ethanol	1.339
TBS <sup>-</sup>	0.04	50% ethanol	1.356
TBS <sup>-</sup>	0.03	10% ethanol	1.339

Table (4.2) Fluorescence yields of T<sub>4</sub>CS<sup>-</sup> and TBS<sup>-</sup> in various ethanol compositions.

An error of  $\pm 10\%$  is estimated for these measurements.

- \*  $\phi_F$  was calculated by taking an average of the values obtained from the two standards (which were within 5% of each other).
- \* The refractive indices were measured using an Abbe refractometer illuminated by means of a pearl electric light bulb.

### 4.3.3 Phosphorescence measurements

Since the first excited triplet state of a molecule is generally longer lived than the corresponding singlet state, the triplet state is often involved in the photochemical reactions of the molecule. Therefore it is of great importance to locate the T<sub>1</sub> energy. It was decided to calculate the triplet energy of both T<sub>4</sub>CS<sup>-</sup> and TBS<sup>-</sup> by excitation of these compounds in a glass at 77K, since phosphorescence is most easily observed in rigid matrices that inhibit the quenching collisions that would normally occur in fluid solutions, such as quenching by molecular oxygen.



## Experimental

$T_4CS^-$  and  $TBS^-$  were both dissolved in ethanol, the absorption at the laser excitation wavelength of 354.7 nm was approximately 0.2. The solutions were placed in 1cm x 5cm test tubes and then cooled in liquid nitrogen to form a glass. Likewise benzophenone was prepared into a glass, to use as a standard. The apparatus used to detect the emission was the diode array attachment to the HY laser system (see section 3.4).

## Results

The phosphorescence spectra recorded are shown in figures (4.23a) and (4.23b).

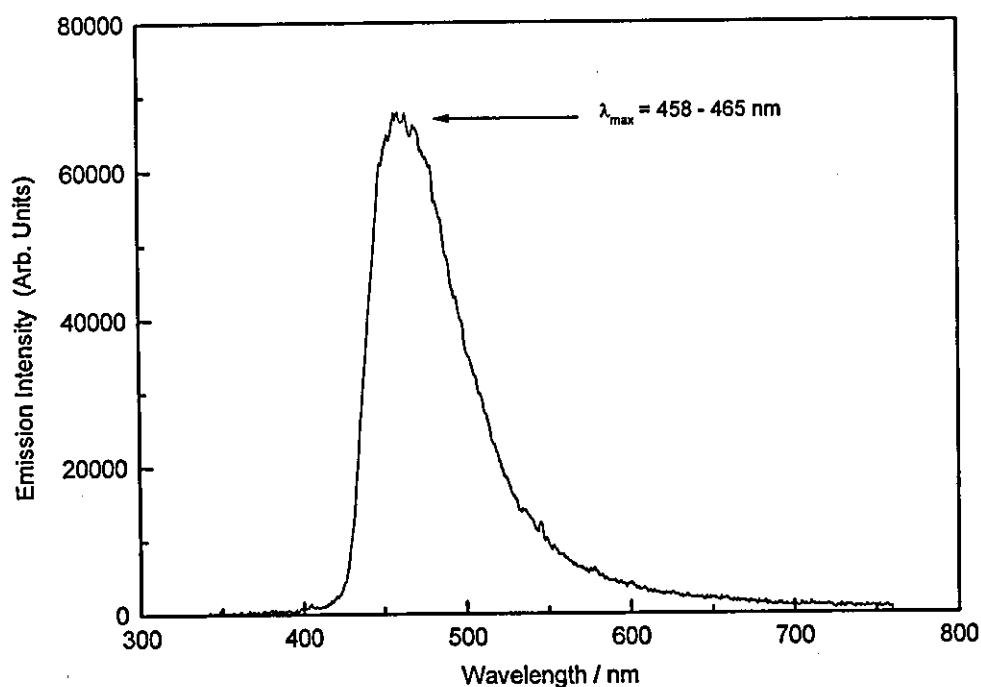
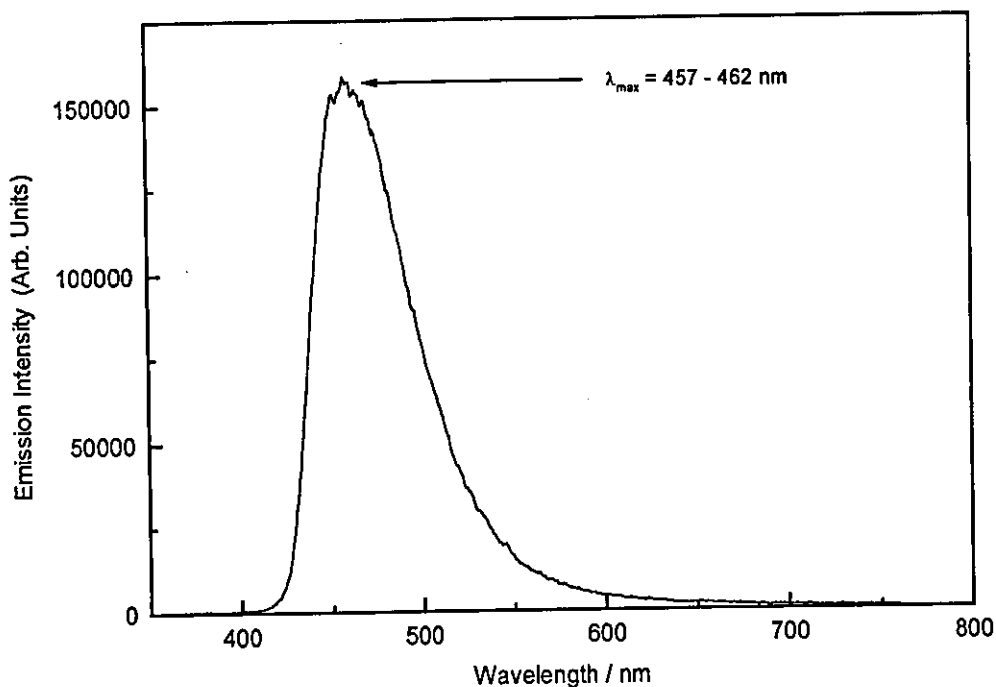


Figure (4.23a) Phosphorescence spectrum of  $T_4CS^-$  in ethanol glass (77 K), excitation wavelength 354.7 nm.



**Figure (4.23b)** *Phosphorescence spectrum of TBS<sup>-</sup> in ethanol glass (77 K), excitation wavelength 354.7 nm.*

The phosphorescence emission bands shown are broad and structureless, therefore locating the position of the 0-0 band which establishes the  $T_1-S_0$  difference is difficult but can be estimated by locating  $\lambda_{\max}$ .

For  $T_4CS^-$   $\lambda_{\max} = 458 - 463$  nm which corresponds to a triplet state energy of between  $258 - 261$   $\text{kJ mol}^{-1}$ ,  $\lambda_{\max}$  for  $TBS^- = 457 - 462$  nm corresponding to a triplet energy of between  $259 - 262$   $\text{kJ mol}^{-1}$ . These values are in accord with fluorescence measurements where  $\lambda_{\max} = 438$  nm since  $E(T_1-S_0) < E(S_1-S_0)$ . The spectrum obtained for the standard benzophenone, gave a triplet energy of  $289$   $\text{kJ mol}^{-1}$  that concurs with reported literature values [4], verifying the accuracy of the data.

#### 4.3.4 Singlet - Triplet Splitting

The singlet - triplet splitting of  $T_4CS^-$  and  $TBS^-$  in ethanolic aqueous solutions can be simply calculated from the difference in singlet state and triplet state energies. The values are given overleaf:

Compound	$\Delta E (S_1 - T_1) / \text{kJmol}^{-1}$
$T_4CS^-$	42 - 45
$TBS^-$	43 - 46

Table (4.3) *Singlet - triplet splitting energies for  $T_4CS^-$  and  $TBS^-$  in alcoholic aqueous solvents.*

The small values obtained for the singlet - triplet splitting energies are general to  $^3(n,\pi^*)$  configurations which have lower singlet - triplet energy splittings than the corresponding  $^3(\pi,\pi^*)$  configurations. For example the  $n \rightarrow \pi^*$  configuration of benzophenone and formaldehyde have singlet - triplet energy splittings of 27 and 36  $\text{kJ mol}^{-1}$  respectively, whereas for the  $\pi \rightarrow \pi^*$  configuration of naphthalene the splitting is 131  $\text{kJ mol}^{-1}$ .

## 4.4 Dark Binding Studies of $T_4CS^-$ with mHSA

The main aim of these dark binding experiments is the quantification of:

- (1) stoichiometry of binding *i.e.* the number of binding sites on the protein (mHSA) for the interacting species  $T_4CS^-$ .
- (2) affinity of the binding sites for  $T_4CS^-$ .

Calculation of the binding constant and number of binding sites due to the non-covalent association of  $T_4CS^-$  with mHSA via changes in fluorescence on binding were carried out.

### Choice of Technique

The measurement of  $T_4CS^-$  binding to mHSA by spectrophotometry requires that the optical properties of the  $T_4CS^-$  - mHSA complex differ from those of the free  $T_4CS^-$  and free mHSA. A great strength of spectrophotometric methods is that the results may be obtained instantly and the progress of an experiment modified accordingly. Another advantage is that the two components:  $T_4CS^-$  and mHSA are allowed to equilibrate and be measured in one vessel, so rapid separations of the free and bound ligand are avoided. However, there are certain drawbacks to this technique; the main disadvantage of the use of spectroscopy to measure binding is that the optical system is used empirically *i.e.* there is no prior knowledge of how large an optical change (in  $T_4CS^-$  or mHSA) is expected on binding. Nor, if multiple binding sites are present, can it be assumed that the spectral change on binding a second or third ligand molecule will be identical to that observed for the first. Fluorescence methods are potentially several orders of magnitude more sensitive than absorption methods in absolute terms. Thus, fluorescence methods require less experimental material than absorption methods and may cover a wide concentration range. Protein or ligand fluorescence is more sensitive than absorption to the environment, thus the signal change (relative sensitivity) is likely to be larger on protein-ligand interaction if a fluorophore is present. In general, changes in

absorption on binding are rather small and of limited use in spectroscopic titrations. Fluorescence despite its sensitivity to interference, was the method of choice. The dark binding experiments were carried out on a Perkin Elmer LS50 luminescence spectrometer.

#### 4.4.1 Emission Spectroscopy ( $T_4CS^-$ with mHSA)

An excitation wavelength of 360 nm was chosen, since this is the wavelength at which maximum absorption occurs the ground state spectrum of  $T_4CS^-$ . This will allow a small excitation slit width to be used, without reducing the emission intensity too much. The excitation slit width is kept narrow in order to avoid any undue photodecomposition which may occur. The emission spectrum of  $T_4CS^-$  alone and in the presence of mHSA (1:1 stoichiometry) was collected and the difference between the two spectra, from which the wavelength of maximum change can be determined is shown in figure (4.24).

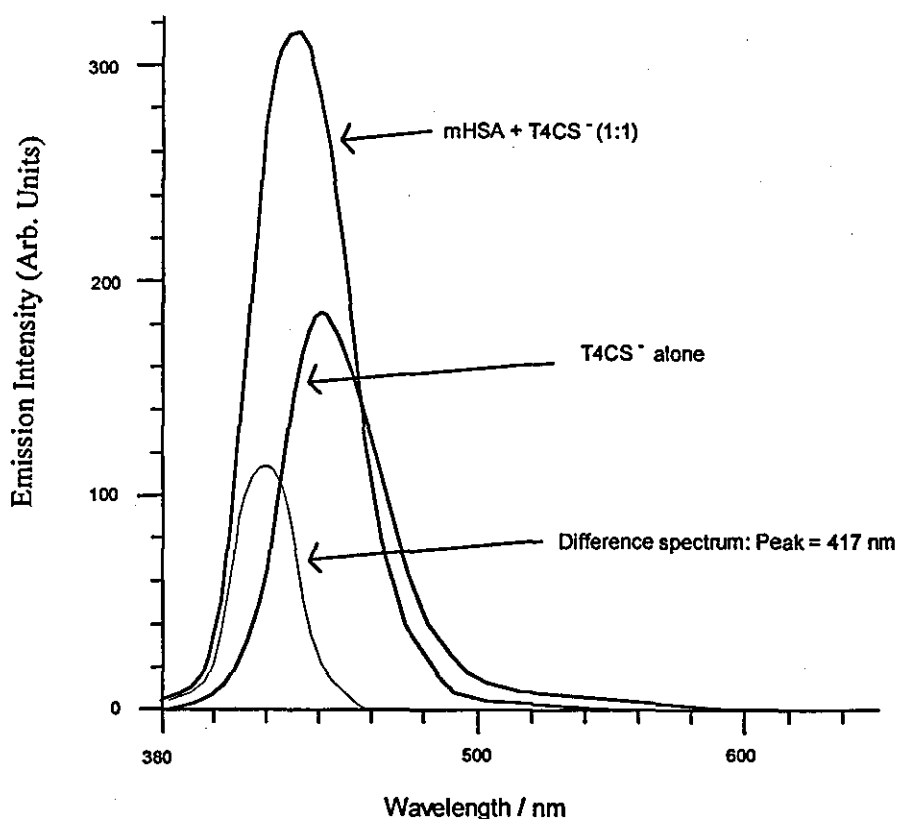


Figure (4.24) Emission spectra of  $T_4CS^-$  - mHSA conjugate,  $T_4CS^-$  alone and the difference spectrum.

An emission scan of the phosphate buffer over the range of interest was also performed, this showed no emission, so no correction was necessary. The difference spectrum, shows that the maximum change occurs at 417 nm, therefore, this was selected as the emission wavelength used for the binding experiments.

## Method

For preparation of mHSA in 0.1M potassium phosphate buffer (pH=7.4) see section (3.6.1). A preliminary titration was carried out by adding 5 $\mu$ l aliquots of T<sub>4</sub>CS<sup>-</sup> sequentially to 3ml of 0.1M potassium phosphate buffer (pH =7.4); to make sure the inner filter effect was not in operation over the desired concentration range. A linear plot was obtained, indicating that no such effect is at work.

To a fluorimeter cuvette 3ml of a known concentration of mHSA was added. A similar cell was prepared containing 3ml of buffer alone. Both cuvettes are allowed to equilibrate at 25 °C.  $\lambda_{ex}$  is set to 360 nm,  $\lambda_{em}$  is set to 417 nm (peak of difference spectrum) as previously determined. The titration is performed by adding 5 $\mu$ l aliquots of T<sub>4</sub>CS<sup>-</sup> sequentially to each cuvette over the desired range. After each addition, the cuvette was stirred and the fluorescence reading at 417 nm read. When this reading stabilized an average of 3-5 values were read and the average fluorescence intensity recorded. The fluorescence intensity after each addition of T<sub>4</sub>CS<sup>-</sup> is then plotted against the T<sub>4</sub>CS<sup>-</sup> concentration after correcting for dilution, to yield two plots. All measurements were carried out at 25 °C.

### 4.4.2 Results of Dark Binding Data

The first titration was carried out using a 0.4  $\mu$ M solution of mHSA. The resultant emission readings plotted against the T<sub>4</sub>CS<sup>-</sup> concentration are shown in figure (4.25). The corresponding blank titration is shown in figure (4.26).

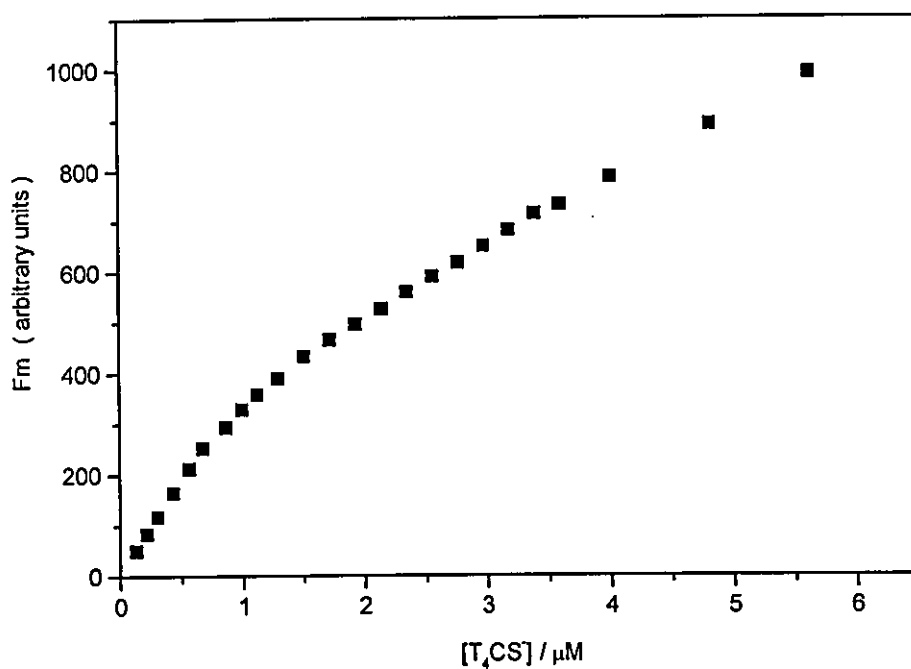


Figure (4.25) Plot to show the emission intensity recorded at 417 nm as  $T_4CS^-$  was titrated with a  $0.4\mu M$  mHSA solution, as a function of  $T_4CS^-$  concentration.

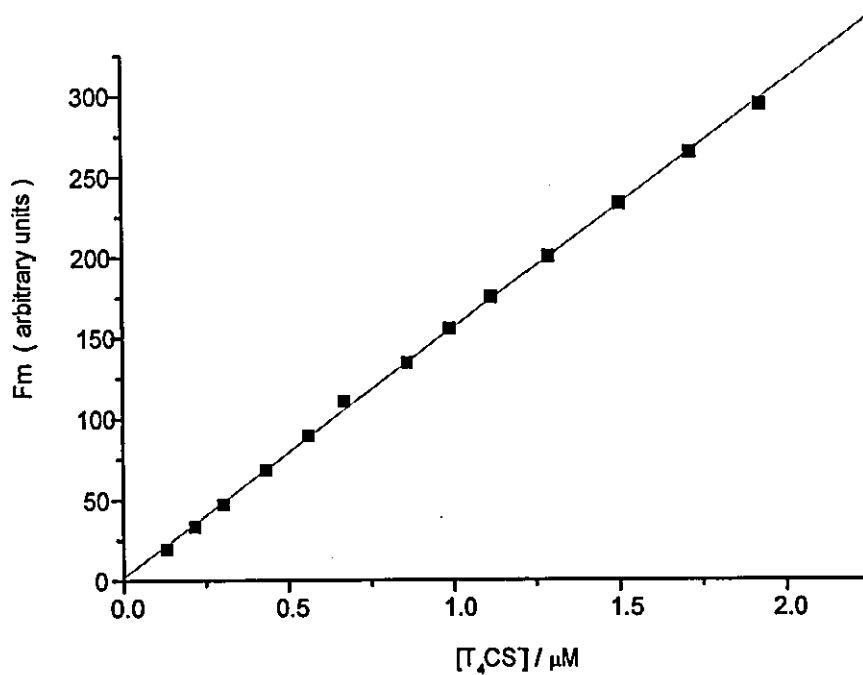


Figure (4.26) Plot to show the emission intensity recorded at 417 nm of  $T_4CS^-$  as a function of increasing  $T_4CS^-$  concentration, with the Best Straight Line Fit to the data.

The second titration was carried out using a 2.1  $\mu\text{M}$  solution of mHSA. The resultant emission readings plotted against  $\text{T}_4\text{CS}^-$  concentration are shown in figure (4.27).

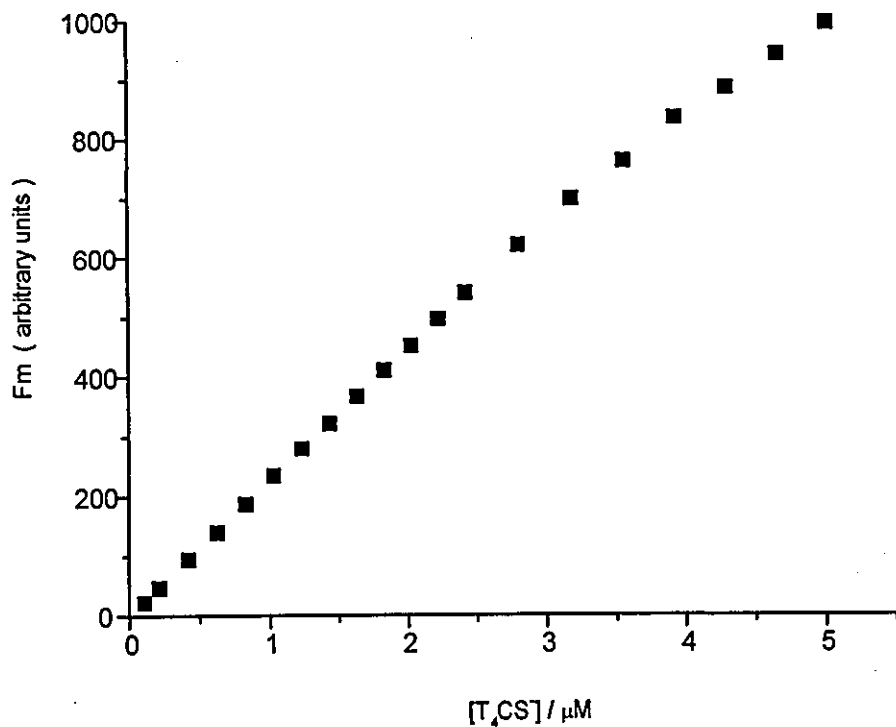


Figure (4.27) Plot to show the emission intensity recorded at 417 nm as  $\text{T}_4\text{CS}^-$  was titrated with a 2.1  $\mu\text{M}$  mHSA solution, as a function of  $\text{T}_4\text{CS}^-$  concentration.

#### 4.4.3 Analysis of Data

The equilibrium can be represented as:





where:

$l^{\circ}$ ,  $l$  = total, free concentration of added  $T_4CS^-$  at equilibrium

$b$  = concentration of bound  $T_4CS^-$

$e^{\circ}$  = total concentration of binding sites for  $T_4CS^-$

$e$  = concentration of free binding sites at equilibrium

The fluorescence intensity measured, denoted by  $F_m$  is given by:

$$F_m = bF^b + (l^{\circ} - b) F^u \quad (4.14)$$

where:

$F^b$  = fluorescence increase per  $\mu M$  of bound  $T_4CS^-$  (tangent of early part of curve, where it is assumed all  $T_4CS^-$  is bound.)

$F^u$  = fluorescence increase per  $\mu M$  of unbound  $T_4CS^-$  (gradient of blank titration).

The binding dissociation constant is given by:

$$K_d = [T_4CS^-] [mHSA] / [T_4CS^- \cdot mHSA] \quad (4.15)$$

or

$$K_d = el / b \quad (4.16)$$

This can be written as:

$$K_d = (e^{\circ} - b) (l^{\circ} - b) / b \quad (4.17)$$

$\Rightarrow$

$$K_d = (b^2 - (e^{\circ} + l^{\circ}) b + e^{\circ} l^{\circ}) / b \quad (4.18)$$

This can be rearranged to give:

$$b^2 - (e^{\circ} + l^{\circ} + K_d) b + e^{\circ} l^{\circ} = 0 \quad (4.19)$$

Solving quadratically gives:

$$b = ((e^0 + I^0 + K_d) \pm [(e^0 + I^0 + K_d)^2 - 4e^0 I^0]^{1/2}) / 2 \quad (4.20)$$

Equation (4.20) can be substituted into equation (4.14).

A computer program was written by Dr. D.R. Worrall here in Loughborough to fit the plots shown in figures (4.25) and (4.27) according to equation (4.14). This was done where the parameters from equation (4.14) can be made variable or set.

#### Data set no. 1

The first set of binding data (figures 4.25 and 4.26) produced the following values:

$$F^u = 153$$

$$F^b = 373$$

The program which resulted in the best fit and closest agreement with the calculated  $F^u$  and  $F^b$  values, was obtained using a program which fitted all the parameters. This gave the following values:

$$F^u = 126$$

$$e^0 = 0.83$$

$$F^b = 490$$

$$K_d = 0.2$$

Where the total number of binding sites ( $e^0 = 0.83 \mu\text{M}$ ). Since the actual concentration of mHSA used in the titration was  $0.4 \mu\text{M}$  then the number of binding sites per mHSA molecule is two, with a corresponding binding dissociation constant,  $K_d$ , of  $0.2 \mu\text{M}$ .

### Data set no. 2

The second set of binding data (figure 4.27) yielded the following values:

$$F^u = 79$$

$$F^b = 232$$

Similarly the program which resulted in the best fit and closest agreement with the calculated  $F^u$  and  $F^b$  values was obtained using a program which fixed  $F^u$  but varied the other parameters. The following values were obtained:

$$F^u = 79$$

$$e^o = 4.43$$

$$F^b = 237$$

$$K_d = 0.2$$

For the second titration the total number of binding sites:  $e^o = 4.43 \mu\text{M}$ , the actual concentration of mHSA used was  $2.1 \mu\text{M}$ , therefore the calculated number of binding sites per mHSA molecule is two with binding dissociation constants of  $K_d$  of  $0.2 \mu\text{M}$ .

These results can be compared with the findings of Rickwood and Barratt [5] who investigated the non-covalent binding of a spin analogue of  $T_4CS^-$  to mHSA (see section 2.6) and reported a strong binding site with  $K_a = 6.1 \times 10^6 \text{ M}^{-1}$  or  $K_d = 0.16 \mu\text{M}$ , but report a number of additional sites with much lower binding constants.

## 4.5 FLASH PHOTOLYSIS STUDIES

### 4.5.1 Excited State Photochemistry of $T_4CS^-$ in Solution

The molar absorption coefficients of the anion of  $T_4CS-H$  in various alcoholic / buffer solvent compositions were found to be in the region of  $9000 \text{ dm}^3 \text{ mol}^{-1} \text{ cm}^{-1}$  at the laser excitation wavelength of  $354.7 \text{ nm}$  (see section 4.1.3). Therefore, a ground state concentration of approximately  $70\text{-}100 \text{ }\mu\text{M}$  is required to gain sufficient absorbance in order to perform laser flash photolysis experiments.

$T_4CS^-$  in 50% ethanolic aqueous solution was prepared, the ground state absorbance at the laser excitation wavelength was 0.70. Using a laser energy of  $50 \text{ mJ/pulse}$ , the transient absorption spectrum of a degassed solution at five time delays is shown in figure (4.28).

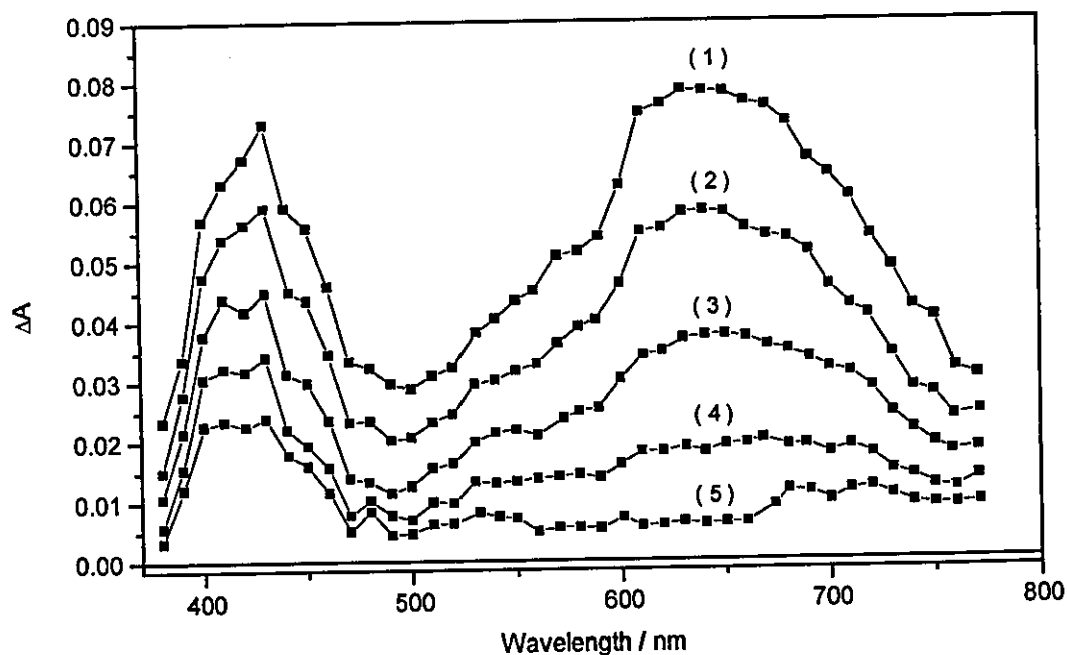


**Figure (4.28)** *Transient absorption spectrum of  $T_4CS^-$  in a degassed 50% ethanolic aqueous solution at five time delays following the laser pulse. Delay times are (1)  $1.3 \mu\text{s}$ . (2)  $3.2 \mu\text{s}$ . (3)  $7.0 \mu\text{s}$ . (4)  $14.6 \mu\text{s}$ . (5)  $45.3 \mu\text{s}$ .*

Following laser excitation, transient absorption is observed throughout the visible region; the spectrum appears to consist of two bands: the shorter wavelength band has  $\lambda_{\text{max}} = 440 \text{ nm}$ , the longer wavelength band has  $\lambda_{\text{max}} = 650 \text{ nm}$ . There appears to be at least some residual absorption right across the spectrum - being far greatest between the wavelengths of 400 - 460 nm. In addition, flash photolysis studies using identical experimental parameters performed on aerated solutions, produced the transient absorption spectrum shown in figure (4.29). The aerated transient absorption spectrum again shows residual absorption right across the spectrum, however, only the shorter wavelength band ( $\lambda_{\text{max}} = 440 \text{ nm}$ ) is observed but with approximately a 50% reduced absorbance change and the long wavelength band ( $\lambda_{\text{max}} = 650 \text{ nm}$ ) is almost completely gone.

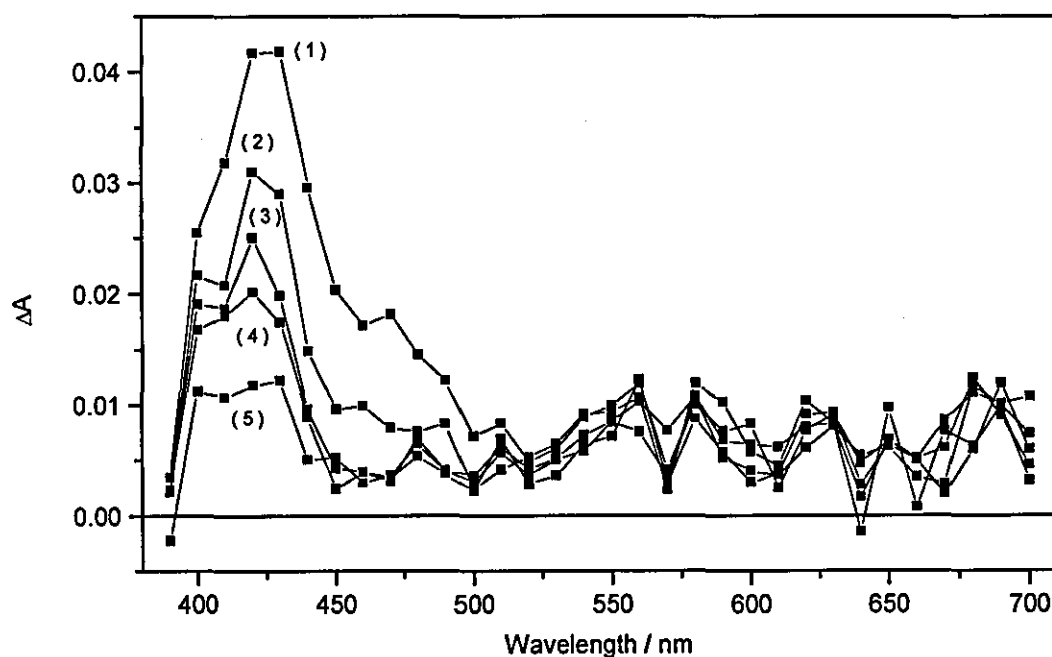


**Figure (4.29)** *Transient absorption spectrum of  $T_4CS^-$  in an aerated 50% ethanolic aqueous solution at five time delays following the laser pulse. Delay times are (1)  $1.3 \mu\text{s}$ . (2)  $3.2 \mu\text{s}$ . (3)  $7.0 \mu\text{s}$ . (4)  $14.6 \mu\text{s}$ . (5)  $45.3 \mu\text{s}$ .*

#### 4.5.2 Analysis of the Long Wavelength Band ( $\lambda_{\text{max.}} = 650 \text{ nm}$ )

Nanosecond flash photolysis was carried out on degassed 50% ethanolic aqueous solutions, using a laser energy of approximately 19 mJ/pulse. The resultant traces when analyzed at 650 nm, gave mixed first and second order kinetics - the second order component believed to arise from triplet-triplet annihilation. In order to reduce this second order component the laser energy was attenuated by means of sodium nitrite filters placed in front of the laser beam. The optimum laser energy for a good first order decay was found to be approximately 10 mJ/pulse; this however, resulted in a low signal to noise ratio - but was improved by recording many traces and averaging. The first order rate constant for the intramolecular deactivation of the excited  $T_4CS^*$  transient was found to be  $1.2 \times 10^5 \text{ s}^{-1}$  corresponding to a lifetime of 8.3  $\mu\text{s}$ . The decay is given in figure (4.30).

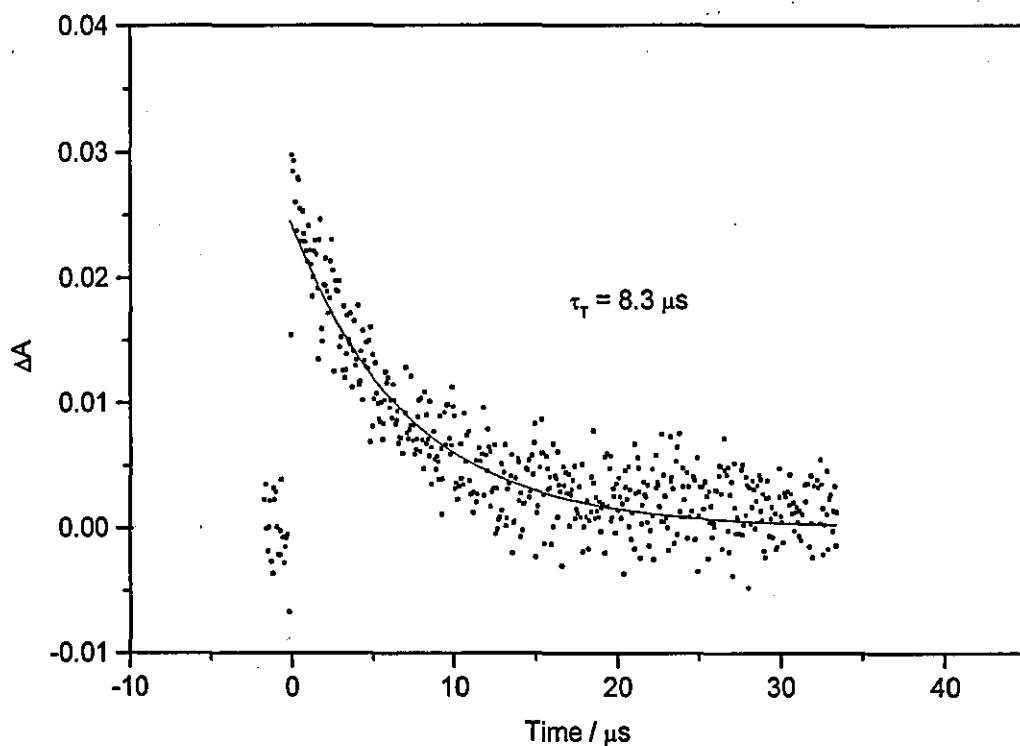


Figure (4.30) Decay and fitting of the  $T_4CS^*$  transient signal analysed at 650 nm.

The experiment was repeated, only this time flash exciting an aerated solution. Fitting the decay by first order kinetics results in a rate constant of  $3.3 \times 10^6 \text{ s}^{-1}$  - corresponding to a lifetime of  $0.3 \mu\text{s}$ .

The oxygen quenching rate constant is given in the equation:

$$k = k_d + k_{O_2} [O_2] \quad (4.21)$$

where:

$k$  = rate constant in the presence of  $O_2$

$k_d$  = rate constant in the absence of  $O_2$

$k_{O_2}$  = oxygen quenching rate constant

$[O_2]$  = oxygen concentration

Values for the rate constants obtained from the decay of  $T_4CS^*$  excited state, in the presence and absence of oxygen are:

$$k = 3.3 \times 10^6 \text{ s}^{-1}$$

$$k_d = 1.2 \times 10^5 \text{ s}^{-1}$$

The oxygen concentrations in aerated solution are given by:

$$[O_2] \text{ in water} = 0.29 \times 10^{-3} \text{ mol / dm}^3 \text{ [6]}$$

$$[O_2] \text{ in ethanol} = 2.10 \times 10^{-3} \text{ mol / dm}^3 \text{ [6]}$$

The estimated oxygen concentration in an aerated 50% ethanolic aqueous solution (using a simple v/v ratio) =  $0.61 \times 10^{-3} \text{ mol / dm}^3$ . With these values the oxygen rate quenching constant,  $k_{O_2}$ , is calculated as  $5.2 \times 10^9 \text{ dm}^3 \text{ mol}^{-1} \text{ s}^{-1}$ .

It is well known that molecular oxygen is a strong quencher of triplet states, ranging from approximately  $1 \times 10^9 \text{ dm}^3 \text{ mol}^{-1} \text{ s}^{-1}$ , e.g. 2-methyl-1,4-naphthoquinone in  $H_2O$  [7] to

approximately  $1 \times 10^{10} \text{ dm}^3 \text{ mol}^{-1} \text{ s}^{-1}$ , e.g. indole in cyclohexane [8]. The value obtained ( $5.2 \times 10^9 \text{ dm}^3 \text{ mol}^{-1} \text{ s}^{-1}$ ) lies in this range - strongly suggesting that in the transient absorption spectrum of degassed solutions, the long wavelength band ( $\lambda_{\text{max}} = 650 \text{ nm}$ ) is due to the excited triplet state of  $\text{T}_4\text{CS}^-$  and the shorter wavelength band ( $\lambda_{\text{max}} = 430 \text{ nm}$ ) appears to be a combination of both triplet state absorption and a much longer lived component whose lifetime is not quenched by molecular oxygen. This would explain why on these time-scales in aerated solutions the long wavelength band is lost and there is a reduction in absorption of the shorter wavelength band.

Figure (4.31) shows the transient absorption spectrum at four time delays of  $\text{T}_4\text{CS}$  in a degassed 10% ethanolic aqueous solution. The ground state absorption at the laser excitation wavelength was 0.83, the laser energy was approximately 35 mJ/pulse.

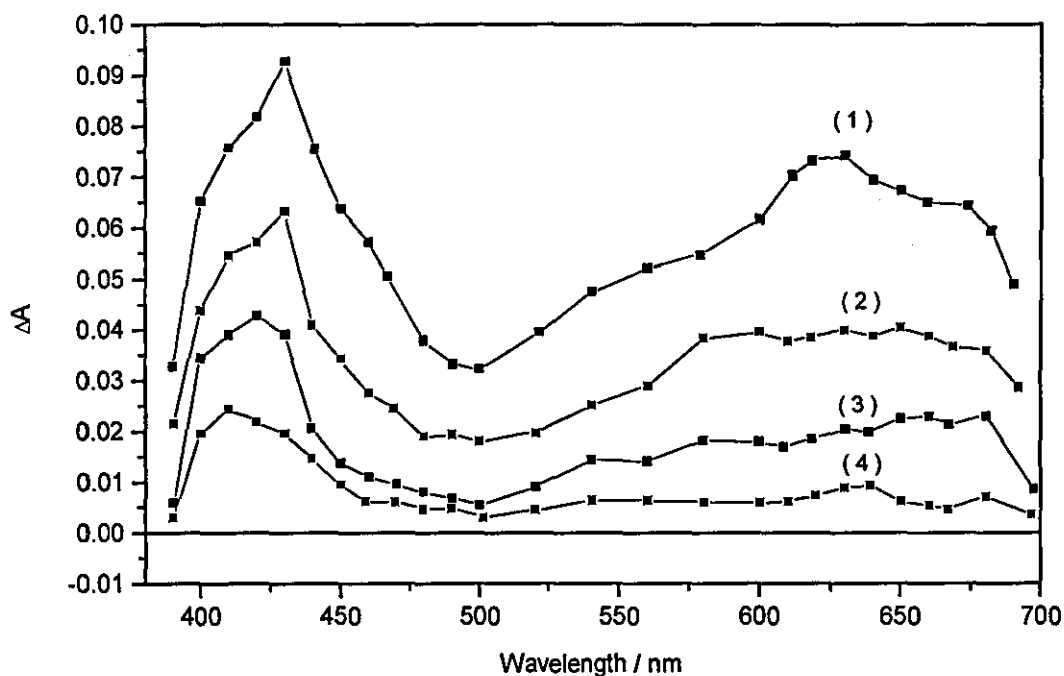


**Figure (4.31)** *Transient absorption spectrum of  $\text{T}_4\text{CS}^-$  in a degassed 10% ethanolic aqueous solution at five time delays following the laser pulse. Delay times are (1)  $1.3 \mu\text{s}$ . (2)  $3.2 \mu\text{s}$ . (3)  $7.0 \mu\text{s}$ . (4)  $14.6 \mu\text{s}$ . (5)  $45.3 \mu\text{s}$ .*



In addition, flash photolysis studies using identical experimental parameters performed on aerated solutions, produced the transient absorption spectrum shown in figure (4.32).

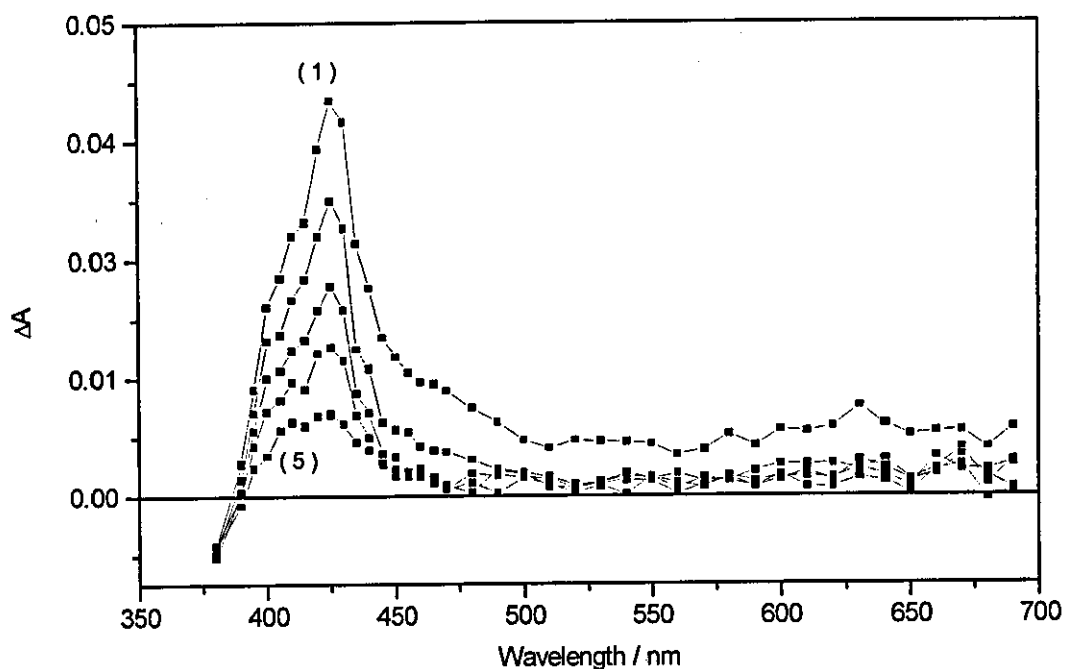


**Figure (4.32)** *Transient absorption spectrum of  $T_4CS^-$  in an aerated 10% ethanolic aqueous solution at five time delays following the laser pulse. Delay times are (1)  $1.3\mu s$ . (2)  $3.2\mu s$ . (3)  $7.0\mu s$ . (4)  $14.6\mu s$ . (5)  $45.3\mu s$ .*

When the alcohol content of the mixed solvent is reduced, the lifetime of the triplet state of  $T_4CS^-$  is reduced. Shown in figure (4.33) is the decay and first order fitting of the  $T_4CS^-$  triplet state in a degassed 10% ethanolic aqueous solution analysed at 650 nm. The lifetime is approximately  $3\mu s$ . In aerated solutions the lifetime of the triplet state was found to be quenched by molecular oxygen to approximately  $0.5\mu s$ .

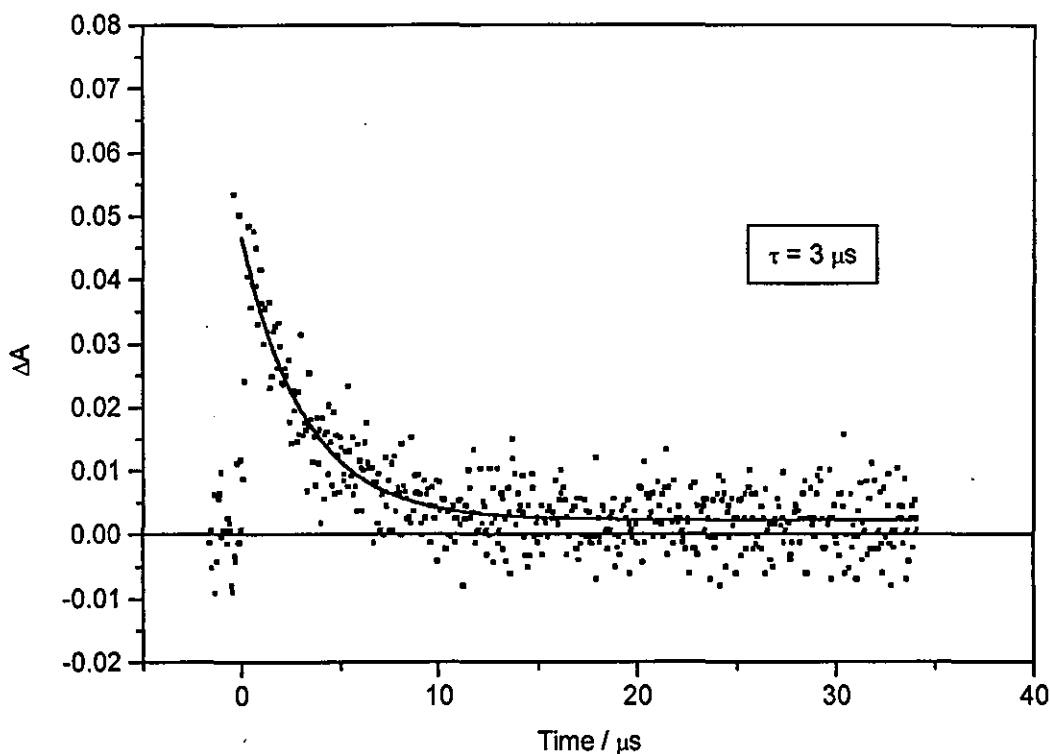


**Figure (4.33)** *Decay and fitting of the  $T_1CS^{\cdot}$  triplet state, analyzed at 650 nm in a degassed 10% ethanolic aqueous solution.*

Again using the equation:  $k = k_d + k_{O_2} [O_2]$ , the value of  $k_{O_2}$  can be calculated using the following values:

$$k = 2.0 \times 10^6 \text{ s}^{-1}$$

$$k_d = 3.3 \times 10^5 \text{ s}^{-1}$$

Estimated  $[O_2]$  in 10% ethanolic aqueous solution using a simple v/v ratio =  
 $3.54 \times 10^{-3} \text{ mol / dm}^{-3}$  [6]

This results in a value for  $k_{O_2}$ , of  $3.5 \times 10^9 \text{ dm}^3 \text{ mol}^{-1} \text{ s}^{-1}$ .

### 4.5.3 Triplet - Triplet Energy Transfer

Triplet-triplet energy transfer can occur when the relative energies of the lowest excited states of the donor and acceptor are as shown in figure (4.34).

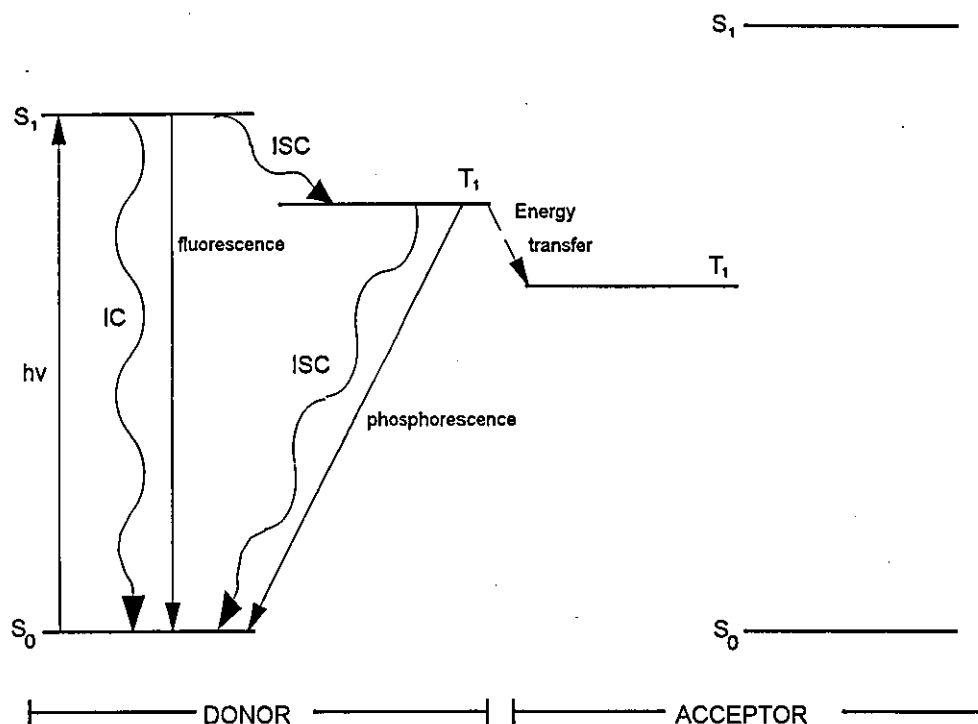
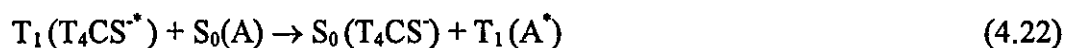


**Figure (4.34)** Favourable arrangement of donor-acceptor energy levels for triplet-triplet energy transfer.

Hence, energy transfer from the  $S_1$  state of the donor to the  $S_1$  and to the  $T_1$  of the acceptor are energy and spin forbidden respectively and are inefficient processes compared to  $T_1 - T_1$  transfer which is both energy and spin allowed for the situation in figure (4.34). Similarly, transfer from the  $T_1$  state of the donor to the  $S_1$  state of the acceptor will be highly inefficient since this process is both energy and spin forbidden. The energy transfer between  $T_4CS^*$  excited triplet state and an acceptor molecule (A) can be represented as:



Rate constants for triplet-triplet energy transfer can be obtained from flash photolysis measurements by selectively exciting the donor in the presence of an acceptor and comparing the transient absorption spectrum of the mixture at suitable times after flashing with that of a flash excited solution of the donor alone. At low triplet concentrations of donor when there is no self-quenching of triplet states (*i.e.* no second order kinetics), the rate of decay of the triplet state will be equal to the sum of the rates of intramolecular and intermolecular deactivation processes as expressed by the equation:

$$-\frac{d}{dt}[T_1] = k_d[T_1] + k_q[T_1][Q] \quad (4.23)$$

where:  $k_d$  = the overall rate constant for intramolecular deactivation of the  $T_1$  state

$k_q$  = the rate constant for triplet-triplet energy transfer

$[Q]$  = the concentration of quencher

$[T_1]$  = the concentration of donor triplet

The first order rate constant,  $k$ , for the decay of the triplet in presence of quencher for the above processes is given by the equation:

$$k = k_d + k_q [Q] \quad (4.24)$$

So a plot of  $k$  versus  $[Q]$  should give a straight line of slope  $k_q$  and intercept  $k_d$ .

## Naphthalene as Quencher

It was decided to see if naphthalene ( $E_T = 254 \text{ kJ mol}^{-1}$ ) [9] whose triplet energy is lower than that calculated for  $T_4CS$  from phosphorescence measurements (section 4.3.3) would quench the signal attributed to the triplet state of  $T_4CS^*$ . Naphthalene being a suitable acceptor molecule because its ground state shows no absorption at the laser excitation wavelength of 354.7 nm, therefore all the exciting radiation will be absorbed solely by the donor. A transient absorption spectrum of a degassed 50% propan-2-ol aqueous solution of  $T_4CS$  with naphthalene added ( $150 \mu\text{M}$ ) was recorded and is shown in figure (4.35). For comparison using identical experimental parameters the transient absorption spectrum of  $T_4CS^*$  alone is shown in figure (4.36) at the same time delays. What is clear from examining the long wavelength band ( $\lambda_{\text{max}}$  650 nm) in each spectrum, is that the triplet state of  $T_4CS^*$  is being quenched by the naphthalene.

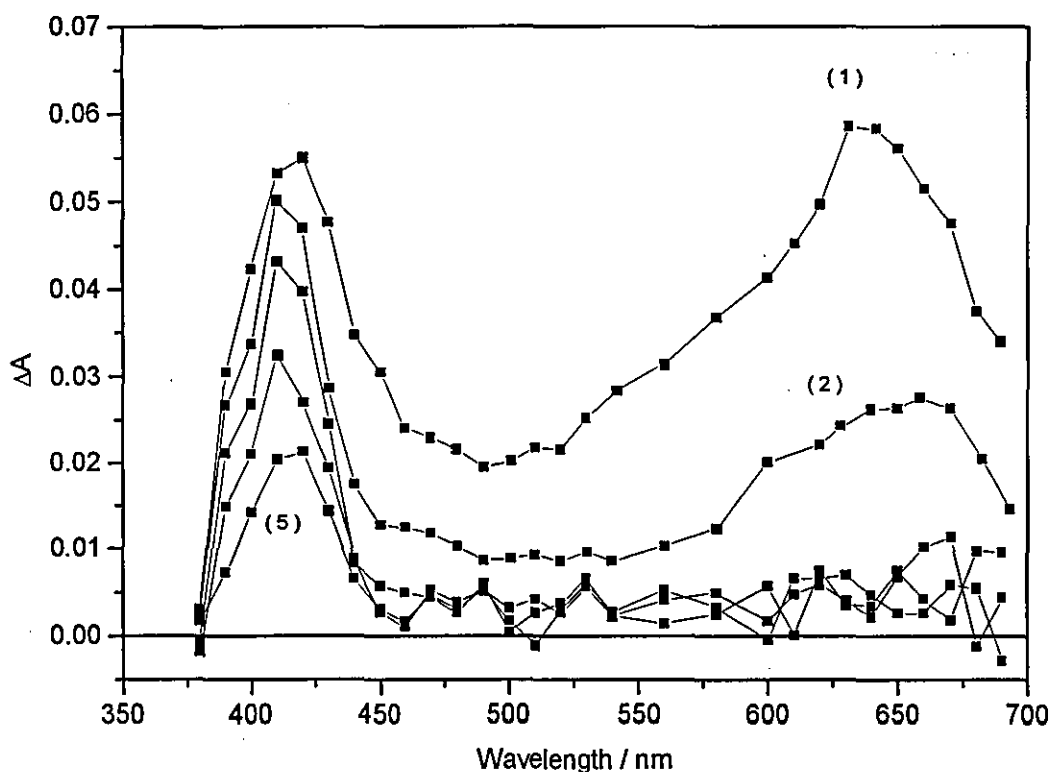


**Figure (4.35)** *Transient absorption spectrum of  $T_4CS^*$  with naphthalene added ( $150 \mu\text{M}$ ) to a degassed 50% propan-2-ol aqueous solution at five time delays following the laser pulse. Delay times are (1)  $1.4 \mu\text{s}$ . (2)  $5.3 \mu\text{s}$ . (3)  $7.7 \mu\text{s}$ . (4)  $16.0 \mu\text{s}$ . (5)  $39.0 \mu\text{s}$ .*

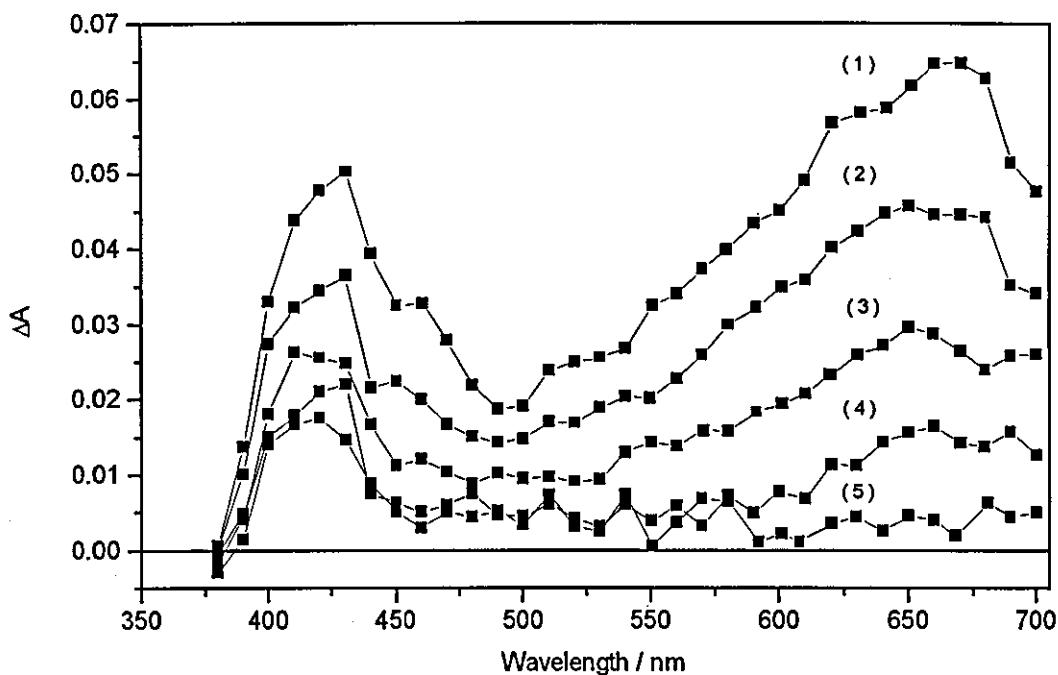


**Figure (4.36)** *Transient Absorption Spectrum of  $T_4CS^-$  in a degassed 50% propan-2-ol aqueous solution at five time delays following the laser pulse. Delay times are (1) 1.4  $\mu s$ . (2) 5.3  $\mu s$ . (3) 7.7  $\mu s$ . (4) 16.0  $\mu s$ . (5) 39.0  $\mu s$ .*

There is overlap between  $T_4CS^-$  and naphthalene transient absorption; naphthalene's triplet-triplet transient absorption is well documented as occurring in the region 400 - 430 nm of the spectrum [10]. This is well below the long wavelength band ( $\lambda_{max} = 650$  nm) for  $T_4CS^-$ , and therefore this wavelength can be selected to analyse the  $T_4CS^-$  triplet-triplet absorption free from any naphthalene signal.

### **Experimental for Naphthalene Quenching**

Solutions of T<sub>4</sub>CS in 50% propan-2-ol with various concentrations of naphthalene (14 - 412 μM ) were prepared, the concentration of T<sub>4</sub>CS itself being kept constant. These solutions were degassed on the vacuum line to remove dissolved oxygen. Using approximately 10 mJ/pulse laser energy the decay of the T<sub>4</sub>CS triplet in the various solutions was monitored at 650 nm.

### **Biphenyl as Quencher**

Likewise biphenyl ( $E_T = 274 \text{ kJ mol}^{-1}$ ) [11] a compound whose triplet energy is close to, but higher than that calculated for T<sub>4</sub>CS was selected. Biphenyl also shows no absorption at the laser excitation wavelength.

### **Experimental for Biphenyl**

Solutions of T<sub>4</sub>CS in 50% propan-2-ol alone and with a concentration of 90 μM biphenyl present was made up - the absorbances at the excitation wavelength were matched. The solutions were degassed and the decay of the triplet state in the presence and absence of biphenyl was monitored at 650 nm.

## 4.5.4 Quenching Results

### Naphthalene

The traces fitted by first order kinetics gave the results shown in table (4.4).

Concentration of Naphthalene / $\mu\text{M}$	Rate Constant $k / \text{s}^{-1}$ *	Lifetime / $\mu\text{s}$
-	$1.23 \times 10^5$	8.1
14	$1.61 \times 10^5$	6.2
69	$3.37 \times 10^5$	3.0
138	$4.90 \times 10^5$	2.0
412	$12.1 \times 10^5$	0.9

Table (4.4) Rate constants for the decay of  $T_4CS^-$  with varying naphthalene concentration added.

\* An error of  $\pm 10\%$  is estimated for these measurements.

A plot of rate constant ( $k$ ) versus the naphthalene concentration is shown in figure (4.38).

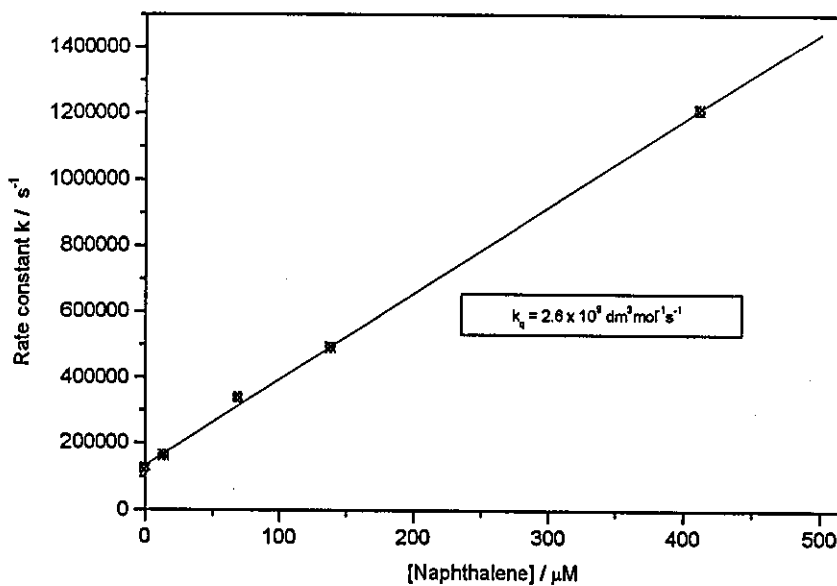


Figure (4.36) Plot of rate constant ( $k$ ) versus naphthalene concentration.



The gradient of the plot gives a value of  $2.60 \times 10^9 \text{ dm}^3 \text{ mol}^{-1} \text{ s}^{-1} \pm 10\%$  for the rate constant of triplet-triplet energy transfer from  $T_4\text{CS}^-$  to naphthalene. The rate for a collisional process cannot be greater than the rate at which the molecules diffuse through the solvent medium. Therefore, the upper limit for the rate constant will be equal to the rate constant for a diffusion controlled bimolecular process. An approximate value for this rate constant can be calculated from the Debye equation shown below:

$$k_{\text{diff}} = \frac{8RT}{3\eta} \quad (4.25)$$

where: R is the gas constant:  $8.314 \text{ JK}^{-1} \text{ mol}^{-1}$

T is the temperature: 298 K

$\eta$  is the solvent viscosity

$\eta$  was estimated by taking the average viscosity of  $\text{H}_2\text{O}$  and propan-2-ol at 298 K

Then:

$$\eta_{\text{H}_2\text{O}} = 0.8904 \text{ cp [12]}$$

$$\eta_{\text{Propan-2-ol}} = 1.988 \text{ cp [12]}$$

$$\text{Average } (\eta) = 1.44 \text{ cp } (1 \text{ cp} = 10^{-2} \text{ g s}^{-1} \text{ cm}^{-1})$$

In this approximation the rate constant is independent of the identities of the reactants, and depends only on the temperature and the viscosity of the solvent. Applying these numbers to the Debye equation yields  $k_{\text{diff}} = 4.60 \times 10^9 \text{ dm}^3 \text{ mol}^{-1} \text{ s}^{-1}$  for bimolecular diffusion in 50% propan-2-ol solution at 298 K. The efficiency of the energy transfer will depend on the proximity of the triplet state energy level of the donor to that of the acceptor. As the acceptor energy is lowered the energy transfer

efficiency is increased until the rate approaches the diffusion controlled rate [13]. The fact that the energies of the  $D^*(T_4CS^-)$  and  $A^*(Np)$  are comparable ( $<10 \text{ kJ mol}^{-1}$  difference) means that it is not unreasonable to expect some back energy transfer from  $A^*(Np)$  to  $D(T_4CS^-)$ . This would mean that the measured value of  $k_q$  should be less than that estimated for  $k_{diff}$ , which we do find:

$$k_q 2.60 \times 10^9 \text{ dm}^3 \text{ mol}^{-1} \text{ s}^{-1} < k_{diff} 4.60 \times 10^9 \text{ dm}^3 \text{ mol}^{-1} \text{ s}^{-1}$$

## Biphenyl

Analysis by first order kinetics revealed no change in the lifetime of the  $T_4CS^-$  triplet in the presence or absence of biphenyl.

## 4.5.5 Discussion

The flash photolysis experiments performed confirm that triplet-triplet energy transfer does take place between  $T_4CS^-$  and naphthalene, therefore validating the assumption that the transient absorption that occurs with  $\lambda_{max} = 650 \text{ nm}$  is indeed due to the excited triplet state of  $T_4CS^-$ . The value of  $2.6 \times 10^9 \text{ dm}^3 \text{ mol}^{-1} \text{ s}^{-1}$  is lower than that calculated for the maximum possible rate of bimolecular diffusion,  $k_{diff}$ , of  $4.60 \times 10^9 \text{ dm}^3 \text{ mol}^{-1} \text{ s}^{-1}$ . As was expected, no energy transfer occurs between  $T_4CS^-$  and biphenyl, confirming that  $254 \text{ kJ mol}^{-1} < E_T T_4CS^- < 274 \text{ kJ mol}^{-1}$ .

For unequivocal proof that the excited triplet state of  $T_4CS^-$  is quenched by naphthalene by the triplet-triplet energy transfer mechanism, the triplet-triplet absorption of naphthalene itself needs to be observed. The naphthalene triplet-triplet absorption is well documented to occur in the region of 400 - 430 nm of the spectrum, this however overlaps with the shorter wavelength band in the transient absorption spectrum of  $T_4CS^-$  ( $\lambda_{max} = 430 \text{ nm}$ ), therefore in order to see the signal arising from the naphthalene triplet alone it is necessary to subtract any absorption arising from the transient absorption of  $T_4CS^-$ . Degassed solutions of  $T_4CS^-$  alone, and with  $150 \mu\text{M}$  naphthalene added, were flashed under identical conditions using matching absorbances of 0.70 at the laser excitation wavelength. Analysis took place at 415 nm and a time-

base of 400ns per point was used and after subtracting any absorption due to  $T_4CS^+$  absorption alone from the trace with naphthalene results in a signal from the naphthalene triplet alone, which is shown in figure (4.37).

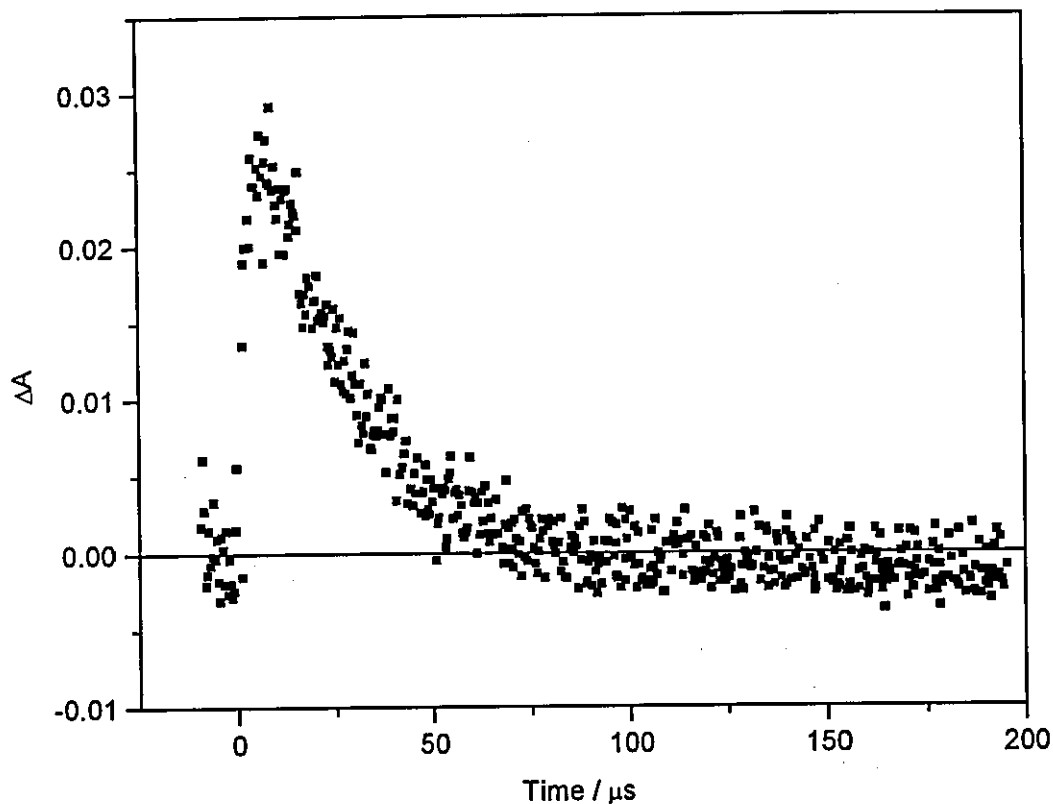


**Figure (4.37)** *Naphthalene decay trace, monitored at 415 nm using a 400 ns / point time-base.*

Using a shorter time-base of 40 ns per point enables us to observe the rise in production of the naphthalene triplet and its subsequent decay, and this is shown in figure (4.38).

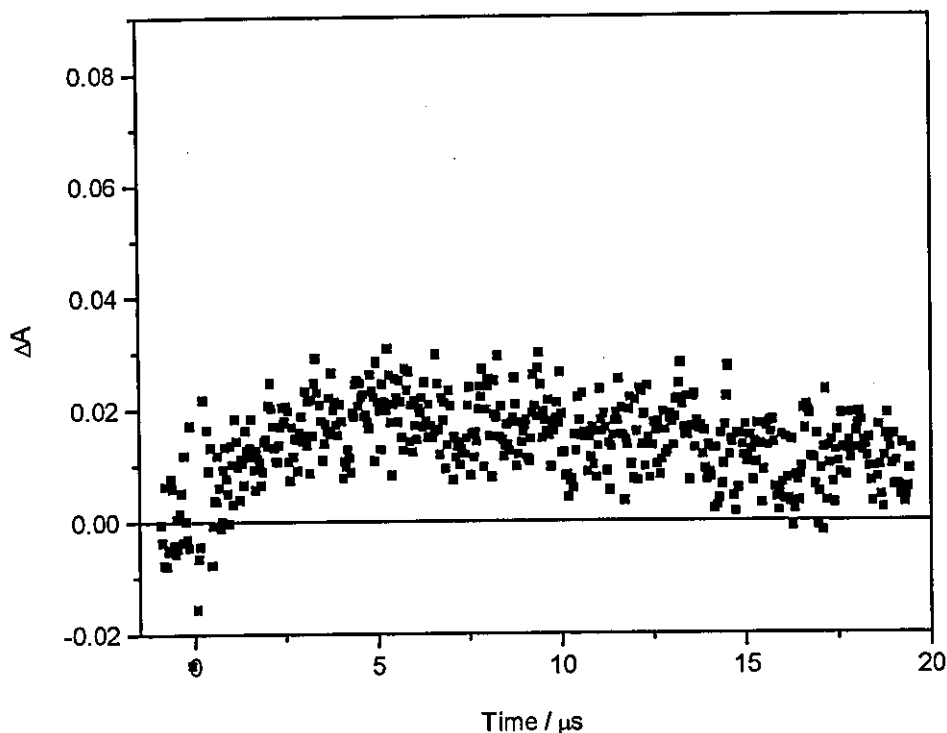


Figure (4.38) Rise and decay of naphthalene triplet, using a 40 ns / point time-base.

### Summary of Evidence for the Existence of the $T_4CS^-$ Triplet State

1. Phosphorescence measurements (see section 4.3.3).
2. Oxygen strongly quenches the transient:  $k_{O_2} = 5.2 \times 10^9 \text{ dm}^3 \text{ mol}^{-1} \text{ s}^{-1}$ .
3. At high laser energies decay by first and second order kinetics is observed.  
The second order component arising from triplet-triplet annihilation is reduced by cutting down the laser energy to give first order kinetics.
4. Quenching by naphthalene ( $E_T = 254 \text{ kJ mol}^{-1}$ ) the triplet energy of which is lower than that of  $T_4CS^-$  at a rate close to the diffusion controlled rate ( $k_q = 2.6 \times 10^9 \text{ dm}^3 \text{ mol}^{-1} \text{ s}^{-1}$ ) and observing a rise and subsequent decay of the triplet quencher.
5. No quenching observed by biphenyl ( $E_T = 274 \text{ kJ mol}^{-1}$ ) the triplet state energy of which is greater than that of  $T_4CS^-$ .

#### 4.5.6 Radical anion and product absorption ( $\lambda_{\text{max.}} = 425 \text{ nm}$ )

Having identified the part of the transient absorption spectrum due to the excited triplet state of  $T_4CS^-$ , a closer examination of the longer lived species which absorbs in the shorter wavelength band ( $\lambda_{\text{max.}} = 425 \text{ nm}$ ) the lifetime of which is not affected by molecular oxygen, was undertaken. This longer lived species is believed to be the radical anion  $T_3CS^{\cdot -}$ , which has been shown to be formed upon irradiation of  $T_4CS^-$  by homolytic cleavage of the 3 C-Cl bond to produce a free radical (see section 2.7). An appropriate time-base was chosen, long enough to miss out transient absorption due to the much shorter lived triplet state ( $\tau_T \approx 8.0\mu\text{s}$ ).  $T_4CS^-$  in 50% aqueous ethanolic solution, with an absorbance of 0.67 at the laser excitation wavelength was flashed using a laser energy of 27 mJ/pulse. Degassed and aerated spectra at four time delays are shown in figures (4.39) and (4.40).

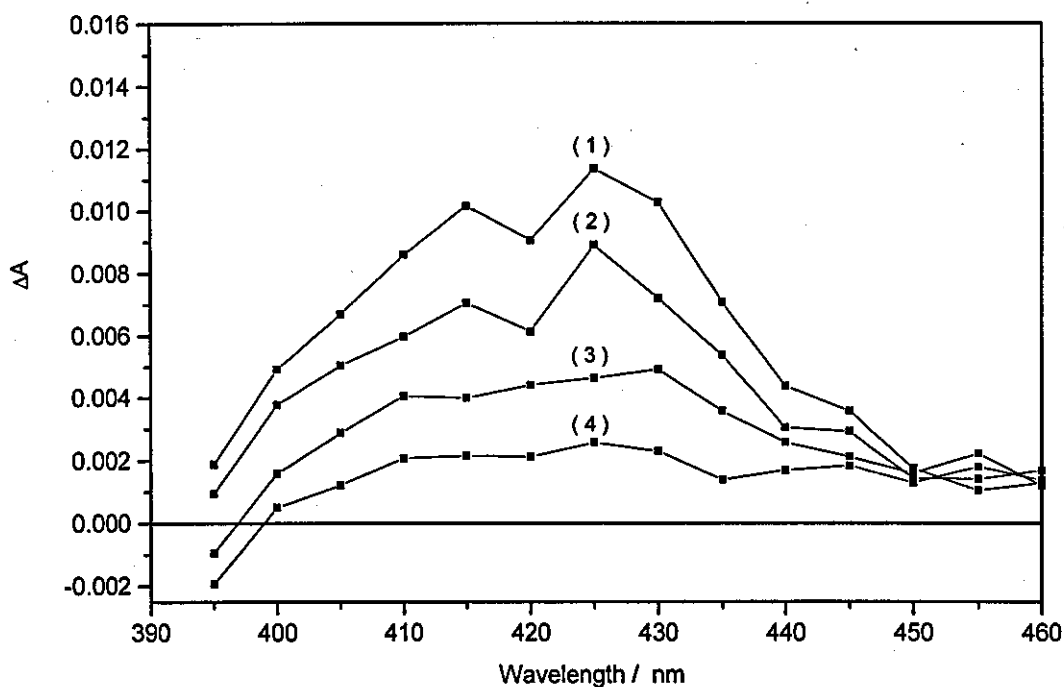
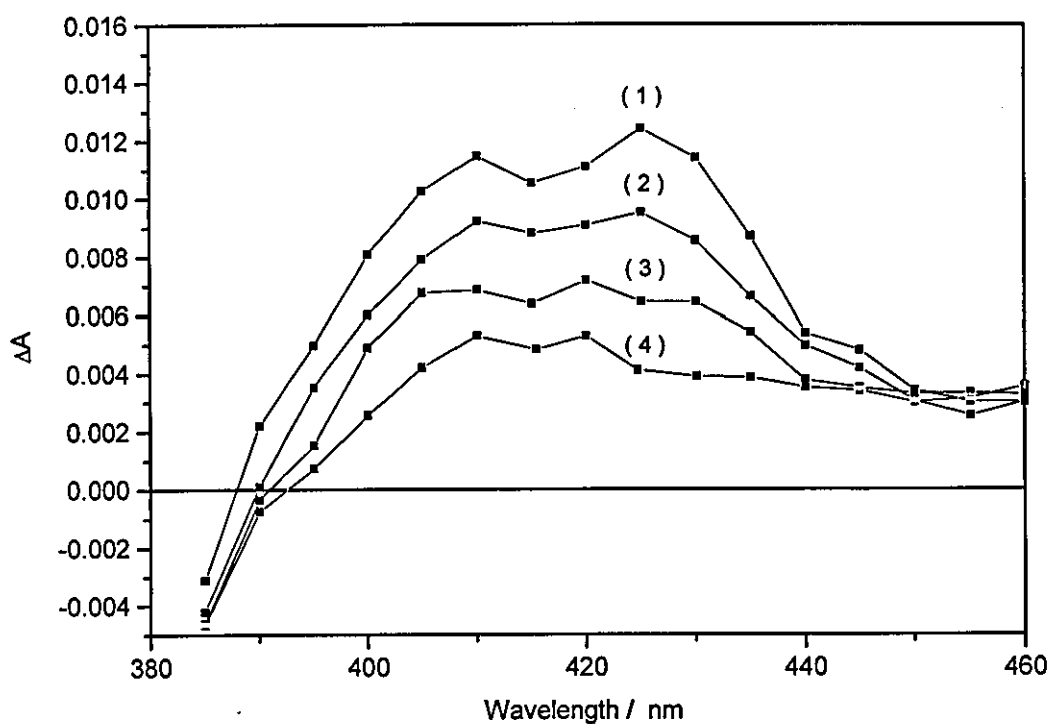
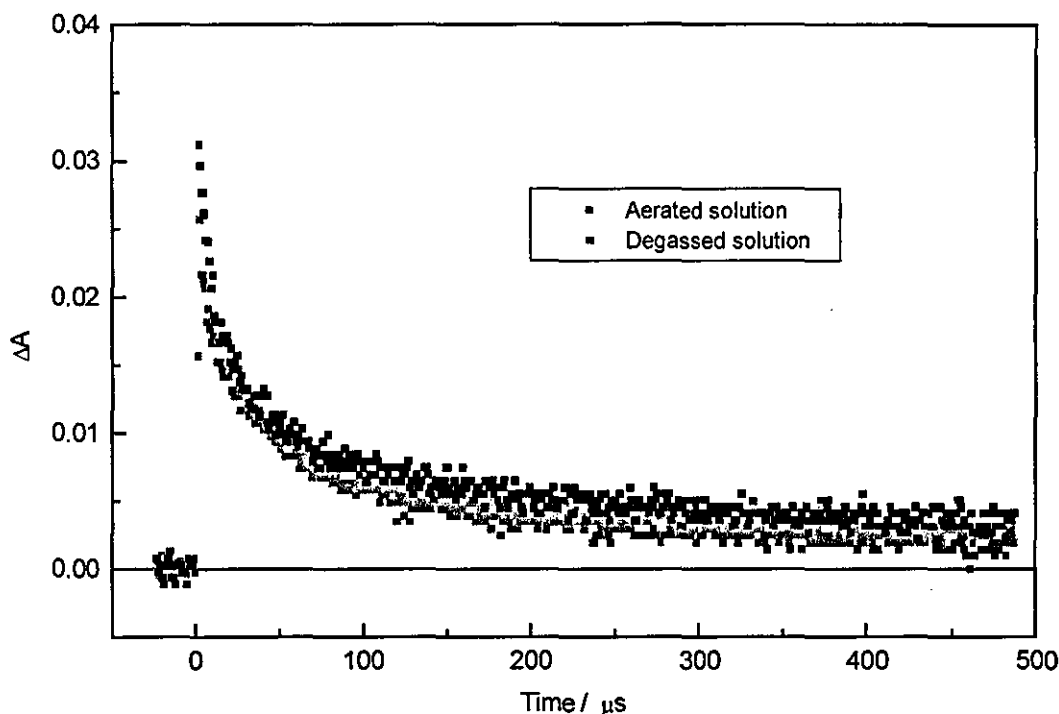


Figure (4.39) *Transient absorption spectrum from  $T_4CS^-$  in an aerated 50% ethanolic aqueous solution at four time delays following the laser Pulse. Delay Times are (1) 41.0  $\mu\text{s}$ . (2) 75.8  $\mu\text{s}$ . (3) 159  $\mu\text{s}$ . (4) 464  $\mu\text{s}$ .*



**Figure (4.40)** *Transient absorption spectrum from  $T_4CS^-$  in degassed 50% ethanolic aqueous solution at four time delays following the laser pulse. Delay Times are (1) 41.0  $\mu s$ . (2) 75.8  $\mu s$ . (3) 159  $\mu s$ . (4) 464  $\mu s$*

If this transient state is produced solely via the triplet state, then quenching of the triplet state by dissolved molecular oxygen which occurs in aerated solutions, ( $k_{O_2} = 5.2 \times 10^9 \text{ dm}^3 \text{ mol}^{-1} \text{ s}^{-1}$ ) should prevent its formation. At first sight, comparison of the two spectra appear to exhibit little difference. However, if the individual traces taken from each spectrum are overlaid, they do show a difference in the amount of radical and product produced upon flashing. This is exemplified in figure (4.41), which shows decay traces from each spectrum analysed at 425 nm.



**Figure (4.41)** *Kinetic traces analysed at 425 nm, comparing the traces obtained from flashing  $T_4CS^-$  in degassed and aerated 50% aqueous ethanol solution.*

The fact that almost no fluorescence quenching was occurring between the degassed and aerated solutions showed that there was no quenching of the first excited singlet state. This indicates that at least some of the radical is being formed via the triplet state.

To determine how much the singlet state is a precursor in the production of the radical state, the effect of fluorescence quenching was investigated. It was found that pumping an already degassed 50% ethanolic aqueous solution with oxygen to approximately three atmospheres resulted in 10% fluorescence quenching. Upon flash photolysis, it was found that the radical and product formation was  $76\% \pm 10\%$  of that formed in aerated solution. However, the ground state absorbances required for flash photolysis (typically 0.8) are much higher than the absorbances normally used in fluorescence measurements ( $< 0.1$ ), and therefore may not yield accurate fluorescence quenching values - since self-absorption affects may effect the corresponding yields (see section 4.3.2). Using absorbances of less than 0.1 at the laser excitation wavelength in

order to eliminate any inner-filter effects, showed no change in the amount of fluorescence quenching, showing that the oxygen quenching of the solutions prepared for the flash photolysis experiments are valid.

To obtain an even more significant amount of quenching it was decided to use a higher concentration of ethanol - since the oxygen solubility is greater in ethanol compared with water. An 80% ethanolic aqueous stock solution of  $T_4CS^-$  was prepared, with an absorbance of 0.80 at 354.7 nm. Using this stock solution, one cell was degassed and then saturated with oxygen at a pressure of approximately three atmospheres, the other cell was left aerated. Saturating the degassed solution with oxygen at a high pressure had the desired effect - resulting in 50% quenching of fluorescence.

Flash photolysis studies were then carried out on the two solutions, exciting at 354.7 nm and monitoring the decays at 425 nm. The resultant traces obtained for the two solutions are shown in figure (4.42).

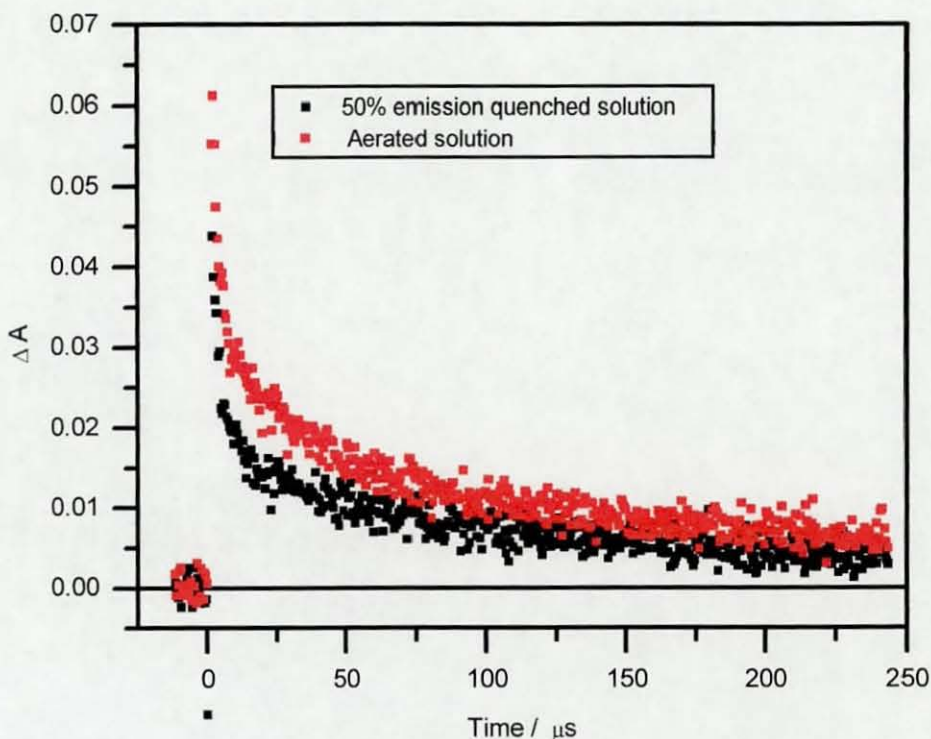


**Figure (4.42)** *Decay traces from flashing  $T_4CS^-$  in an aerated 80% ethanolic aqueous solution and in a degassed plus oxygen saturated (3 atm.) 80% ethanolic aqueous solution, analysed at 425 nm.*



The percentage decrease in the amount of radical and product produced is plotted on the same time axis in figure (4.43). The average percentage decrease was found to be 34% or 66% of the signal found in aerated solutions. An error of  $\pm 10\%$  is estimated for these calculations.

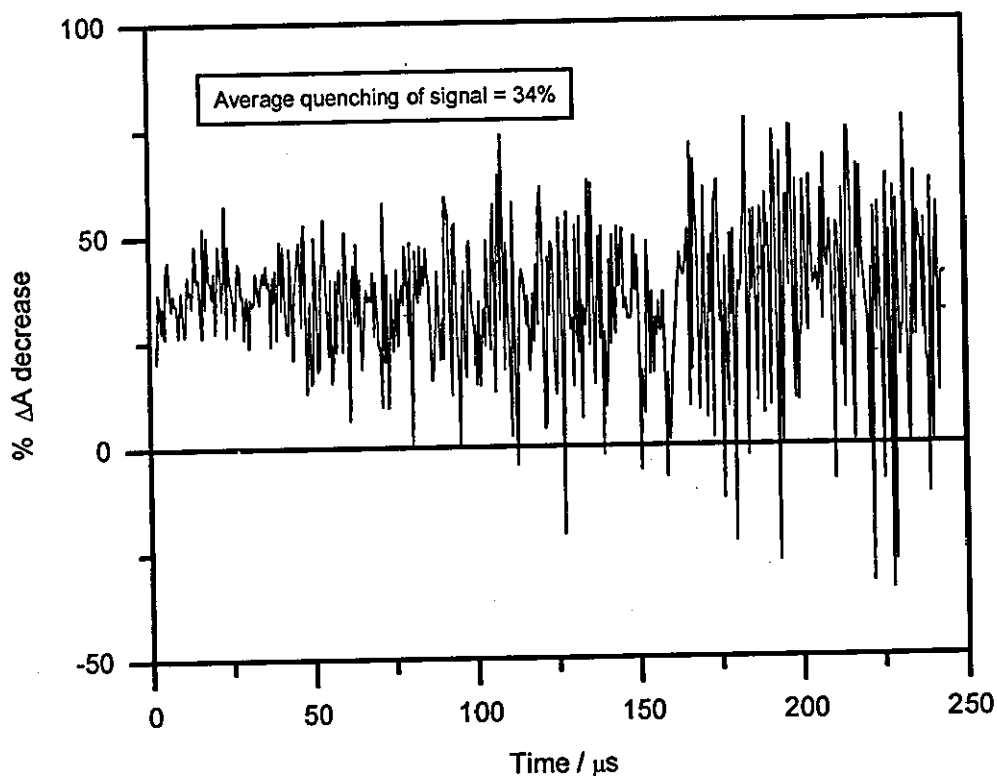


Figure (4.43) *Percentage quenching of radical trace per data point.*

### Discussion of Results

If the radical state is derived from both the singlet and triplet state in degassed solutions then:

$$\phi_R = \phi_R(S) + \phi_R(T) \quad (4.26)$$

And for aerated solutions:

$$\phi_R^{O_2} = \phi_R^{O_2}(S) + \phi_R^{O_2}(T) \quad (4.27)$$

In degassed 50% alcoholic aqueous solutions the lifetime of the  $T_4CS^*$  triplet state is 8.0  $\mu s$  and in aerated solution the lifetime is reduced to 0.3  $\mu s$ . This represents about 96% quenching of the triplet state of  $T_4CS^*$ .

Therefore, we would expect  $\phi_R^{O_2}(T) \rightarrow 0$

so we can write:

$$\phi_R^{O_2} = \phi_R^{O_2}(S) \quad (4.28)$$

Between aerated and degassed solutions of  $T_4CS^*$  in 50% alcoholic aqueous solutions, no significant fluorescence quenching is observed, but there is a decrease in the amount of radical and product produced upon flash photolysis - the amount of radical and product detected in the aerated solution was found to be about  $66\% \pm 7\%$  of that detected in degassed solutions. Since there is no significant quenching of the excited singlet state, with these results it appears that 34% radical and product formation is formed via the excited triplet state, leaving 66% formed via the excited singlet state. This would mean the ratio of singlet:triplet contributing to the radical and product is approximately 2:1.

When oxygen is pumped in at approximately three atmospheres into 50% ethanolic aqueous solutions, the fluorescence is quenched by 10% when compared with aerated solutions. Flash photolysis of the solution containing three atmospheres of oxygen gives approximately  $76\% \pm 8\%$  of radical and product formation produced in aerated solutions, which equates to 50% of that found in degassed solutions.

The contribution from the triplet state will be zero in both cases (see equation 5.4) but now we would expect the contribution to the radical state and product on the basis of 10% quenching of the fluorescence to be in the ratio of 1.8:1, singlet:triplet, from the original 2:1. This would equate to  $1.8/3 \times 100\% = 60\%$  of the original signal. When taking experimental error into account ( $\pm 10\%$ ) the values obtained are plausible.

On going to higher ethanol concentrations, that is 80% ethanolic aqueous solution and pumping oxygen in at three atmospheres, results in 50% fluorescence quenching. The resulting flash photolysis experiments produce  $66\% \pm 7\%$  radical and product absorption of that detected in aerated solutions, which equates to 43% of degassed. If the solvent change does not affect the ratio of 2:1 then we would expect now to get approximately 1:1 singlet:triplet, equating to  $1.0/3 \times 100\% = 33\%$  of the original signal. This is lower than what we observe.

But what we are dealing with now is a different solvent composition which has not had its photochemistry investigated, and we have found that the photochemical paths of  $T_4CS^-$  following excitation is very dependant on the alcohol and water content. A possible explanation for these discrepancies is that  $\phi_R(S)$  arises from upper singlet states ( $S_n^*$ ) and is not quenched by oxygen at least in the case of 50% quenched solution. This is not unreasonable since the C-Cl bond could break in a single vibration in a higher singlet state ( $S_n^*$ ) and then will be less likely to break from  $S_1$ .

Whatever the complications that arise due to solvent composition and oxygen concentration, what is not in dispute is the fact that the radical species and product originates both from the excited singlet and triplet state. Hilal also investigated the contribution of the triplet and singlet to product formation. He carried out continuous photolysis of 50% aqueous alcoholic solutions of tetrachlorosalicylanilide (pH = 6), using a 220 watt Hanovia medium pressure mercury lamp as a light source with filters to isolate the 365 nm line. Monitoring conductivity changes due to formation of  $Cl^-$  ions, Hilal showed that oxygen was found to reduce the initial rate of chloride ion formation to about half that obtained in nitrogen-saturated solution. To confirm this using anthracene as a triplet energy acceptor, he found that both the excited singlet and triplet states of  $T_4CS$  are responsible for the photolysis, with a singlet:triplet ratio of 0.7:1.

### 4.5.7 Kinetics of the Radical Species

A typical example of a trace analysed at 425 nm produced from photolysis of  $T_4CS^-$  in an aerated 50% ethanolic aqueous solution with a ground state absorption of 0.7 at the laser excitation wavelength is shown in figure (4.44). The half-life of the radical species was found to be approximately 60  $\mu s$ .

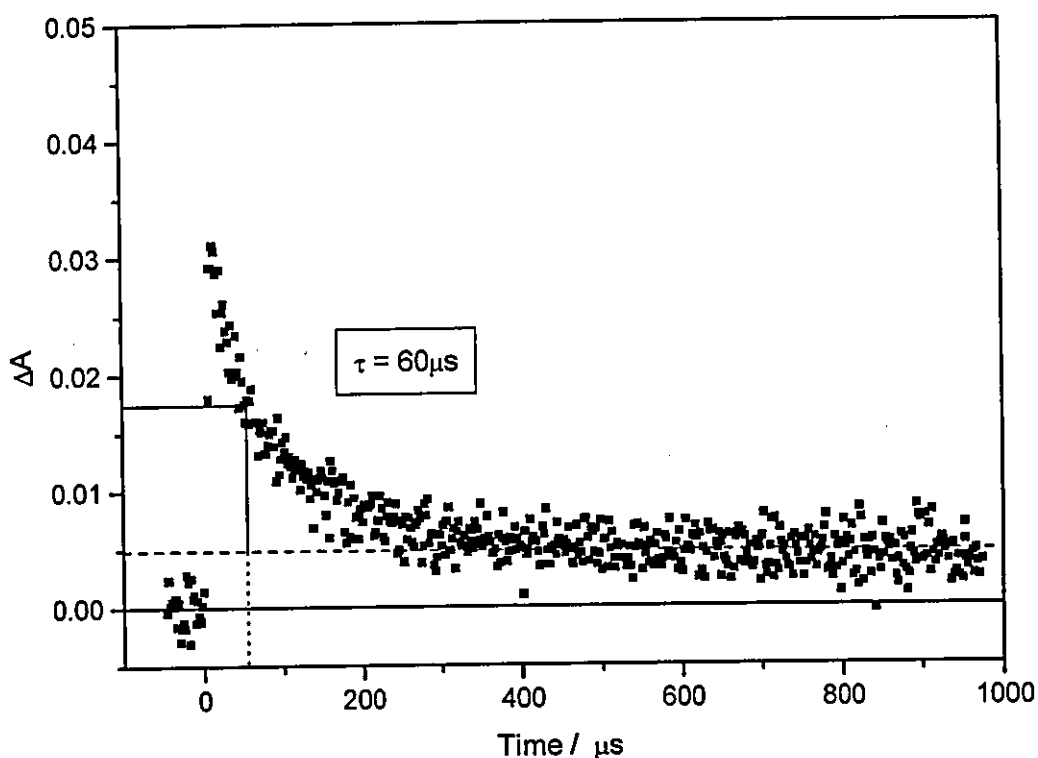


Figure (4.44) Typical trace of radical species, analysed at 425 nm.

### Product Absorption

The residual absorption is present even when the longest workable time-base available to the JK laser system (approximately 10  $\mu s$  / point) is used. This is strong evidence of product formation. To verify this, it was possible to observe the trace over a much greater time span, by using a flash gun as an excitation source, and operating

the trigger on the JK laser manually. A trace collected over 2.6 seconds is shown in figure (4.45). This clearly shows there is no decay, which is conclusive proof that a permanent product is being observed. This concurs with the laser induced degradation experiments shown in figures (4.15 - 4.18), which show the build of permanent product in the ground state absorption spectra following laser excitation.

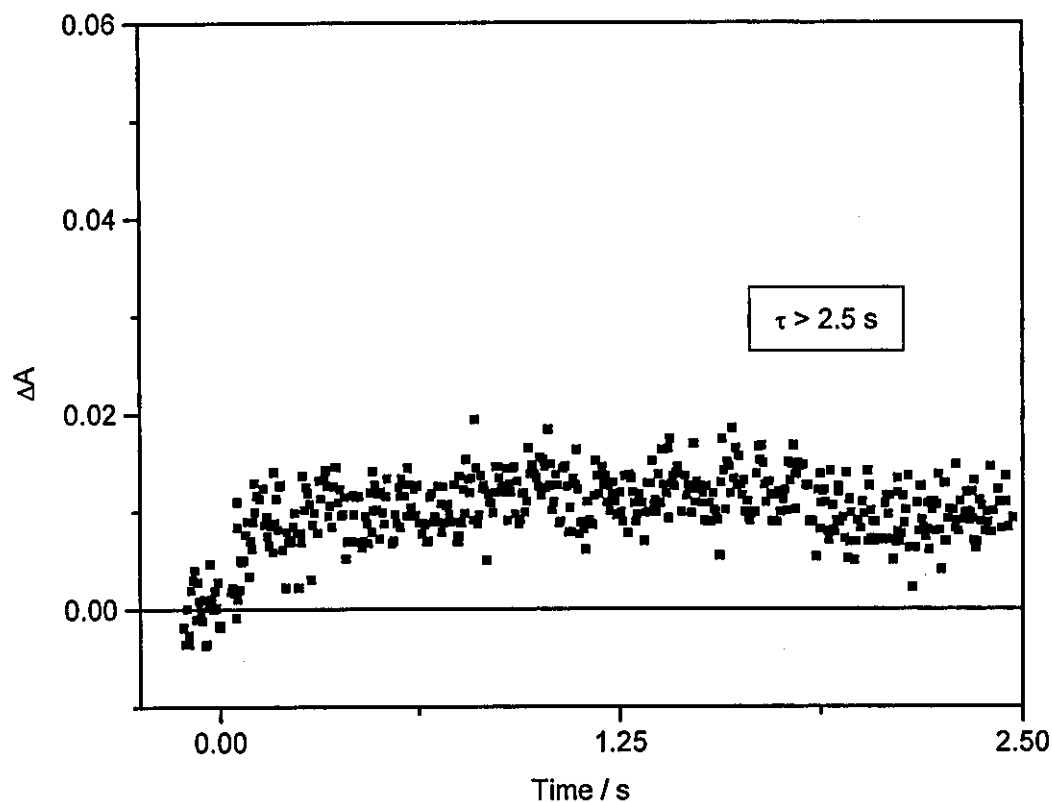
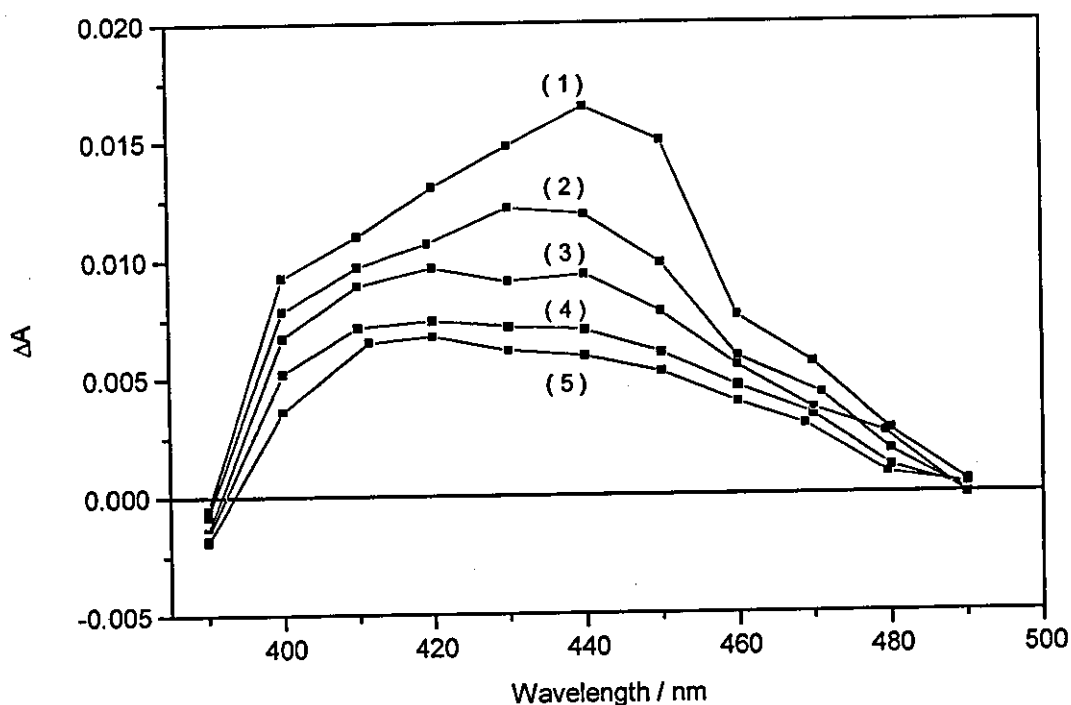


Figure (4.45) *Kinetic trace of the permanent product, analysed at 425 nm over 2.5 seconds.*

### 4.5.8 Excited State Photochemistry of $\text{TBS}^-$ in Solution

$\text{TBS}^-$  in 50% ethanolic aqueous solution was prepared, the ground state absorbance at the laser excitation wavelength of 354.7 nm was 0.85. Using a laser energy of 20 mJ / pulse, degassed and aerated transient absorption spectra were collected and are shown at five time delays in figures (4.46) and (4.47):



**Figure (4.46)** *Transient absorption spectrum from  $\text{TBS}^-$  in an aerated 50% ethanolic aqueous solution at five time delays following the laser pulse. Delay times are (1) 3.7  $\mu\text{s}$ . (2) 23.4  $\mu\text{s}$ . (3) 53.1  $\mu\text{s}$ . (4) 147  $\mu\text{s}$ . (5) 218  $\mu\text{s}$ .*

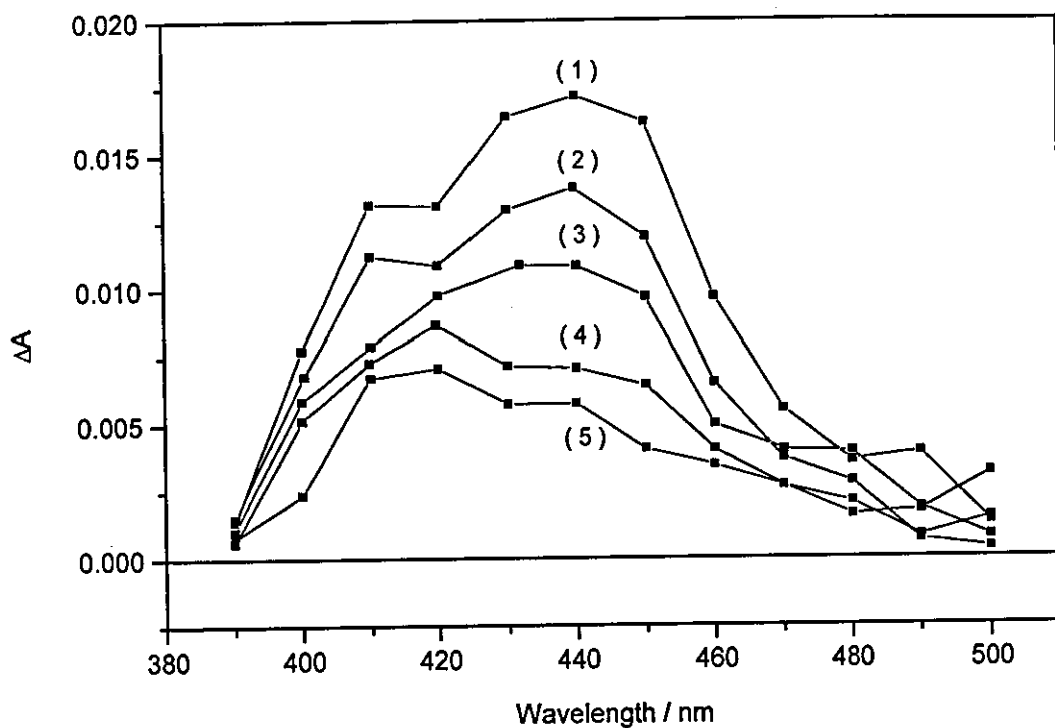


**Figure (4.47)** *Transient absorption spectrum from  $TBS^-$  in a degassed 50% ethanolic aqueous solution at five time delays following the laser pulse. Delay times are (1) 3.7  $\mu s$ . (2) 23.4  $\mu s$ . (3) 53.1  $\mu s$ . (4) 147  $\mu s$ . (5) 218  $\mu s$ .*

The above spectra show that  $\lambda_{max} = 440$  nm for the early time delays, the longer time delays give  $\lambda_{max} = 410-420$  nm. This absorption is long lived and displays no sign of decay, even on the longest time-base used. As with  $T_4CS^-$  this can be attributed to product formation. Overlapping individual decay traces of the same wavelength obtained from the degassed and aerated spectra showed there to be no difference, *i.e.* the presence of oxygen has negligible effect, thereby ruling out the possibility that any of the transient absorption is due to excited triplet state formation - a triplet state would be expected to be quenched by molecular oxygen on these time scales. Therefore, it would appear the transient absorption is due to radical formation, a typical decay is shown in figure (4.48) - the half-life of this radical species is found to be approximately 30  $\mu s$ .

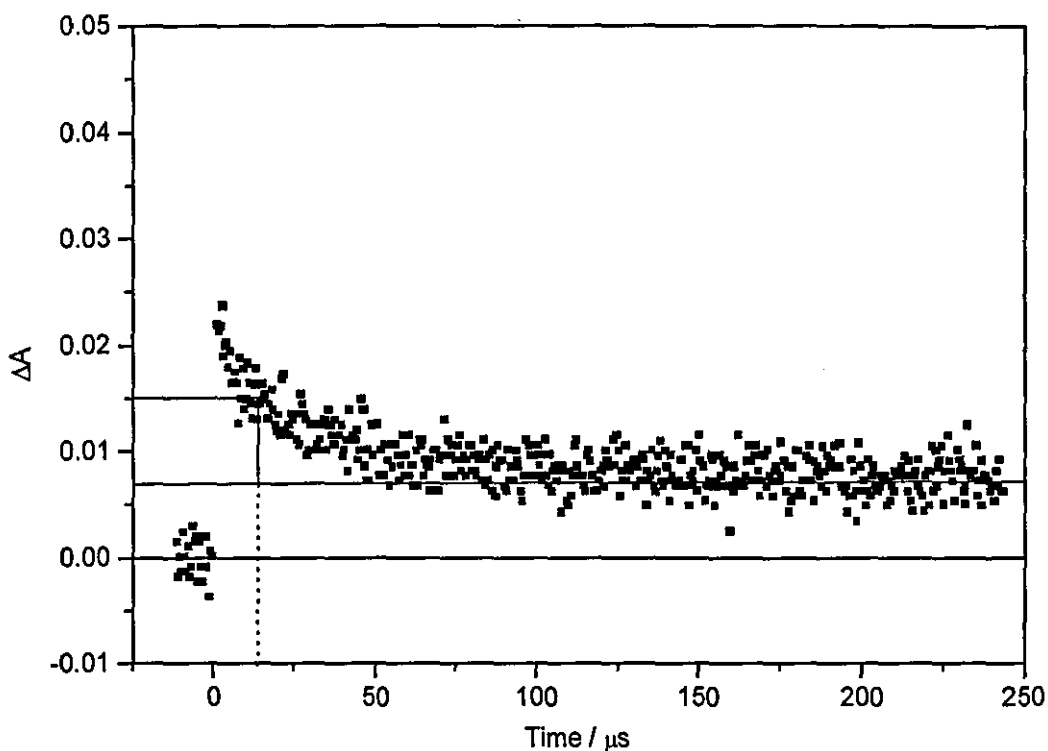


**Figure (4.48)** *Typical decay following photolysis of TBS<sup>-</sup> analysed at 440 nm, showing radical decay ( $\tau \approx 30 \mu\text{s}$ ) and product absorption.*

There is indirect evidence that the excited triplet state of TBS<sup>-</sup> is produced upon excitation from energy transfer experiments using naphthalene as a quencher (see section 4.5.10). An attempt to observe the TBS<sup>-</sup> triplet state using the HY laser system, which has a slightly shorter time resolution capability was carried out.

TBS<sup>-</sup> in a degassed 50% ethanolic aqueous solution was prepared, using a laser energy of 13 mJ / pulse at the laser excitation wavelength of 354.7 nm and analysing at 660 nm produced a transient whose resultant decay is shown in figure (4.49).



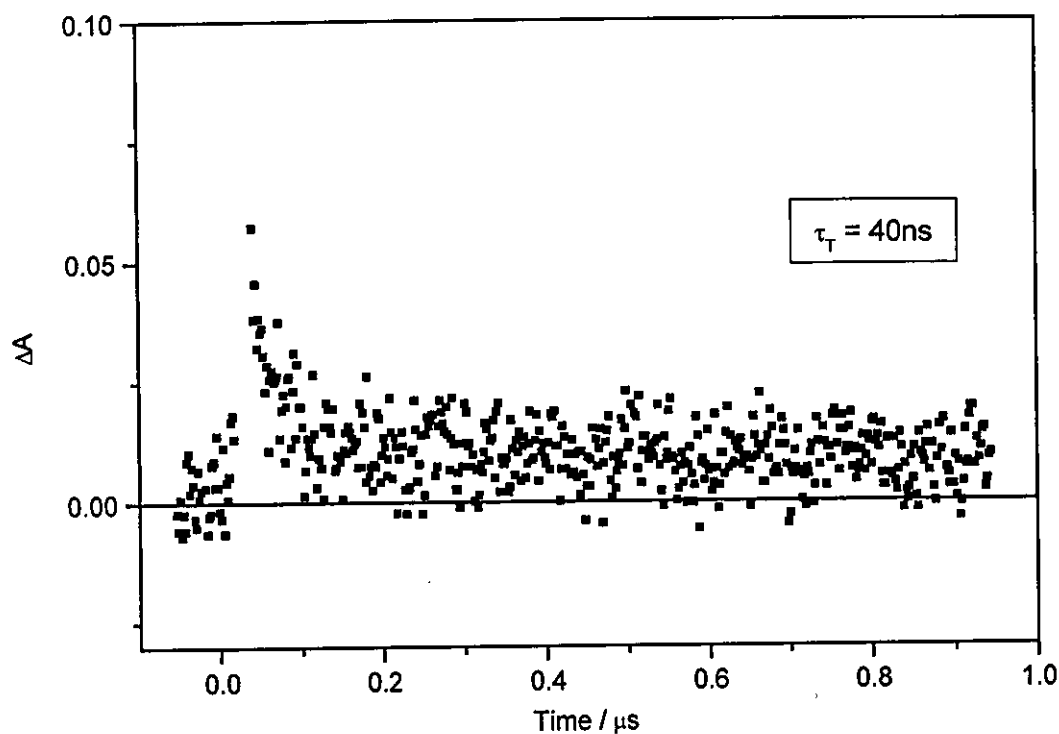
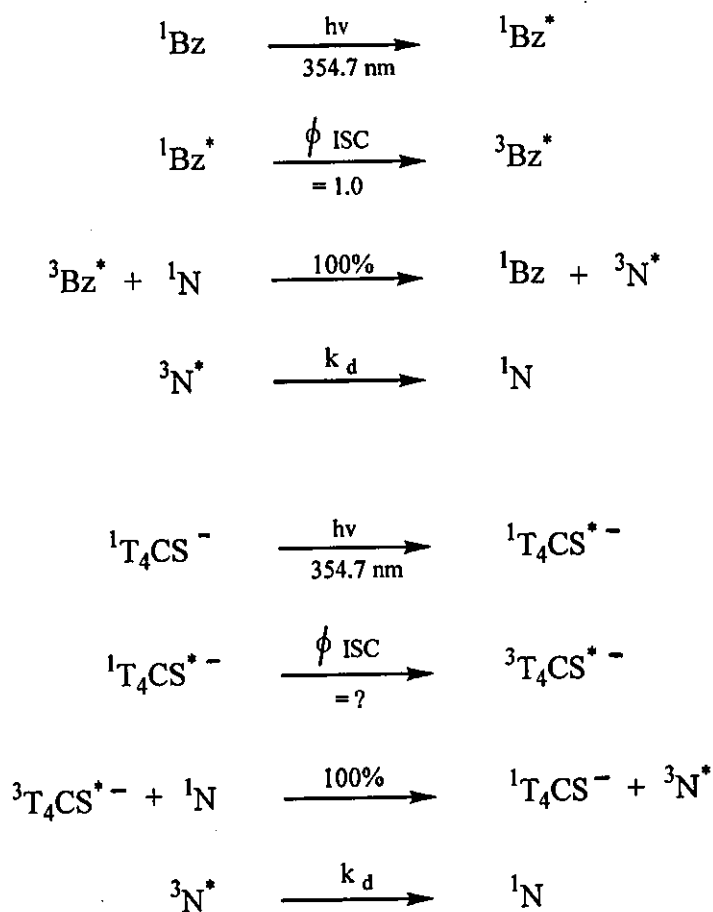


**Figure (4.49)** *Transient decay of TBS\* in a degassed 50% ethanolic aqueous solution analysed at 660 nm.*

Fitting the data by first order kinetics gives a lifetime of approximately 40 ns. The same degassed solution was then pumped with oxygen at a pressure of approximately three atmospheres resulting in the loss of the transient absorption signal - strong evidence that the observed signal is due to the excited triplet state of TBS\*.

### 4.5.9 Singlet - Triplet Intersystem Crossing Quantum Yields

The intersystem crossing quantum yield, ( $\phi_T$ ), was measured for  $T_4CS^-$  in 50% and 10% alcoholic aqueous solutions. Benzophenone is well documented to have a intersystem crossing quantum yield of near unity [14] and was therefore used as a standard for these experiments. The triplet quantum yield was measured by sensitisation of naphthalene by both  $T_4CS^-$  and benzophenone, and comparing the two. Excitation at 354.7 nm of a solution containing a mixture of benzophenone and naphthalene must result in the initial formation of the benzophenone  $S_1$  state only, since insufficient energy is provided in a 354.7 nm photon to excite the naphthalene  $S_1$  state. The initially formed benzophenone  $S_1$  state undergoes intersystem crossing to the  $T_1$  state, naphthalene having a triplet state lower in energy than benzophenone can be sensitised by triplet-triplet energy transfer from the benzophenone excited triplet state. If the concentration of naphthalene molecules is high (ca.  $0.1 \text{ mol dm}^{-3}$ ), all photo induced triplet states of benzophenone will be quenched instantaneously on the time scales of these experiments. The resultant decay of the naphthalene triplet state can then be monitored and a value for  $\Delta A_0$  obtained from the decay (extrapolated to zero time after the laser pulse), this value will represent a quantum yield of one. Likewise, photoinduced  $T_4CS^-$  triplet states have been shown to be quenched by naphthalene by triplet-triplet energy transfer see (see section 4.5.3), again a value for  $\Delta A_0$  can be determined, and the two  $\Delta A_0$  values compared. A reaction scheme depicting these two processes is shown in figure (4.50).



N - Naphthalene

Bz - Benzophenone

**Figure (4.50)** Reaction scheme for the two systems under study after excitation.

Using an aqueous solvent can provide solubility problems when trying to dissolve naphthalene, despite this it was possible to make up to a 0.05 M solution of naphthalene in a 50% alcoholic aqueous solution. This was achieved by first dissolving the naphthalene in the alcohol, and then adding the 0.1 M potassium phosphate buffer. A concentration of 0.05 M is sufficient to intercept all photo-induced triplet states of  $\text{T}_4\text{CS}^-$ .

Ideally in this experiment the same solvent system for both systems would be preferable. However, a different solvent system is required for the naphthalene / benzophenone system, this is because carbonyl compounds with a  $(n,\pi^*)$  triplet state abstract  $H^\bullet$  from donor molecules efficiently. The radical-like structure of the  $(n,\pi^*)$  triplet states are much more able to abstract  $H^\bullet$  from donor molecules. The primary products from  $H^\bullet$  abstraction by a carbonyl compound are ketyl radicals ( $R_2\dot{C}-OH$ ) and the radical of the hydrogen donor molecule. So if other photochemical reactions occur, between the benzophenone triplet and solvent before interception by the naphthalene occurs, the resultant  $\phi_T$  value for naphthalene will be less than unity. For this reason it is not recommended to use an alcoholic solvent for the standard determinations since the yield will not be known exactly and may well be less than unity. The solvent chosen for the benzophenone / naphthalene system was acetonitrile.

Since two different solvent mediums are to be used it is essential to make sure there are no significant solvent shifts in the recorded sensitised naphthalene triplet-triplet absorption spectra between the two solvent systems. Therefore transient absorption spectra of naphthalene / benzophenone in acetonitrile and naphthalene /  $T_4CS^\bullet$  in 50% alcoholic aqueous solution were recorded. The resultant spectra are shown in figure (4.51), which shows the characteristic sharp absorption bands of the naphthalene triplet ( $\lambda_{max} = 395 \text{ nm}$  and  $415 \text{ nm}$ ) with no spectral shift between the two solvent systems, therefore assuming that the molar absorption coefficient ( $\epsilon_T$ ) for both solvent systems will be approximately the same.

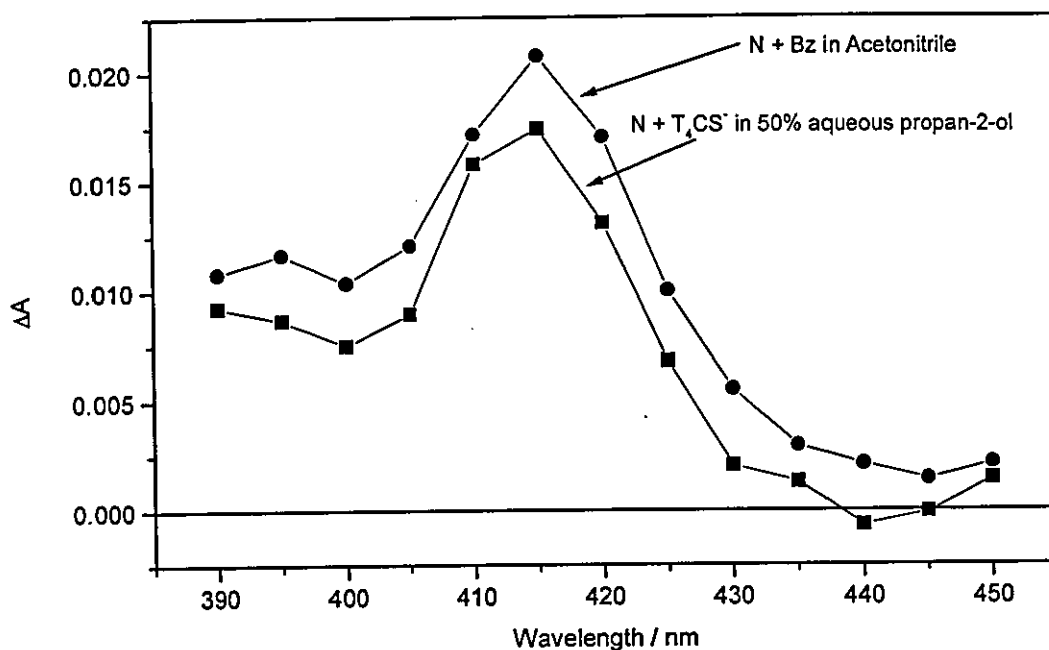


Figure (4.51) *Transient absorption spectra of sensitised naphthalene from the two solvent systems under study.*

In the absence of oxygen, the change of absorbance at 390 nm ( $\Delta A_0$ ) due to the formation of triplet naphthalene as a function of laser intensity is monitored. The laser intensity was attenuated by means of sodium nitrite filters of known transmittance at the laser excitation wavelength of 354.7 nm.

Solutions of both samples were optically matched at the laser excitation wavelength -to ensure equal number of photons are absorbed by each sample. Typical absorbances being approximately 0.8 at 354.7 nm. The triplet quantum yield ( $\phi_T$ ) for T<sub>4</sub>CS<sup>-</sup> can be determined using the equation (4.29):

$$\Phi_T = \frac{\text{slope } T_4CS^-}{\text{slope } Bz} \times \frac{(1 - 10^A)_{Bz}}{(1 - 10^A)_{T_4CS^-}} \quad (4.29)$$

where the first term is the ratio of the slopes of  $\Delta A^{390 \text{ nm}}$  (extrapolated to zero time after laser pulse) as a function of laser intensity for the unknown (T<sub>4</sub>CS<sup>-</sup>) and

benzophenone (Bz) respectively. The second term in the equation, accounts for any difference in absorbance at the laser excitation wavelength of 354.7 nm. A plot of the calculated values of  $\Delta A_0$  measured at 390 nm versus laser energy gave the plots shown in figure (4.52). An error of  $\pm 10\%$  is estimated for each plot.

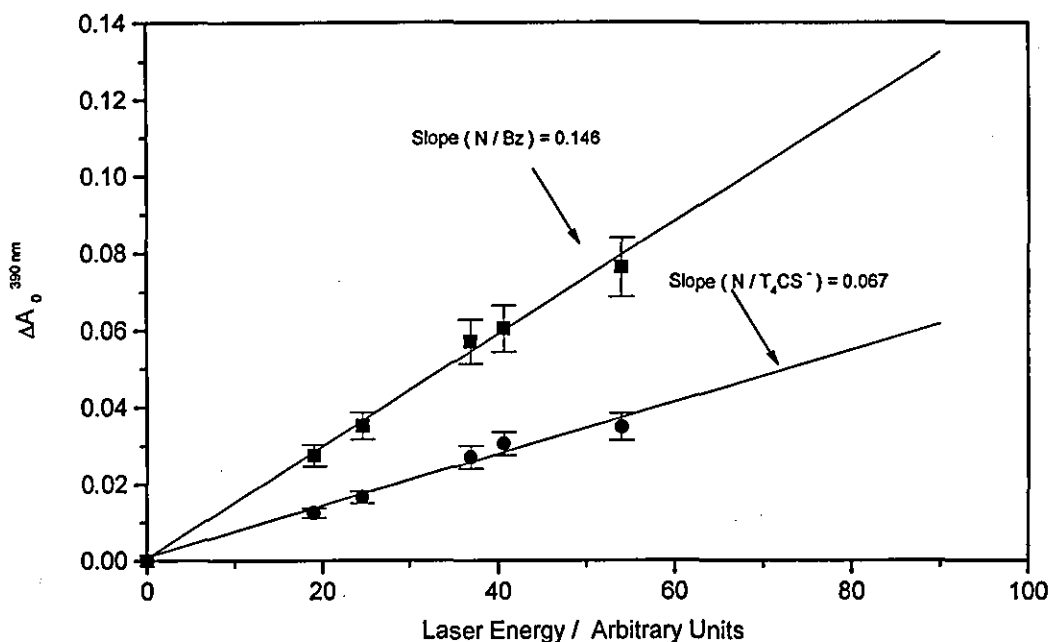


Figure (4.52) A plot of  $\Delta A^{390 \text{ nm}}$  as a function of laser intensity with benzophenone and  $T_4CS^-$  as sensitizers together with the Best Straight Line Fit to the data.

Linear regression analysis was performed using the two plots, and this yielded slopes of  $0.146 \pm 0.15$  and  $0.067 \pm 0.07$  for the benzophenone / naphthalene and  $T_4CS^-$  / naphthalene systems respectively. Applying these to equation (4.29) results in a value  $0.46 \pm 0.09$  for the triplet yield ( $\phi_T$ ) of  $T_4CS^-$  in 50% alcoholic aqueous solution.

Calculation of the triplet quantum yield of  $T_4CS^-$  in a 10% alcoholic aqueous solution cannot be as easily achieved using the same method, because it is not possible to make up a high enough concentration of naphthalene to intercept all the photo-induced  $T_4CS^-$  triplets.

This is due to:

1. Insolubility of naphthalene in water - which is now 90% by volume.
2. A higher rate constant of the  $T_4CS^-$  triplet state decay in 10% alcoholic ( $\tau \approx 3\mu s$ ) solutions compared with 50% alcoholic ( $\tau \approx 8\mu s$ ) solutions.

However, assuming that the molar absorption coefficients in 10% and 50% alcoholic aqueous mixtures are approximately the same, then the quantum yield in a 10% solution can simply be determined by comparing the relative changes in absorbance at the  $\lambda_{max}$  of the transient absorption spectrum for each optically matched sample. The results shown in table (4.4) yield a value of  $0.36 \pm 0.07$  for the triplet yield ( $\phi_T$ ) of  $T_4CS^-$  in a 10% alcoholic aqueous solution.

Solvent *	$\Delta A_0$ at $\lambda_{max}$ .	$\phi_T$
50% propan-2-ol	4.24	$0.46 \pm 0.09$
10% propan-2-ol	2.80	$0.36 \pm 0.07$

Table (4.4) Triplet yield values for  $T_4CS^-$  in 10% and 50% propan-2-ol aqueous solutions.

\* Direct comparison of  $T_4CS^-$  in propan-2-ol aqueous solutions with  $T_4CS^-$  in ethanolic aqueous solutions did not reveal any difference in the corresponding triplet yield values.

#### 4.5.10 Triplet State Molar Absorption Coefficient of $T_4CS^-$

The molar absorption coefficient of triplet  $T_4CS^-$  in 50% alcoholic aqueous solution was measured in a degassed solution relative to that of the benzophenone (Bz)

triplet at 525 nm ( $\epsilon = 7220 \text{ l mol}^{-1} \text{ cm}^{-1}$ ) [15]. The change in absorbance at the  $\lambda_{\text{max}}$  of the transient absorption for each optically matched sample (absorbance approximately 0.75 at the laser excitation wavelength) was recorded. Results are shown in table (4.5).

Compound	$\phi_T$	$\lambda_{\text{max}}^{T-T} / \text{nm}$	$\epsilon (\lambda_{\text{max}})$ $\text{dm}^3 \text{ mol}^{-1} \text{ cm}^{-1}$
$T_4CS^-$ in 50% propan-2-ol	0.46	660	6980*
Benzophenone	1	525	7220

\* An error of  $\pm 10\%$  is estimated.

Table (4.5) *Triplet molar absorption coefficient of  $T_4CS^-$  in 50% alcoholic aqueous solution.*

#### 4.5.11 Singlet-Triplet Intersystem Crossing Quantum Yield for $TBS^-$

The lifetime of the excited triplet state of  $TBS^-$  in a degassed 50% ethanolic aqueous solution was found to be approximately 40 ns (see section 4.5.7), this is a much shorter lived transient species than the corresponding  $T_4CS^-$  triplet state (lifetime  $\approx 8\mu\text{s}$ ). The maximum concentration of naphthalene obtainable in 50% alcoholic aqueous solution is ca 0.05M - which may not be a high enough concentration of the sensitiser to intercept all the  $TBS^-$  triplet states formed. If this is the case then the calculated  $\Delta A_0$  value will result in a triplet quantum yield of  $TBS^-$  less than its intrinsic yield. However, a minimum value for its triplet yield can be obtained, and this was found to be 0.3.



## 4.6 Excited State Photochemistry of $T_4CS^-$ and $TBS^-$ with the addition of monomer Human Serum Albumin (mHSA)

### 4.6.1 Addition of mHSA to $T_4CS^-$

mHSA was added to solutions of  $T_4CS^-$  in 0.1M potassium phosphate buffer solution (pH = 7.4). The concentration of ethanol never exceeded 10% (for preparation and calculation of the concentration of mHSA used see section 3.6.1).

The ground state absorption spectrum of mHSA in buffer solution is displayed in figure (4.53), and shows negligible absorption at the laser excitation wavelength of 354.7 nm.

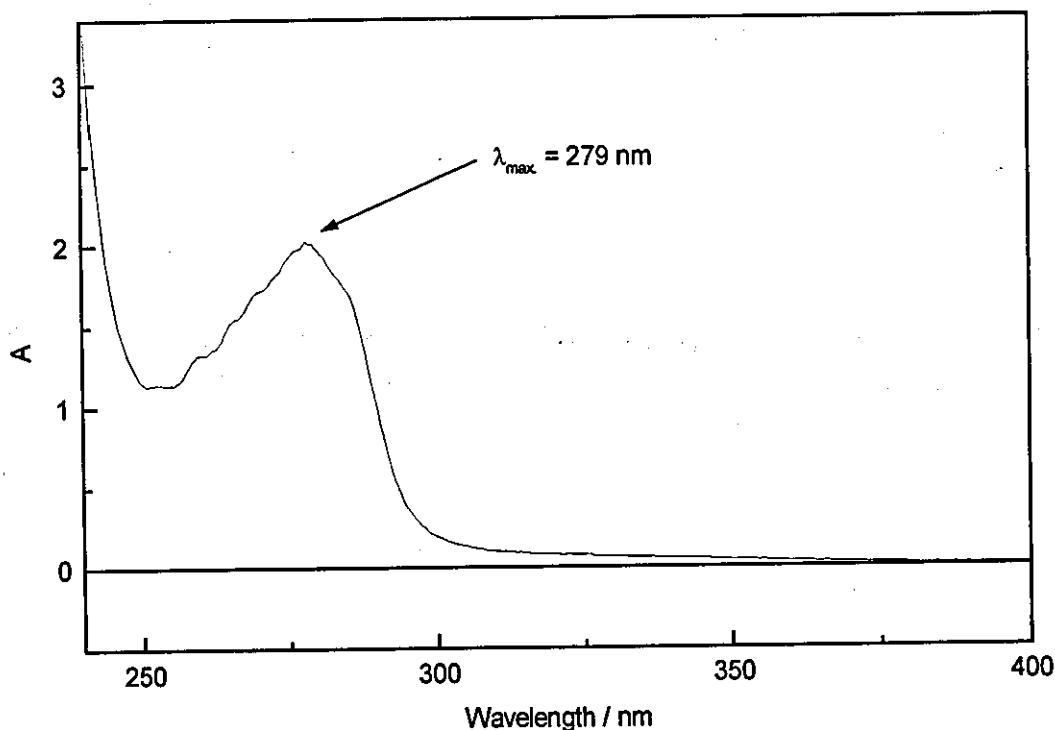
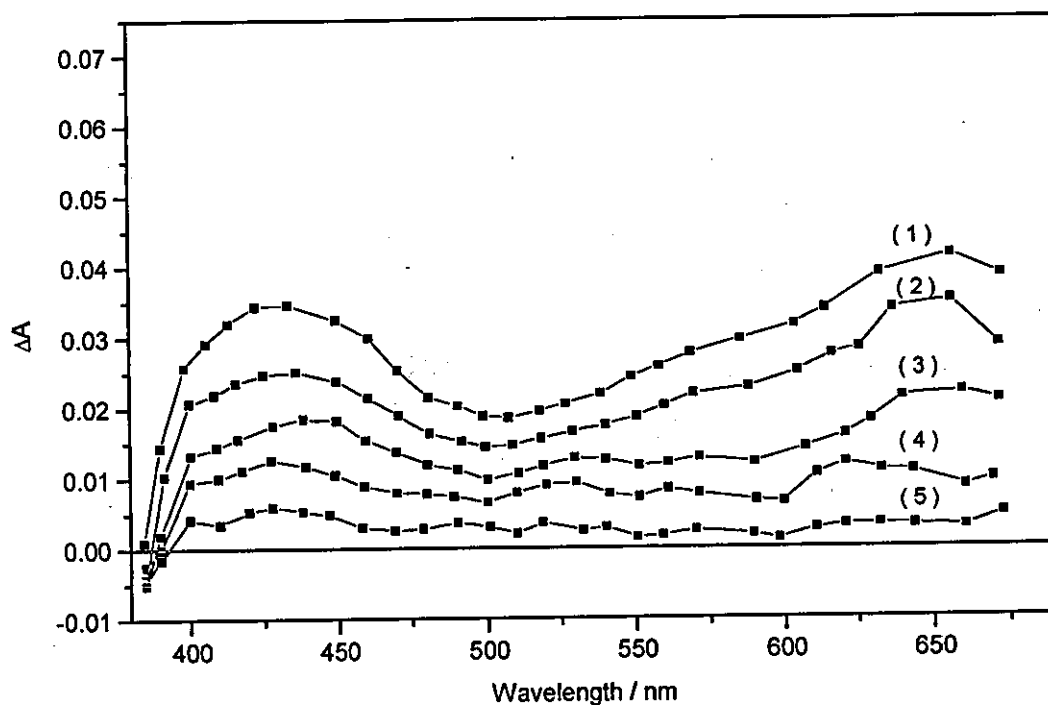


Figure (4.53) *Ground state absorption spectrum of human serum albumin (500  $\mu\text{M}$ ) in 0.1M potassium phosphate buffer, pH = 7.4.*

The band with the peak at 279 nm, is due to the aromatic residues, tyrosine and tryptophan [16].

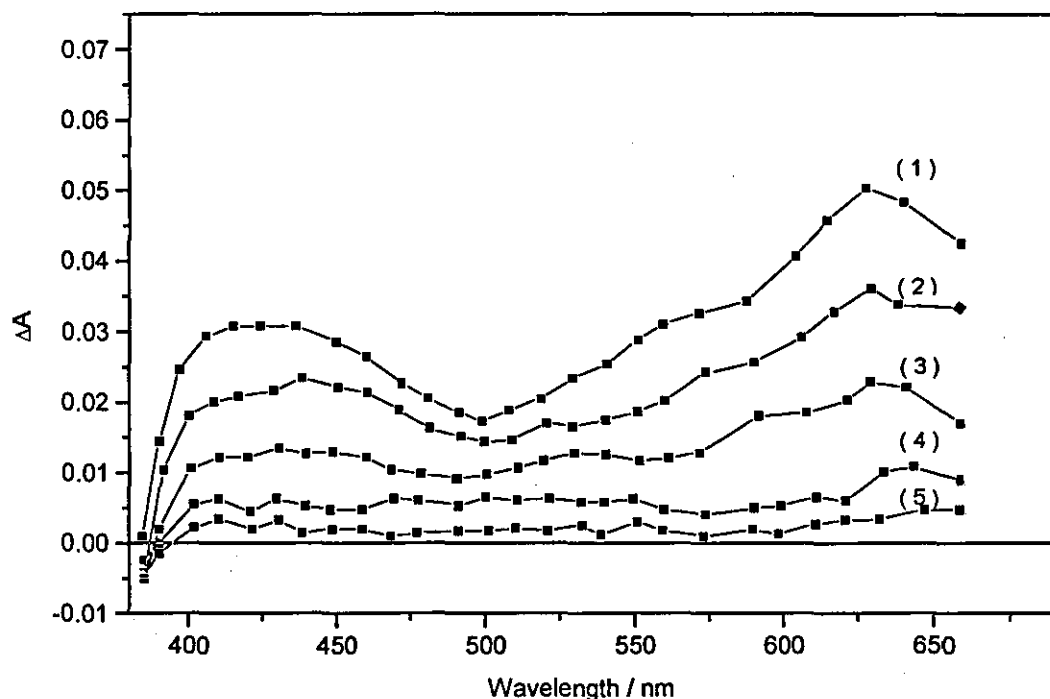
Flash photolysis studies were carried out on the first fractions collected containing the conjugate. The molar ratio of mHSA: $T_4CS^-$  was normally greater than 1:1 respectively. For flash photolysis experiments the absorbances of the solutions at the laser excitation wavelength of 354.7 nm were typically between 0.50 and 0.80, with laser energies between 18 and 40 mJ / pulse.

Figure (4.54) shows a typical transient absorption spectrum at five time delays of an aerated solution of mHSA /  $T_4CS^-$  in 10% aqueous ethanolic solution. In this particular experiment using an absorption of 0.7 at the laser excitation wavelength, with a laser energy of 19 mJ / pulse.



**Figure (4.54)** *Transient absorption spectrum of  $T_4CS^-$  with mHSA in an aerated 10% aqueous ethanolic solution at five time delays following the laser pulse. Delay times are (1) 1.0  $\mu s$ . (2) 3.1  $\mu s$ . (3) 6.7  $\mu s$ . (4) 12.9  $\mu s$ . (5) 38.7  $\mu s$ .*

The same stock was purged with nitrogen gas to remove the dissolved oxygen content. The resultant transient absorption spectrum again shown at five time delays is given in figure (4.55).



**Figure (4.55)** *Transient absorption spectrum of  $T_4CS^-$  with mHSA in a degassed 10% aqueous ethanolic solution at five time delays following the laser pulse. Delay times are (1) 5.3  $\mu s$ . (2) 12.0  $\mu s$ . (3) 22.0  $\mu s$ . (4) 51.0  $\mu s$ . (5) 143.0  $\mu s$ .*

The two spectra show the same structure, and appear to exhibit one transient species. The only difference being that the lifetime of the transient has increased upon degassing. This is very strong evidence that the same transient species is responsible for the entire transient absorption spectrum, as the quenching by oxygen appears to be very similar throughout. This can be exemplified by overlapping the transient decays obtained from the spectrum shown in figure (4.54) which were analysed at 430 nm and 590 nm. These two wavelengths displayed in figure (4.56) were chosen because their  $\Delta A_0$  values are almost identical.

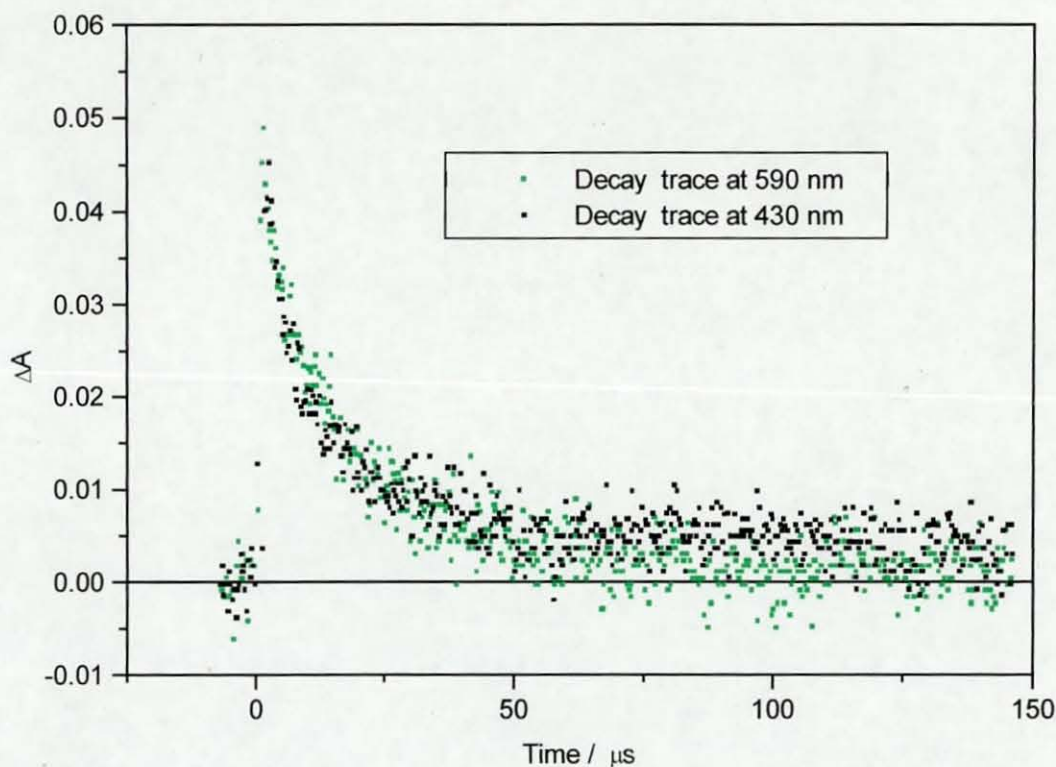


**Figure (4.56)** *Transient absorption decays of  $T_4CS^-$  with mHSA in an aerated 10% aqueous ethanolic solution, analysed at 430 nm and 590 nm.*

Analysis of the decay traces fitted first order kinetics. Typically lifetimes for aerated solutions were found to be between 6 and 8  $\mu s$ . Upon nitrogen purging the lifetime was found to increase to between 20 and 22  $\mu s$ . Furthermore, pumping oxygen into the system under study quenched the lifetime of the transient down to between 2 and 3  $\mu s$ . This degree of quenching is in accord with the transient observed being that of the triplet state of  $T_4CS^-$ .

Using these lifetimes a value can be obtained for the oxygen rate quenching constant,  $k_{O_2}$ . This was calculated to be between  $1.6-3.3 \times 10^8 \text{ dm}^3 \text{ mol}^{-1} \text{ s}^{-1}$ . If we compare this value with the value obtained in mHSA free solutions of  $3.5 \times 10^9 \text{ dm}^3 \text{ mol}^{-1} \text{ s}^{-1}$  (see section 4.5.2), we see that the triplet state upon binding to mHSA is protected from molecular oxygen at least ten fold.

Having identified the transient as being that of the triplet state of  $T_4CS^-$  when mHSA is added, a comparative look at the transient spectra obtained from the same stock solution of  $T_4CS^-$  with and without the presence of mHSA using identical experimental parameters was examined.

An absorption of 0.8 at the laser excitation wavelength and a laser energy of 36 mJ/pulse was used. Using identical time delays figure (4.57) shows the transient absorption spectrum of an aerated solution of  $T_4CS^-$  with mHSA added, and figure (4.58) shows the spectrum in mHSA free solution, *i.e.*  $T_4CS^-$  alone

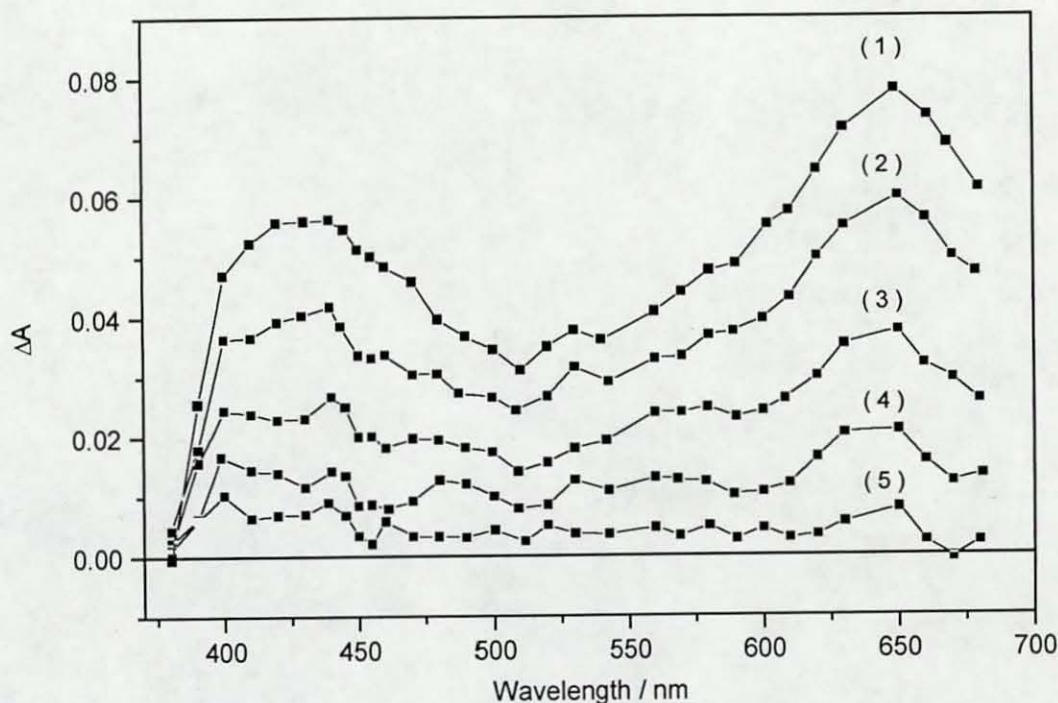


**Figure (4.57)** *Transient absorption spectrum of  $T_4CS^-$  with mHSA in an aerated 10% aqueous alcoholic solution at five time delays following the laser pulse. Delay times are (1) 1.1  $\mu s$ . (2) 3.1  $\mu s$ . (3) 6.4  $\mu s$ . (4) 12.5  $\mu s$ . (5) 45.7  $\mu s$ .*

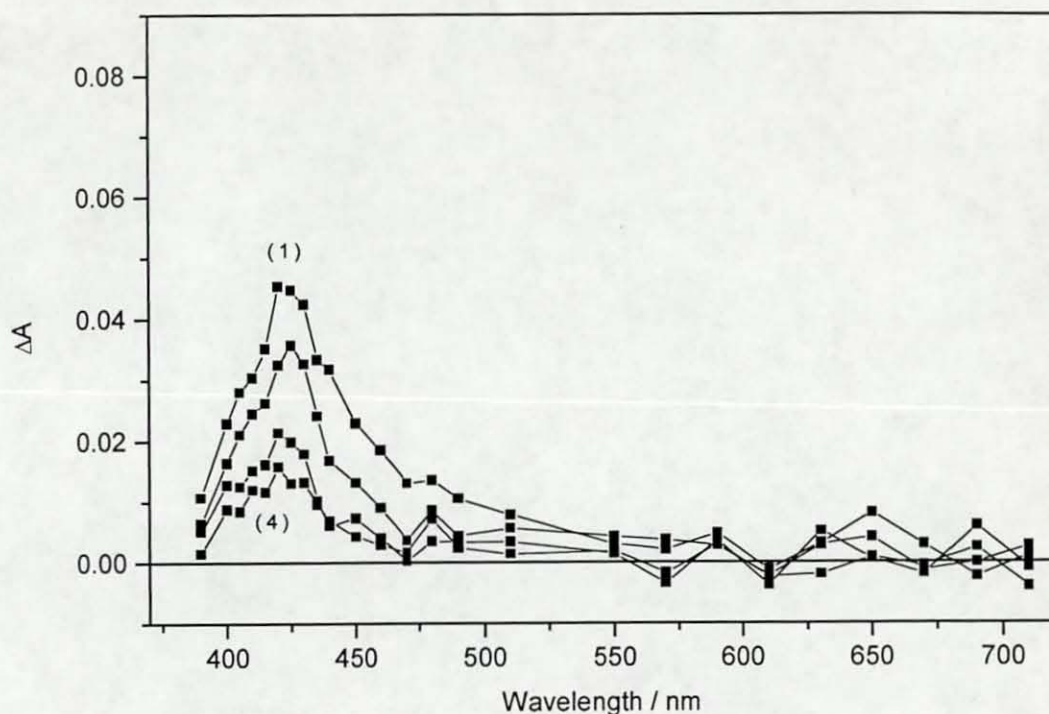


**Figure (4.58)** *Transient absorption spectrum of  $T_4CS^-$  in an aerated 10% aqueous alcoholic solution at five time delays following the laser pulse. Delay times are (1) 1.1  $\mu s$ . (2) 3.1  $\mu s$ . (3) 6.4  $\mu s$ . (4) 12.5  $\mu s$ . (5) 45.7  $\mu s$ .*

The kinetic traces analysed at 430 nm obtained from each spectrum are shown in figure (4.59). When mHSA is added to  $T_4CS^-$  solution the kinetic trace is clearly altered. The transient absorption assigned to being that of the radical anion of  $T_3CS^-$  in section 4.5.7 is clearly absent and what remains is the triplet state and reduced residual absorption assigned as a product of photolysis. This loss of the radical signal and reduction in product will be discussed in chapter 5.

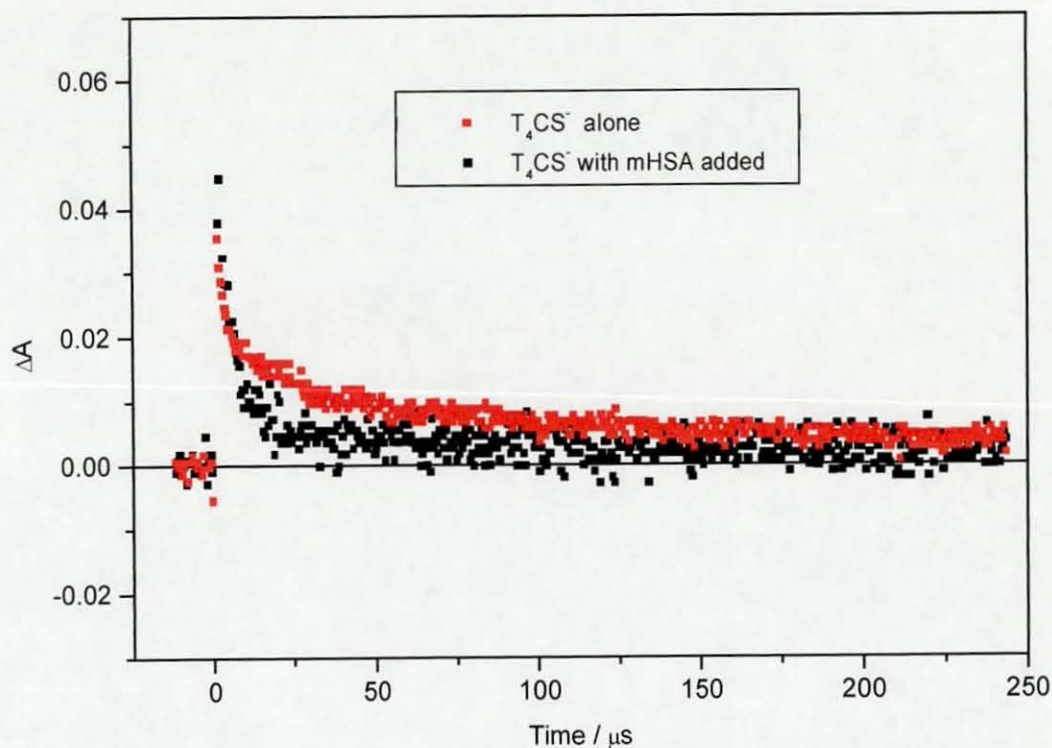


**Figure (4.59)** Kinetic traces obtained from flash photolysis of  $T_4CS^-$  alone and when mHSA is added, analysed at 430 nm.

#### 4.6.2 Laser Induced Degradation of $T_4CS^-$ / mHSA solutions

As with solutions of  $T_4CS^-$  (section 4.2), the degradation when mHSA is present in aerated solution was recorded by taking the ground state spectrum after flashing a comparable number of times (100 laser shots) using a laser energy of approximately 24 mJ/pulse. The resultant spectrum is shown in figure (4.60).

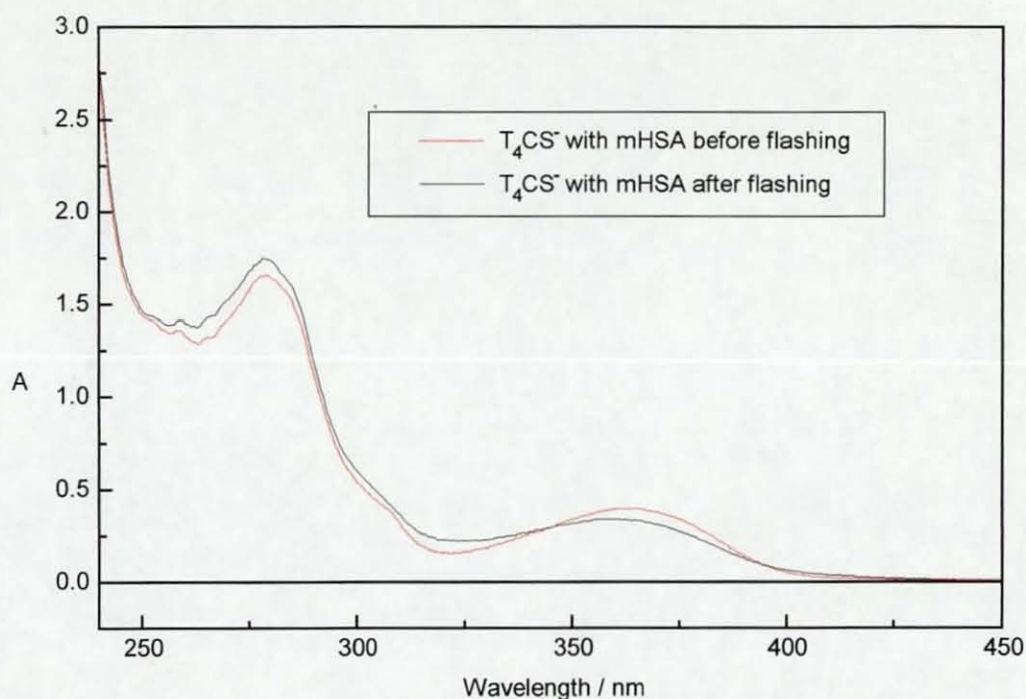


**Figure (4.60)** *Ground state absorption spectra of  $T_4CS^-$  with mHSA before and after flash photolysis.*

The amount of degradation and product formation is greatly reduced when compared to solutions of  $T_4CS^-$  alone (see figures 4.15 and 4.16), this will be discussed in chapter 5.

### 4.6.3 Addition of Bovine Serum Albumin (BSA) to solutions of $T_4CS^-$

Similarly BSA was added to solutions containing  $T_4CS^-$ . The mole ratio of BSA: $T_4CS^-$  being greater than 1:1. Using an absorbance at the laser excitation wavelength of 354.7 nm of 0.80 and a laser energy of 30 mJ/pulse the transient absorption spectrum obtained from flash photolysis of an aerated solution is shown at five time delays in figure (4.61).



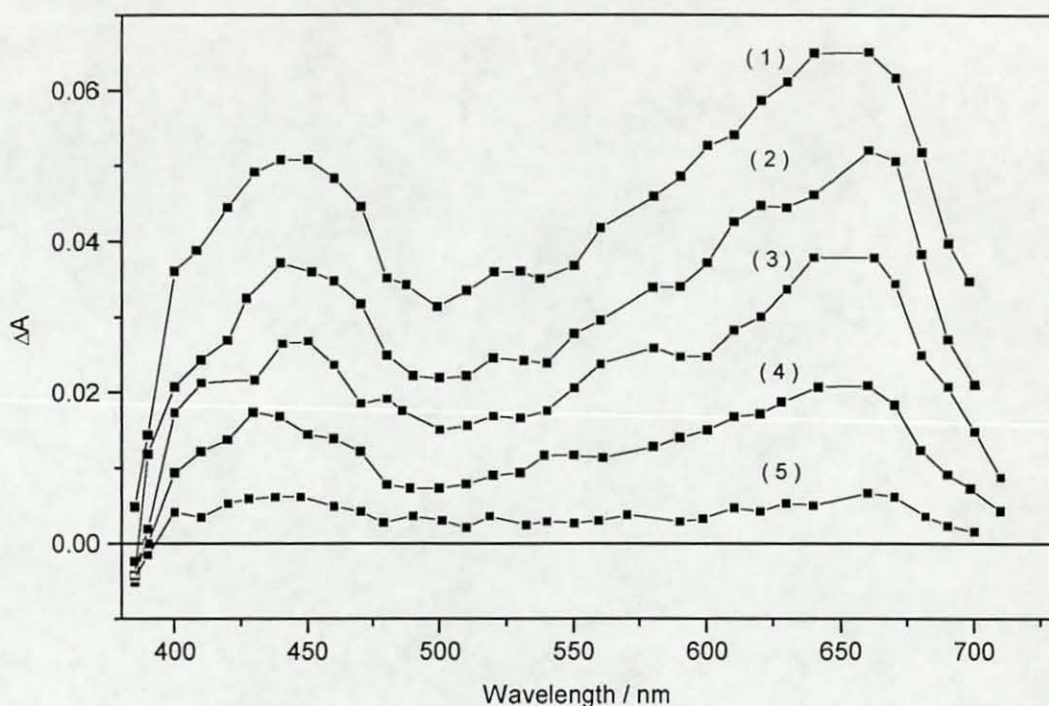


**Figure (4.61)** *Transient absorption spectrum of  $T_4CS^-$  with BSA added in an aerated 10% aqueous alcoholic solution at five time delays following the laser pulse. Delay times are (1) 3.3  $\mu s$ . (2) 10.0  $\mu s$ . (3) 24.0  $\mu s$ . (4) 51.3  $\mu s$ . (5) 130  $\mu s$ .*

The observed transient absorption spectrum mirrors that when mHSA is added, *i.e.* displaying the two bands with  $\lambda_{max.} = 440$  nm and 650 nm. However, there is a significant difference in the measured lifetimes, when compared to when mHSA is added. Analysis by first order kinetics on the aerated solution results in a lifetime of approximately 40  $\mu s$ . Upon purging with nitrogen the lifetime increased to approximately 80  $\mu s$ . These values result in an oxygen rate constant,  $k_{O_2}$ , of  $3.2 \times 10^7$   $dm^3 mol^{-1} s^{-1}$ . This is at least five times less than the value obtained for the addition of mHSA ( $k_{O_2}$  1.6 - 3.3  $\times 10^8$   $dm^3 mol^{-1} s^{-1}$ ).

#### 4.6.4 Addition of mHSA to $TBS^-$

$TBS^-$  in a 10% aqueous ethanolic solution was prepared. The absorbance at the laser excitation wavelength was approximately 0.7. A solution of  $TBS^-$  was flashed and analyzed at 430 nm. The same solution but with mHSA added (molar ratio of mHSA: $TBS^- > 1:1$ ) was prepared and flashed using exactly the same experimental conditions, again the transient was monitored at 430 nm. The resultant traces are shown below in figure (4.62).

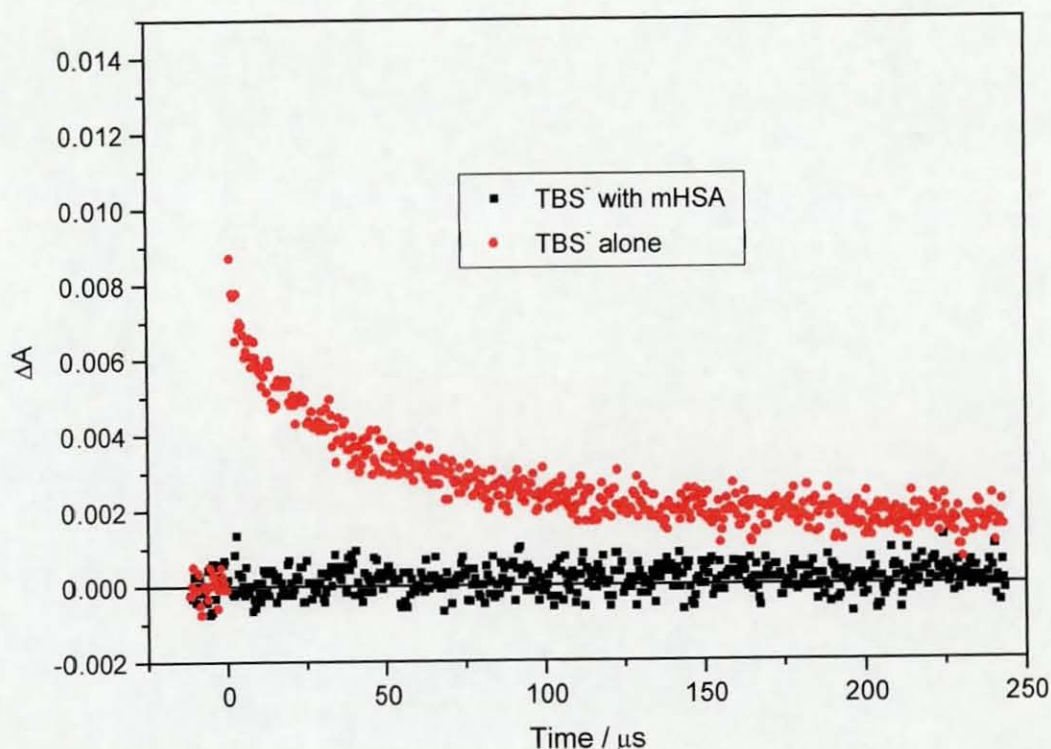


**Figure (4.62)** Decay traces of  $TBS^-$  with and without mHSA, analysed at 430 nm.

As can be seen the addition of mHSA clearly results in the loss of any transient signal. Other wavelengths were monitored, these too revealed no transient absorption.

## 4.7 Singlet Oxygen Formation Quantum Yield Determinations

It is known that many phototoxic compounds react upon irradiation producing singlet oxygen, which consequently can produce cellular damage such as oxidation of amino acid residues. Kochevar and Harber [17] reported that in aerated samples of  $T_4CS^-$  with HSA, upon irradiation there was a 15% reduction in the histidine content of the HSA, however analysis in the absence of oxygen revealed no difference in the histidine content when compared with solutions of HSA alone. They suggest that  $T_4CS^-$  is sensitising the photooxidation of histidine. Therefore, it was decided to see if  $T_4CS^-$  is capable of producing singlet oxygen ( $^1\Delta_g(O_2)$ ) which may lead to phototoxic action.

Details of singlet oxygen production, lifetimes in various solvents and quenching mechanisms are given in section (1.1.12), with details of the apparatus used for singlet oxygen phosphorescence detection given in section (3.4).

Preliminary experiments utilising  $D_2O$  as a solvent, after first dissolving the salicylanilides in small amounts of ethanol (5% by volume) for solubility purposes, indicated that upon excitation with 354.7 nm light, solutions containing  $T_4CS^-$  and TBS $^-$  sensitise the production of singlet oxygen, albeit, in small yields. To verify that the observed signal is actually singlet oxygen phosphorescence and not caused by any apparatus artefact - such as noise or detector overloading, the aforementioned solutions were purged with nitrogen gas in order to remove the dissolved oxygen. This clearly resulted in the loss of the phosphorescence signal - showing that the observed signal was due to singlet oxygen phosphorescence. Therefore, having established that the formation of singlet oxygen is sensitised by these compounds, the next step was to determine their quantum yields,  $\phi_\Delta$ . This can be achieved by comparing the phosphorescence intensity sensitised from  $T_4CS^-$  with the phosphorescence intensity produced using an appropriate standard. The standard selected was benzophenone in benzene solution, for which the quantum yield of singlet oxygen production,  $\phi_\Delta$ , is reported to be 0.36 [18].

The quantum yield of singlet oxygen production ( $\phi_\Delta$ ) can thus be calculated from equation (4.30).

$$\phi_{\Delta} = \frac{\text{slope of } T_4CS^-}{\text{slope of } Bz} \times \frac{(1 - 10^{-A_u}) n^2}{(1 - 10^{-A_s}) n_0^2} \times \frac{k_r^{Bz}}{k_r^{D_2O}} \times \phi_{\Delta}(Bz) \quad (4.30)$$

where the slopes are obtained from plots of  $I_{\Delta}^0$  versus laser intensity -  $I_{\Delta}^0$  is the singlet oxygen luminescence intensity extrapolated to zero time following the laser pulse. The second term in the equation corrects for any differences in ground state absorption,  $n$  and  $n_0$  are the index of refraction of the solvent containing the unknown and standard respectively,  $k_r^{Bz}/k_r^{D_2O}$  corrects for the variation in the radiative rate constants between the two solvents and  $\phi_{\Delta}(Bz)$  is the quantum yield of singlet oxygen production sensitised from benzophenone.

where:

$$n = 1.34 \quad \text{and} \quad n_0 = 1.498 \quad [12]$$

$$\phi_{\Delta}(Bz) = 0.36$$

$$\text{and } k_r^{Bz}/k_r^{D_2O} = 5.0 \quad [19]$$

## Experimental

For the luminescence data collection, the solutions were contained in 1 cm x 1 cm quartz cuvettes with the singlet oxygen luminescence detector being aligned orthogonal to the direction of the laser beam.

$T_4CS^-$  and  $TBS^-$  were prepared in a solution containing a concentration of  $D_2O$  of (Ca. 95%), benzophenone was prepared in benzene. The absorbances of the solutions were optically matched at the laser excitation wavelength of 354.7 nm to ensure equal number of photons are absorbed by each sample, typically absorbances being 0.60.

In the presence of oxygen (all samples were aerated), the solutions were excited using varying laser energies - this was achieved by attenuating the laser intensity by placing sodium nitrite filters in front of the laser beam.

## Results

The singlet oxygen luminescence decay traces that were collected were analysed at 1270 nm by fitting with 1st order kinetics, and extrapolation to zero time after the laser pulse yields a value for  $I_{\Delta}^0$ . Shown in figure (4.63) is a plot of  $I_{\Delta}^0$  as a function of laser intensity for the standard benzophenone, the data are fitted according to linear regression best line fit.

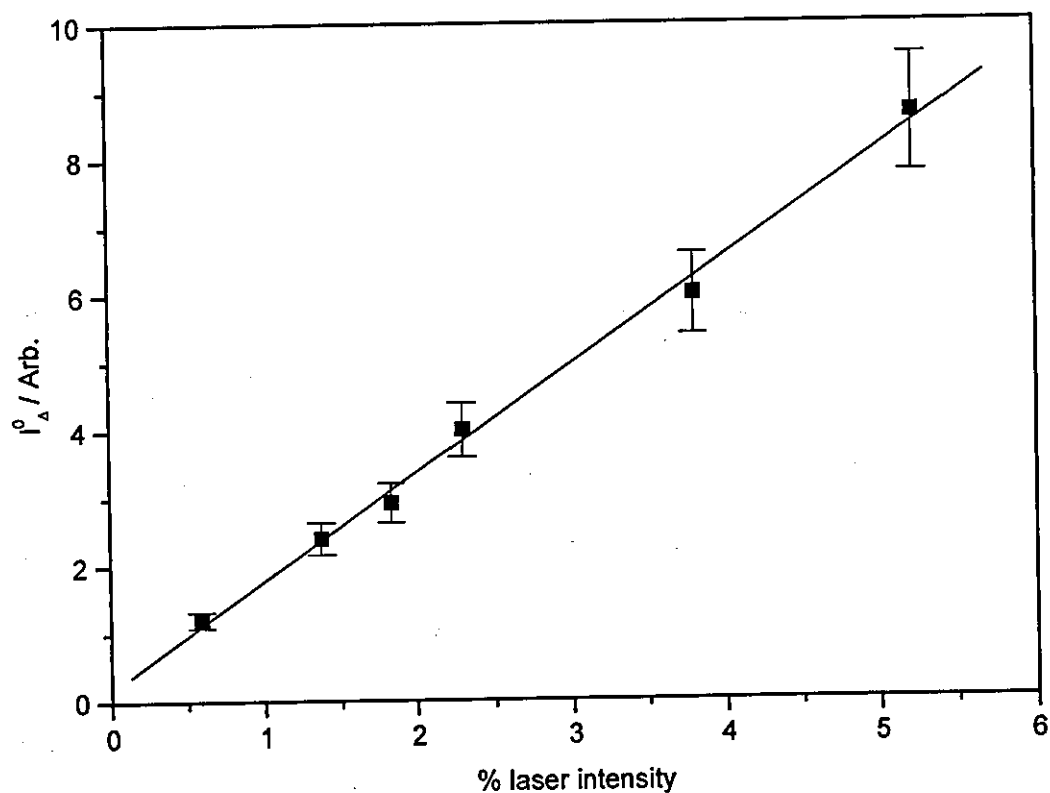
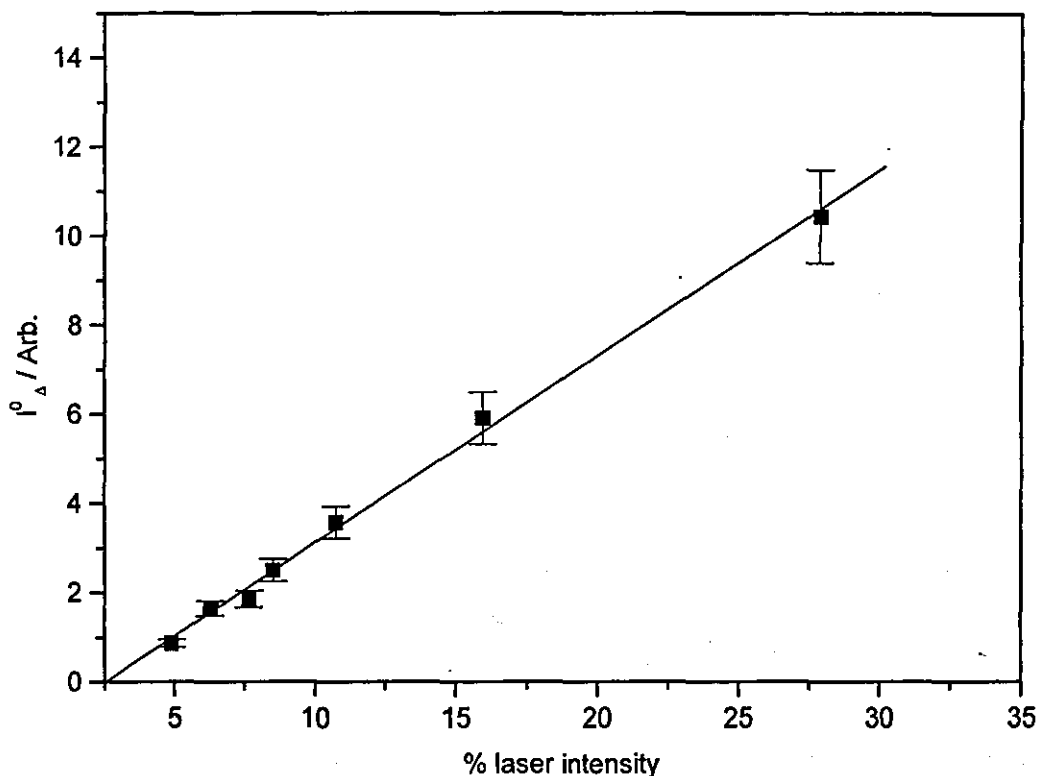


Figure (4.63) Plot of  $I_{\Delta}^0$  versus laser intensity for benzophenone in benzene.

An error of  $\pm 10\%$  is estimated for these measurements.

The best line fit was only performed at sufficiently low laser intensities to ensure that the plots of  $I_{\Delta}^0$  as a function of laser intensity were linear - the plot yielded a slope of

$1.52 \pm 1.5$ . Likewise, the plot acquired from analysing the data obtained with  $T_4CS^-$  is shown in figure (4.64), linear regression analysis on this yielded a value of  $0.28 \pm 0.028$ .



**Figure (4.64)** Plot of  $P_A$  versus laser intensity for  $T_4CS^-$  in 95 %  $D_2O$ .

An error of  $\pm 10\%$  is estimated for these measurements.

Using these values, the quantum yield of photosensitised singlet oxygen formation ( $\Phi_A$ ) from  $T_4CS^-$  was found using equation (4.30) to be  $0.23 \pm 0.05$ .

The sensitised singlet oxygen quantum yield from  $TBS^-$  was similarly investigated. The yield was found to be extremely small, thereby making accurate analysis difficult, however a value of approximately 0.06 was obtained for  $\Phi_A$ . Preliminary experiments with the addition of mHSA failed to produce any singlet oxygen signal.

## 4.8 1-Hydroxypyridine-2-thione (Omadine - Sodium Salt)

Omadine (pyrithione) is a known photoallergen [20]. It has been shown to bind photochemically to HSA but unlike  $T_4CS^-$  exhibits no specificity on binding [21]. Omadine is soluble in water, its ground state absorption spectrum in this solvent is shown in figure (4.65).

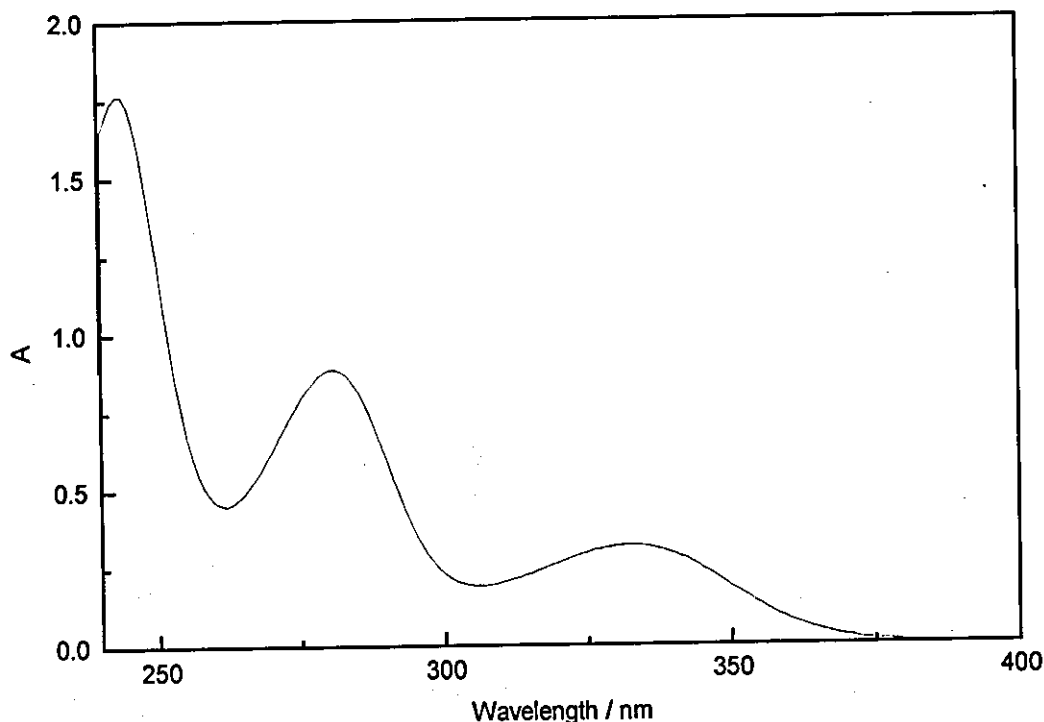


**Figure (4.65)** *Ground state absorption spectrum of omadine in water [100 μM]*

The laser excitation wavelength of 354.7 nm occurs within the long wavelength absorption band, and so was used as the excitation source. A solution was prepared with an absorbance of approximately 0.8 at 354.7 nm. Using a laser energy of 19mJ / pulse, a transient absorption spectrum was collected using the shortest timebase available (5ns / point) to the JK laser system, the resultant trace is shown in figure (4.66).

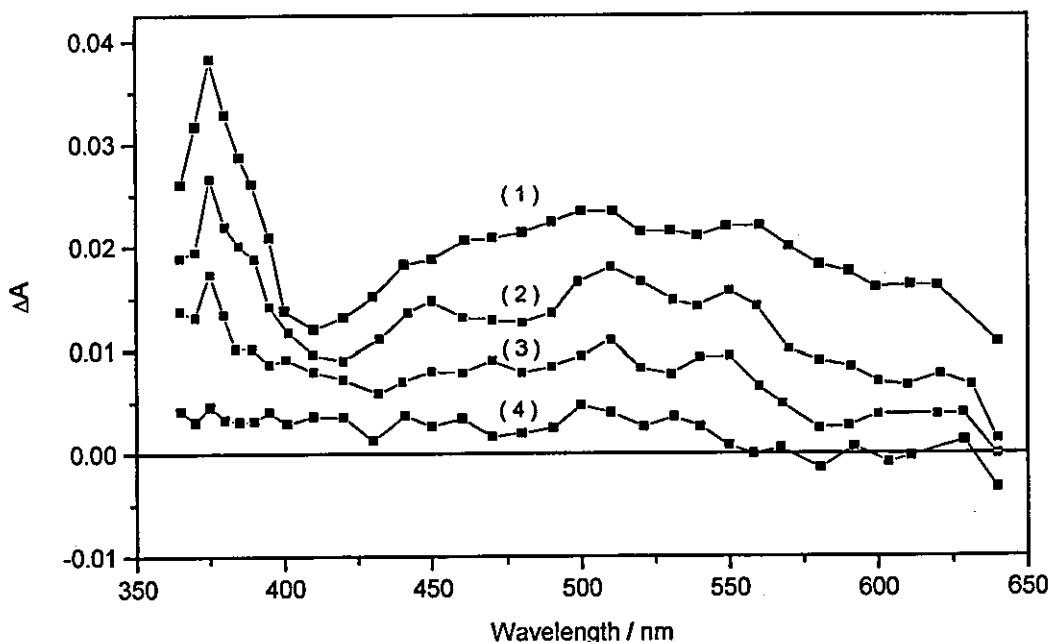


**Figure (4.66)** *Transient absorption spectrum of omadine in water at four time delays following the laser pulse. Delay times are (1) 90 ns (2) 130 ns (3) 200 ns (4) 700 ns*

The spectrum appears to decay uniformly at the same rate, which is verified by kinetic analysis of individual wavelengths which give a lifetime of approximately 90 ns when fitted by 1st order kinetics. Upon degassing, the transient lifetime is found to increase to 115 ns. From these values it is possible to calculate the oxygen quenching rate constant,  $k_{O_2}$ , is found using:  $k = k_d + k_{O_2} [O_2]$

where:

$$k = 1.1 \times 10^7 \text{ s}^{-1}$$

$$k_d = 8.7 \times 10^6 \text{ s}^{-1}$$

$$[O_2] = 0.29 \times 10^{-3} \text{ mol / dm}^3 \text{ in water [6]}$$

Giving a value of  $8 \times 10^9 \text{ dm}^3 \text{ mol}^{-1} \text{ s}^{-1}$  for the oxygen quenching rate constant,  $k_{O_2}$ , this value is consistent with the quenching of triplet states. If this is the excited triplet state of omadine, then purging the solution with oxygen should further quench the



lifetime, and indeed it is found to be quenched below 60 ns. Unlike the findings with the triplet state of  $T_4CS^-$ , the addition of excess HSA had no measurable effect on the transient absorption or lifetimes.

Omadine was excited at 355 nm and other wavelengths where it absorbs to see if any fluorescence occurs, but no emission was observed.

#### 4.9 Rose Bengal

Rose bengal has also been shown to bind to HSA, although not a photoallergen it can be phototoxic. It reacts upon irradiation producing singlet oxygen, this very powerful oxidant can result in cellular damage such as oxidation of amino acid residues and unsaturated lipids, also cross-linking of membrane proteins has been shown to occur [22].

Rose bengal absorbs in the visible region of the spectrum ( $\lambda_{max} = 549$  nm). The fundamental wavelength (1064 nm) of the JK laser can be doubled to produce the 532 nm harmonic (see section 3.3). This wavelength was the excitation source used to investigate the excited states of rose bengal and their reaction with HSA.

A solution with an absorption of 0.8 at the laser excitation wavelength was flashed with a laser energy of 63mJ / pulse, transient absorption spectra of both degassed and aerated solutions were collected.

Values for the rate constants obtained from the decay of the rose bengal triplet state in the presence and absence of oxygen were:

$$k = 4 \times 10^5 \text{ s}^{-1}$$

$$k_d = 1.3 \times 10^4 \text{ s}^{-1}$$

The oxygen concentration in water is given by:

$$[O_2] \text{ in water} = 0.29 \times 10^{-3} \text{ mol / dm}^3 \text{ [6]}$$

This gives a value of  $1.3 \times 10^9 \text{ dm}^3 \text{ mol}^{-1} \text{ s}^{-1}$  for the oxygen quenching rate constant,  $k_{O_2}$ . This agrees within experimental error (25 %) with the literature value of  $9.8 \times 10^8 \text{ dm}^3 \text{ mol}^{-1} \text{ s}^{-1}$  obtained in  $\text{H}_2\text{O}$  (pH = 7.2) [23]. Solutions of rose bengal with mHSA added to make a molar ratio of 0.9:1 respectively were flashed under identical conditions. Analysing at 600 nm the kinetic traces of aerated and nitrogen purged solutions by first order kinetics gave lifetimes of 32 and 120  $\mu\text{s}$  respectively. The oxygen quenching rate constant,  $k_{O_2}$ , is found to be  $8.0 \times 10^7 \text{ dm}^3 \text{ mol}^{-1} \text{ s}^{-1}$ . This value is 17 fold less than that obtained in protein free solutions, indicating that the photochemical interaction of rose bengal with protein results in strong protection of the triplet state from molecular oxygen, similar to the findings with the  $\text{T}_4\text{CS}^{\cdot-}$  triplet state.

# Chapter 4

## References

- [1] Jenkins F.P., Welti D. and Baines D., *Nature* **201**, 213-219. (1964)
- [2] Meech S.R. and Phillips D.J. *Photochem.*, **23**, 193 (1983)
- [3] Hama S. and Hirayama F., *J. Phys. Chem.*, **87**, 83 (1983)
- [4] Leigh W.J. and Arnold D.R.J. *Chem. Soc. Chem. Commun.* 406 (1980)
- [5] Rickwood D.M. and Barratt M.D., *Biophysical Chemistry* **19** 69-73 (1984)
- [6] Handbook of Photochemistry Murov S.L., Carmichael I. and Hug G.L. Marcell Dekker (1983)
- [7] Fischer G.J. and Land E.J., *Photochem. Photobiol.* **37**, 27-32 (1983)
- [8] Ghiron C.A., Bazin M., Santus R., *Biochem. Biophys. Acta* **957**: 207-216 (1988)
- [9] Evans D.F., *J. Chem. Soc.* 1351-7 (1957)
- [10] Hedstrom J., Sedarous S. and Prendergast F.G., *Biochemistry* **27**, 6203-8 (1988)
- [11] Bensasson R. and Land E.J., *Trans. Faraday Soc.*, **67**, 1904 (1971)
- [12] Handbook of Chemistry & Physics. Chemical Rubber Co. 52<sup>nd</sup> Ed. (1971)
- [13] Birks J.B., *Photophysics of Aromatic Molecules*, Wiley, New York (1970)
- [14] Lamola A.A. and Hammond G.S., *J. Chem. Phys.*, **43**, 2129 (1965)
- [15] Hurley J.K., Sinai N and Linshitz H., *Photochem. Photobiol.*, **38**, 9 (1983)
- [16] Theodore P.Jr., *Advances in Protein Chemistry*. Vol **37**, 161 - 242 (1985)
- [17] Kochever I.E. and Harber L.C., *J. Invest. Dermatol.* **68**, 151-156 (1977)
- [18] *J. Phys. Chem. Ref. Data*, Vol.22, No.1, 262 (1993)
- [19] Schmidt R., Afshari E. *J. Phys. Chem.* **94**, 4377-4378 (1990)
- [20] Maguire H.C.Jr. and Kaidbey K.J., *Invest. Dermatol.* **79**, 147-52 (1982)
- [21] Barratt M.D and Pendlington R.V., *Int. J. Cos. Sc.* **12**, 91-103 (1987)

- [22] Barratt M.D., Evans J.C., Lewis C.A. and Rowlands C.C., *Chem. Biol. Interactions* **38**, 215-30 (1982)
- [23] Yoshimura A. and Ohno T., *Photochem. Photobiol.* **48**, 561-5 (1988)

# **CHAPTER 5**

## **Summary, Conclusions and Recommendations for Further Work**

## 5.1 T<sub>4</sub>CS<sup>-</sup> in alcoholic aqueous solution

### 5.1.1 T<sub>4</sub>CS<sup>-</sup> in 50% alcoholic aqueous solution

The value of the pK<sub>a</sub> for the equilibrium between the ionised and unionised forms of T<sub>4</sub>CS-H has been found to be 6.1 in the same solvent composition [1] and 5.6 in methanol [2]. The molar absorption coefficient at 360 nm (maximum of the ionised form) was found to be 9370 dm<sup>3</sup> mol<sup>-1</sup> cm<sup>-1</sup>.

Using two standards the value measured for the fluorescence quantum yield,  $\phi_F$  of the ionised form of T<sub>4</sub>CS<sup>-</sup> in 50% alcoholic aqueous solutions was found to be  $0.5 \pm 0.05$  with  $\lambda_{\text{max}} = 438$  nm. The fluorescence intensity is the same within experimental error in the presence and absence of air. The half-life of the singlet state of T<sub>4</sub>CS<sup>-</sup> in ethanol measured using single photon counting techniques is 2.3 ns [1]. Rate constants for singlet state quenching by oxygen k<sub>O<sub>2</sub></sub>, are found to be typically between  $5 \times 10^9$  and  $3 \times 10^{10}$  dm<sup>3</sup> mol<sup>-1</sup> s<sup>-1</sup>, examples include indole in H<sub>2</sub>O ( $6.5 \times 10^9$  dm<sup>3</sup> mol<sup>-1</sup> s<sup>-1</sup>) [3] and anthracene in ethanol ( $2.5 \times 10^{10}$  dm<sup>3</sup> mol<sup>-1</sup> s<sup>-1</sup>) [4]. If the lifetime of the singlet state of T<sub>4</sub>CS<sup>-</sup> in 50% alcoholic aqueous degassed solutions is similar to that found in ethanol *i.e.*  $\sim 5$  ns or k<sub>d</sub>  $\sim 2 \times 10^8$  s<sup>-1</sup>, then using an upper value for k<sub>O<sub>2</sub></sub> of  $3 \times 10^{10}$  dm<sup>3</sup> mol<sup>-1</sup> s<sup>-1</sup> and applying these values to  $k = k_d + k_{O_2}[O_2]$  where  $[O_2] = 0.6 \times 10^{-3}$  (see section 4.5.2) gives  $k = 4 \times 10^8$  s<sup>-1</sup> or 4.6 ns. This is equivalent to 8% quenching and fluorescence quenching of this magnitude would be detectable. However, if k<sub>O<sub>2</sub></sub> were  $< 1 \times 10^9$  s<sup>-1</sup> or the singlet state lifetime were 1 ns or less, fluorescence quenching will be lower than 2% which is within experimental error.

These calculations suggest that in 50% ethanolic aqueous solutions the life-time of T<sub>4</sub>CS<sup>-</sup> maybe less than that found in neat ethanol and this is borne out in fluorescence studies which show a decrease in fluorescence yields as the water content is increased (section 4.3.2). The phosphorescence band of T<sub>4</sub>CS<sup>-</sup> in ethanol at 77K peaks between 458 and 465 nm, which corresponded to a first triplet state energy of between 258 - 261 kJ mol<sup>-1</sup>.

Upon flash photolysis the excited triplet state was shown to absorb with  $\lambda_{\text{max}} = 650 \text{ nm}$ , and was found to have a lifetime of approximately  $8 \mu\text{s}$  in degassed solutions. In aerated solutions, the triplet state was quenched by molecular oxygen, reducing the lifetime to approximately  $0.3 \mu\text{s}$  - yielding an oxygen rate quenching constant,  $k_{\text{O}_2}$ , of  $5.2 \times 10^9 \text{ dm}^3 \text{ mol}^{-1} \text{ s}^{-1}$ , which is in the range for oxygen quenching of most triplet states.

Triplet-triplet energy transfer experiments using naphthalene as an acceptor molecule ( $E_{\text{T}} = 254 \text{ kJ mol}^{-1}$ ) were found to quench the triplet state of  $\text{T}_4\text{CS}^-$ , with a quenching constant,  $k_{\text{q}}$ , of  $2.6 \times 10^9 \text{ dm}^3 \text{ mol}^{-1} \text{ s}^{-1}$ . This is not quite the diffusion controlled rate, *i.e.*, lower than the maximum possible rate of bimolecular diffusion,  $k_{\text{diff}}$ , estimated at  $4.60 \times 10^9 \text{ dm}^3 \text{ mol}^{-1} \text{ s}^{-1}$ . The rise and decay of the sensitised naphthalene triplet-triplet absorption was observed confirming that triplet-triplet energy transfer was taking place. As expected no energy transfer occurs between  $\text{T}_4\text{CS}^-$  and biphenyl ( $E_{\text{T}} = 274 \text{ kJ mol}^{-1}$ ), the triplet state energy of which is higher than that of  $\text{T}_4\text{CS}^-$  confirming that  $254 \text{ kJ mol}^{-1} < E_{\text{T}} \text{ T}_4\text{CS}^- < 274 \text{ kJ mol}^{-1}$ .

Triplet yield,  $\phi_{\text{T}}$ , determination was performed by sensitising naphthalene with both  $\text{T}_4\text{CS}^-$  and the standard benzophenone. Comparing their relative  $\Delta A_0$  values following laser excitation resulted in a value for  $\phi_{\text{T}}$  of  $0.47 \pm 0.09$ . According to the second law of photochemistry by Stark and Einstein, the absorption of light by a molecule is a one-quantum process, so that the sum of primary process quantum yields ( $\phi$ ) must be unity. That is  $\phi_{\text{F}} + \phi_{\text{ISC}} + \phi_{\text{R}}(\text{S}) + \phi_{\text{IC}} = 1$ , where  $\phi_{\text{R}}(\text{S})$  represents photochemical reaction from excited singlet states and  $\phi_{\text{IC}}$  represents internal conversion. Using the aforementioned values for  $\phi_{\text{T}}$  and  $\phi_{\text{F}}$  leaves  $\phi_{\text{R}}(\text{S}) + \phi_{\text{IC}} = 0.03 \pm 0.14$  for  $\text{T}_4\text{CS}^-$  in 50% ethanolic aqueous solution.

### 5.1.2 $\text{T}_4\text{CS}^-$ in 10% alcoholic aqueous solution

Upon using a smaller concentration of alcohol, that is 10% by volume (maximum alcohol concentration when mHSA was added), the molar absorption coefficient at  $358 \text{ nm}$  (maximum of the ionised band) was found to be  $8810 \text{ dm}^3 \text{ mol}^{-1} \text{ cm}^{-1}$ .

The fluorescence quantum yield,  $\Phi_F$ , was found to be  $0.27 \pm 0.03$ . Upon flash photolysis the excited triplet state was shown to absorb with  $\lambda_{\max} = 630$  nm, and was found to have a lifetime in degassed solutions of approximately 3  $\mu\text{s}$  and in aerated solutions this is quenched down to 0.5  $\mu\text{s}$ . The value of,  $k_{O_2}$ , in this solvent was estimated as  $3.5 \times 10^9 \text{ dm}^3 \text{ mol}^{-1} \text{ s}^{-1}$ .

The triplet yield was found by assuming that the molar absorption coefficient in 50% and 10% aqueous ethanolic solution are approximately the same, and comparing their relative  $\Delta A_0$  at their respective  $\lambda_{\max}$ . - the triplet yield was found to be  $0.36 \pm 0.07$ . This leaves  $\phi_R(S) + \phi_{IC} = 0.37 \pm 0.1$  for  $T_4CS^-$  in 10% ethanolic aqueous solution.

Even when taking experimental error into account, it is clear that in solutions of  $T_4CS^-$  with a higher concentration of water, either the rate constant for the photochemical reaction increases or the non-radiative process (internal conversion) competes much more efficiently.

In various alcoholic aqueous compositions  $T_4CS^-$  shows negligible solvent shifts in absorption and fluorescence maxima, thus the  $\Delta E(S-T)$  values for  $T_4CS^-$  in all alcoholic aqueous solutions was found to be approximately 42 - 45  $\text{kJmol}^{-1}$ . This small energy value for the singlet - triplet splitting suggest ( $n, \pi^*$ ) states.

## 5.2 Degradation of $T_4CS^-$ in alcoholic aqueous solutions

The ground state degradation experiments carried out on  $T_4CS^-$  in both 50% and 10% ethanolic aqueous solutions do show that there is product formation. A long tail tapering from 400 to 900+ nm is observed in the ground state absorption spectrum following laser excitation. Although no attempt was made in this thesis to quantify the yield of product formation these spectra do suggest that the product yield in 10% alcoholic aqueous solutions is considerably more than it is in 50% alcoholic aqueous solutions. This is in accord with the findings discussed earlier which suggest that in 10% alcoholic aqueous solutions photochemical reaction may be greater.

Although the lifetime of the radical species is unaffected by molecular oxygen, it does have an affect on the amount of radical produced, as we shall discuss.

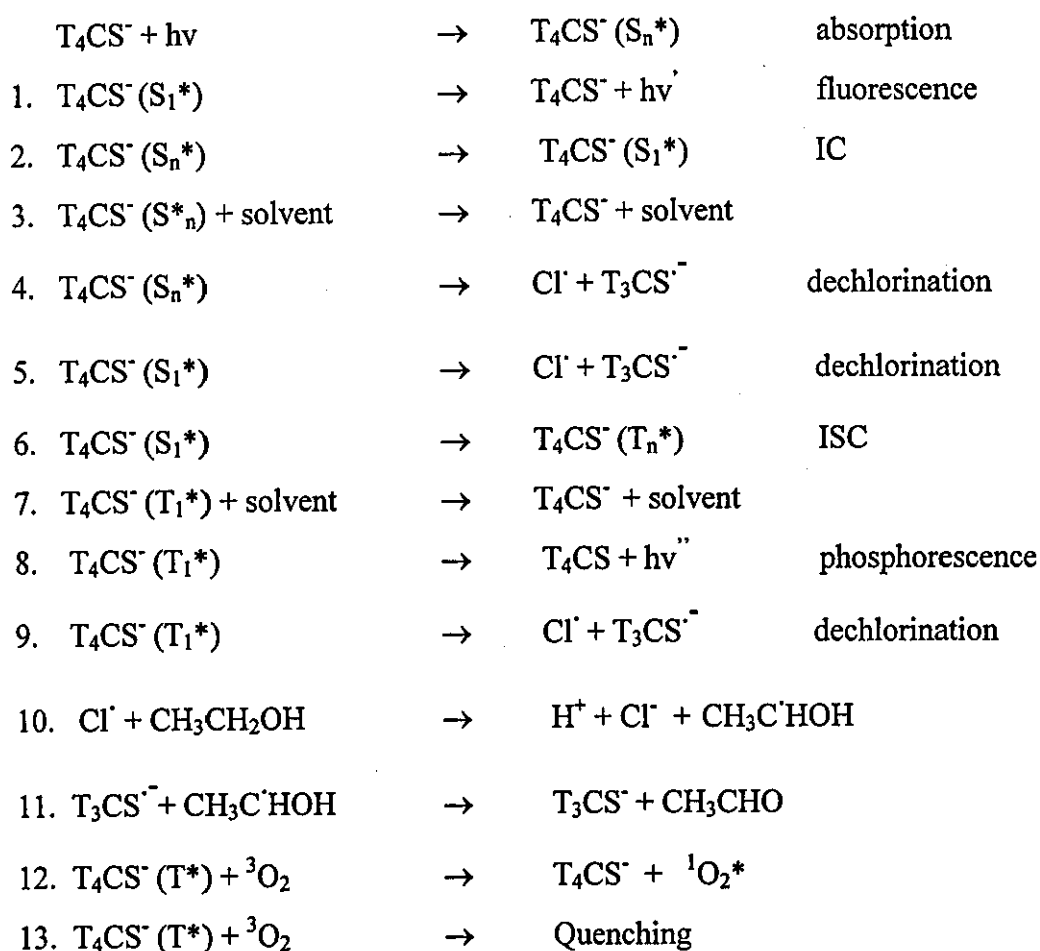


### 5.3 Kinetics of the radical ( $\lambda_{\text{max.}} = 425 \text{ nm}$ )

Although there are four different tri-chlorosalicylanilide's possible, it has consistently been found that the first dechlorination results in the formation of 3',4',5-trichlorosalicylanilide as the primary photoproduct (see section 2.7). Therefore the residual absorption found in all the transient absorption spectra is assigned to this primary product.

The half-life of the radical species produced upon exciting  $T_4CS^-$  in alcoholic aqueous solutions was found to be approximately  $60\mu\text{s}$  - the significance of this lifetime will be discussed shortly.

A possible reaction scheme of the primary photoreactions that occur upon photolysis of  $T_4CS^-$  in aerated alcoholic aqueous solutions which is consistent with the data found in this thesis and previous findings is shown below:



#### 5.4 TBS<sup>-</sup> alcoholic aqueous solution

TBS<sup>-</sup> exhibits similar ground state absorption to that of T<sub>4</sub>CS<sup>-</sup> in alcoholic aqueous solutions. Its pK<sub>a</sub> has been found to be almost identical to that of T<sub>4</sub>CS-H (approx. pK<sub>a</sub> = 5.8 in methanol) [1]. The extinction coefficient at 360 nm (maximum of the ionised band) was found to be 9997 dm<sup>3</sup> mol<sup>-1</sup> cm<sup>-1</sup> in 10% aqueous alcoholic solution.

The value measured for the fluorescence quantum yield,  $\phi_F$ , of the ionised form of the TBS<sup>-</sup> in alcoholic aqueous solutions is approximately 0.04. This is about a tenth of the fluorescence yield found for T<sub>4</sub>CS<sup>-</sup>, a reduction that would be expected for a heavy atom effect - where the heavier bromine atoms increase the rate of ISC due to enhanced spin-orbit coupling. As with T<sub>4</sub>CS<sup>-</sup> the half life of the singlet state measured using single photon counting techniques is 2.35 ns in ethanol [1] and likewise we would not expect to observe oxygen quenching of the singlet state. However, this singlet state half-life which is similar to that found with T<sub>4</sub>CS<sup>-</sup> is in conflict with the reduced value of  $\phi_F$  and requires clarifying (see recommendations for further work).

The phosphorescence band at 77 K almost mirrors that of T<sub>4</sub>CS<sup>-</sup> and peaks between 457 and 462 nm, which corresponds to a first triplet state energy of between 259-262 kJ mol<sup>-1</sup>.

Flash photolysis of TBS<sup>-</sup> in 50% alcoholic aqueous solutions revealed only the radical species and product on the time scales available to the JK laser system. There was found to be no difference between degassed and aerated solutions. The half-life of the radical species was found to be approximately 30  $\mu$ s. Hilal [1] also found that oxygen does not have any marked effect on the photolysis of TBS, stating that either the reaction proceeds exclusively via the singlet state, or if the triplet is involved, the reaction must be so rapid that oxygen does not quench the reaction. However, using the HY laser system, which has a slightly shorter time-base, it was possible to observe the triplet state of TBS<sup>-</sup> in 50% alcoholic aqueous solution. Analysing at 660 nm the lifetime was found to be approximately 40 ns - which is too short lived to be affected

by oxygen in aerated solutions. Upon pumping oxygen at high pressure (approximately three atmospheres) into a degassed cell resulted in loss of the transient signal. This loss of transient signal attributed to the triplet state would be expected if the oxygen rate quenching constant of  $T_4CS^-$  is comparable with that found in solutions of  $T_4CS^-$  ( $k_{O_2}$  of  $5.2 \times 10^9 \text{ dm}^3 \text{ mol}^{-1} \text{ s}^{-1}$ ).

Using the same experimental method as that for finding the triplet yield,  $\phi_T$ , of  $T_4CS^-$ , a minimum value was determined for the triplet yield of  $TBS^-$  and this was found to be 0.3.

### 5.5 Addition of mHSA to $T_4CS^-$

When mHSA was added to solutions of  $T_4CS^-$  there was a dramatic effect on the transient absorption spectrum when compared with the recorded transient spectra of  $T_4CS^-$  alone. Now we observe a transient absorption spectrum assigned to the triplet which appears to decay uniformly. This is backed up by kinetic analysis at individual wavelengths: In aerated solutions, first order kinetic analysis gave lifetimes of between 5 and 6  $\mu\text{s}$ . Verification that the transient spectrum is due to one species was shown by purging the solutions with nitrogen gas to remove the oxygen content - this increased the lifetime of the transient species to between 20 and 22  $\mu\text{s}$ , in contrast purging with oxygen quenched the lifetime down to approximately 1.5  $\mu\text{s}$ . This gives  $k_{O_2}$  as between  $1.6$  and  $3.3 \times 10^8 \text{ dm}^3 \text{ mol}^{-1} \text{ s}^{-1}$  compared to  $3.5 \times 10^9 \text{ dm}^3 \text{ mol}^{-1} \text{ s}^{-1}$  in albumin free solutions, thus clearly showing that the triplet state of  $T_4CS^-$  is being protected from molecular oxygen by at least a factor of ten upon binding to mHSA.

It is the loss of the radical anion absorption under the time resolution of the JK laser that is the most important feature, and may be pivotal in going some way to explaining the specificity of  $T_4CS^-$  binding to mHSA. To explain the loss of the radical anion absorption we need to look at the possibilities. One possibility is that the radical anion formed by the dechlorination of  $T_4CS^-$  that we have observed in non-mHSA solutions is not formed or its yield is greatly diminished in the presence of mHSA. Alternatively the radical's lifetime has decreased greatly enough for it not

to be observed on the time scales of these experiments. What is interesting is that there is still some residual absorption left over, indicating that product is still being formed albeit in a much reduced yield. This is borne out by the ground state absorption spectra shown before and after flash photolysis of  $T_4CS^-$  with mHSA (figure 4.60) showing much reduced degradation when compared to  $T_4CS^-$  alone - indicating that upon binding to mHSA,  $T_4CS^-$  has become much more stable.

### 5.6 Addition of BSA to $T_4CS^-$

When BSA was added to solutions of  $T_4CS^-$ , similar transient absorption spectra were obtained as with the addition of mHSA, the only difference being in the lifetime of the triplet state. In aerated solutions the lifetime is approximately 40  $\mu s$  and upon nitrogen purging it has risen to 80  $\mu s$ , resulting in a value of  $k_{O_2}$  of

$3.2 \times 10^7 \text{ dm}^3 \text{ mol}^{-1} \text{ s}^{-1}$ , which is about five times less than that found with mHSA. The reason for this difference may be due to the respective binding sites, as there are differences in structure between the two albumins. When human and bovine albumins are compared there are found to be 118-135 differences or about 20-23% difference [5].

### 5.7 Addition of mHSA to $TBS^-$

The findings with  $T_4CS^-$  are mirrored when mHSA is added to solutions of  $TBS^-$ , where flash photolysis of solutions containing  $TBS^-$  with mHSA present resulted in the loss of all radical absorption when mHSA was added with a mole ratio of 1:1 (mHSA: $TBS^-$ ) respectively. The association of  $T_4CS^-$  with mHSA resulted in an increase in the triplet lifetime (discussed in 5.5) from about 5  $\mu s \rightarrow 20 \mu s$ , *i.e.*, the decay has slowed down four-fold. If there is a similar effect extending the triplet lifetime of the short lived  $TBS^-$  triplet state which is over a hundred times faster than the corresponding triplet state of  $T_4CS^-$  from 40 ns  $\rightarrow$  160 ns upon association with mHSA it would have been observed using the JK laser system. The limit of detection on this laser is around 60 ns, for example detecting the triplet state of omadine (see section 4.8). This does not rule out the possibility that the lifetime of the  $TBS^-$  triplet

is not extended at all, but does suggest the processes involved upon association with mHSA are very different from those of  $T_4CS^*$ .

### 5.8 Difference in binding between $T_4CS^*$ and other photoallergens to HSA

To recap on section 2.7, it has been shown that  $T_4CS^*$  has high specificity for mHSA when compared with other photoallergens. The majority of photoallergens bind non-specifically to proteins, many with stoichiometries greater than 1:1, photoallergen:protein. Barratt and Rickwood [6] carried out dark-binding studies with  $T_4CS^*$  and mHSA and found only a single strong binding site. In contrast when fentichlor and mHSA were irradiated with UV light (313 nm), it was found at least eight molecules of fentichlor were bound per molecule of protein and fractionation of the protein of fentichlor-mHSA photoadducts showed that the bound fentichlor was distributed fairly evenly throughout the sequence of the mHSA molecule [7]. It has been shown that strong non-covalent binding of  $T_4CS^*$  to protein is a pre-requisite for formation of a photoaddition product [8] and since not all proteins present in the skin are capable of forming covalent photoadducts with  $T_4CS^*$  only those that can form a non-covalent association with  $T_4CS^*$  will go on to form the photoproduct. This is exemplified with fentichlor, which unlike  $T_4CS^*$  will react with almost equal efficiency with both mHSA and  $\gamma$ -globulin [7]. Experiments evidenced by the incorporation of salicylanilide fluorescence into HSA [8] indicated that it is  $T_4CS^*$  alone that acts as a photoallergen rather than the primary products of irradiation such as 3',4',5-trichlorosalicylanilide. This trichloro compound exhibited only weak photobinding to mHSA, and other less chlorinated salicylanilide's showed no tendency to complex with mHSA at all. Morikawa *et al* [9] also found that it is not the stable photochemical dechlorination products that react with protein. So although the other salicylanilide's are quite photoreactive, their weaker complexation with mHSA leads them to be less likely to form covalent photoadducts. Thus it appears that it is the primary photochemical reaction of  $T_4CS^*$  with mHSA that is paramount to causing photoallergy and secondary photochemical reactions are less important.

The difference in specificity between  $T_4CS^*$  when compared to other

photoallergens is thought to arise from the reactive species formed upon irradiation such as free radicals. The lifetime upon irradiation of the  $T_4CS^{\cdot-}$  radical or reactive species is thought to be too short lived to allow diffusion away from the strong non-covalent binding site before a deactivation process occurs, thus leading to high specificity to mHSA because it has the ability to dark-bind to this protein. With other proteins where there is not this non-covalent association, it is believed the reactive species will react with solvent molecules or de-activate through collisions with solvent molecules before the chance of combining with protein. Up to now the lifetime of the radical species:  $T_3CS^{\cdot-}$  produced upon photolysis of  $T_4CS^{\cdot-}$  has not been established. In the absence of protein, the half-life of the radical anion was found to be approximately 60  $\mu s$ . If we compare this lifetime to other photoallergens like fentichlor and bithional, they have been shown using electron spin resonance spectroscopy to produce free radicals that have long lifetimes of a few minutes [7]. Research by Anita Jones [unpublished] in this laboratory support these findings, she has observed radical production from fentichlor and bithional in solution with lifetimes of approximately 0.1 seconds - this lifetime is a thousand times as long lived as any radical produced from  $T_4CS^{\cdot-}$  upon irradiation, thus enabling diffusion to sites throughout the HSA molecule or the photobinding to other proteins contained in the skin.

### 5.9 Phototoxicity of $T_4CS^{\cdot-}$

In Hilal's conclusions he stated that in a 'Persistent Light Reactor' PLR the chlorosalicylanilide-protein conjugate would be retained in the skin for long periods, which is capable of further photochemical reaction. Here it would act as an active centre in the skin and on subsequent exposure to light, both phototoxic and photoallergic responses would be anticipated. The phototoxicity he states is due principally to the production of hydrochloric acid which would have the effect of lowering the pH of the skin and causing localised irritation. Later Kochevar [10] proposed a mechanism (see figure 5.1) that may explain the weak phototoxicity of  $T_4CS^{\cdot-}$  and an explanation for PLR. It was shown that irradiation of  $T_4CS^{\cdot-}$  with

mHSA in aerated samples resulted in a 15% reduction in the histidine content. However, analysis in the absence of oxygen revealed no difference in the histidine content. These results indicate that  $T_4CS^-$  is capable of photosensitising the destruction of histidine in the presence of oxygen and it is this sensitised photooxidation of cell components that has been proposed to be the mechanism underlying the phototoxicity of a number of chemicals and the weak phototoxicity of  $T_4CS^-$  may be due to this mechanism.

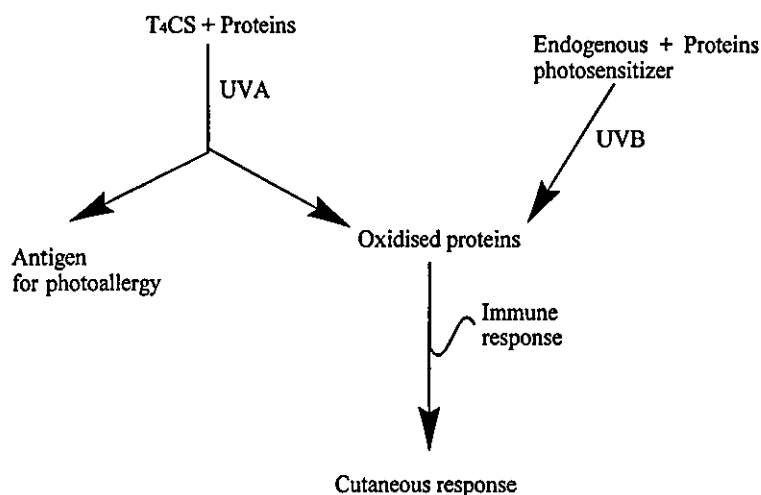


**Figure (5.1)** *A postulated mechanism for persistent light reactivity showing possible initiation by a photoallergic compound.*

$T_4CS^-$  and  $TBS^-$  were found to be capable of producing singlet oxygen, the generation of which can cause cellular damage such as oxidation of amino acid residues. The production of singlet oxygen sensitised from  $T_4CS^-$  was measured by direct comparison with the standard benzophenone. These investigations resulting in  $\phi_\Delta$  of  $0.23 \pm 0.05$  for  $T_4CS^-$  and 0.06 for  $TBS^-$ . Upon the addition of mHSA no singlet oxygen was detected.

## Recommendations for further work

The work detailed in this thesis has gone part of the way towards an understanding of the excited state photochemistry of  $T_4CS^-$  and  $TBS^-$  in alcoholic aqueous solutions buffered at physiological pH (7.4) upon flash photolysis at 354.7 nm. The excited states that are produced along with the lifetimes and quantum yields have built up a picture of the primary photochemical processes, but what is required is some collaborating evidence using other techniques, for example quantification of the product yields. It is clear that the photochemical yields are very dependent on the solvent composition. Laser degradation experiments (shown in section 4.2) show qualitatively that the yield of permanent product is dependent on the solvent composition. The same experimental procedure showed that the addition of mHSA to  $T_4CS^-$  (section 4.62) appears to stabilise  $T_4CS^-$  with a reduction in the yield of permanent product. What is required is the quantification of the permanent products produced from irradiation of  $T_4CS^-$  in the different solvent compositions in the presence and absence of oxygen and upon the addition of mHSA. Also the effect of change in the wavelength of irradiation on product yields would be interesting. This can be achieved by using an appropriate chemical actinometer as a standard. A reliable actinometer in the solution phase which has been widely used in photochemical research is the potassium ferrioxalate system developed by Parker and Hatchard. Details concerning its experimental use are given in most good photochemistry books.

It has been reported that the secondary photochemical transformation of  $T_4CS^-$  appear significantly less important in causing photochemically transformed proteins. Flash photolysis studies on the secondary products of  $T_4CS^-$  photolysis have not been investigated, so it would be of interest to see how the transient absorption spectra of other less chlorinated salicylanilide's compare with that of  $T_4CS^-$ .

To resolve the apparent inconsistency in the measured singlet lifetimes of  $T_4CS^-$  and  $TBS^-$  (section 5.4) with respect to the heavy atom effect and fluorescence yields, it would be desirable to repeat the determination of the singlet state lifetimes of these



two photoallergens using the same method of time-correlated single-photon counting under identical conditions.

### **Experiments with Human Serum Albumin**

Dark-binding experiments revealed at least two strong binding sites of  $T_4CS^-$  to mHSA with a binding dissociation constant  $K_d$  of  $0.16 \mu M$  (see section 4.4). Using the same methodology, the stoichiometry and binding constant of  $TBS^-$  to mHSA can be found.

Competitive binding between  $T_4CS^-$  with other ligands which exhibit comparable or stronger binding constants to the HSA molecule could be investigated. If competitive binding is found, additional information on the binding sites of  $T_4CS^-$  within the protein molecule may be deduced and may further narrow down the region of binding of  $T_4CS^-$  to HSA that has been previously reported (see section 2.6).  $TBS^-$  binding to the protein molecule may be in close proximity to that of  $T_4CS^-$  and therefore competitive binding studies between these two photoallergens could be a starting point.

Following on from this it would be of great interest to study what affect a competitive ligand would have on the transient absorption species produced upon flash photolysis of solutions containing the  $T_4CS^-$  - mHSA conjugate. In section (4.6) of this thesis, it was shown that the addition of mHSA had a profound affect on both the triplet state of  $T_4CS^-$  and on the amount of radical and permanent product produced.

### **Singlet Energy Transfer from Tryptophan to mHSA**

There is overlap between the fluorescence spectrum of tryptophan and the absorption spectrum of  $T_4CS^-$  and it follows therefore that there is a possibility of electronic energy transfer from the tryptophan residue to  $T_4CS^-$  by both a non-radiative and a radiative mechanism. Unpublished data that is referenced in [11], gave evidence for the proximity of the  $T_4CS^-$  binding site to the lone tryptophan residue of HSA provided by energy-transfer measurements. These experiments

indicated that the distance between the tryptophan residue and a  $T_4CS^-$  molecule located at a binding site of HSA is approximately 1.9 nm. Preliminary fluorescence measurements obtained from exciting the tryptophan residue results in electronic energy-transfer to the acceptor  $T_4CS^-$ , which is indicated by an increasing quenching of the tryptophan fluorescence in the presence of increasing concentration of  $T_4CS^-$ . Details of the experimental procedure and the equations required for calculating the energy transfer radius can be found in a paper by F. Wilkinson and G.P Kelly [12].

The work in this thesis was exclusively carried out in the solution phase. A wealth of further research possibilities would be opened up by carrying out experiments using pig skin as a model for human skin. This would require a different experimental technique called diffuse reflectance spectrometry, details of this technique can be found in [13].

In conclusion, there remains much work to be done in this research area. It is clear that a understanding of the mechanism whereby  $T_4CS^-$  and  $TBS^-$  goes on to form an antigen, leading to a photoallergic response is far from clear and further work is definitely required to reach definitive mechanistic conclusions regarding the primary photochemical step which results in a photoadduct between  $T_4CS^-$  and mHSA.

# Chapter 5

## References

- [1] Hilal N.S., *Ph.D. Thesis*, University of Salford. 77-78 (1973)
- [2] Jenkins F.P., Welti D. and Baines D., *Nature* **201**, 213-219. (1964)
- [3] Lakowicz, J.R., Weber, G., *Biochemistry* **12**, 4171-9 (1973)
- [4] Ware, W.R., *J. Phys. Chem.* **66**, 455-8 (1962)
- [5] Brown J.R., *Federation Proceedings* **35**, No 10 (1976)
- [6] Rickwood D.M and Barratt M.D., *Photochem. Photobiol.* **35**, 643-647 (1982)
- [7] Rickwood D.M. and Barratt M.D., *Chem.-Biol. Interactions* **52**, 213-22 (1984)
- [8] Kochever I.E. and Harber L.C., *J. Invest. Dermatol.* **68**, 151-156 (1977)
- [9] Morikawa F., Nakayama Y., Fukuda M., Hamano M., Yokoyama Y., Naguru T  
Ishi M and Toda M., *In Sunlight and Man.* 529-558 Uni.Tokyo Press, Tokyo  
(1974)
- [10] Kochevar I.E., *Photochem-Photobiol.* **30**, 437-442 (1979)
- [11] Rickwood D.M and Barratt M.D., *Biophysical Chemistry* **19**, 69-73 (1984)
- [12] Wilkinson F. and Kelly G.P., *J. Photochem. Photobiol.* **45**, 223-232 (1988)
- [13] Wilkinson F. and Kessler R. W., *J Chem. Soc., Faraday Trans. 1*, **77**, 309 (1981)

